Master's thesis

NTNU
Norwegian University of Science and Technology
Faculty of Information Technology and Electrical Engineering
Department of Electric Power Engineering

Viljar Stensaker Stave

Optimal Utilisation of Grid Capacity for Connection of New Renewable Power Plants in Norway

Master's thesis in Energy and Environmental Engineering
Supervisor: Ümit Cali
Co-supervisor: Magnus Korpås
June 2021

NTNU
Norwegian University of Science and Technology

Viljar Stensaker Stave

Optimal Utilisation of Grid Capacity for Connection of New Renewable Power Plants in Norway

Master's thesis in Energy and Environmental Engineering
Supervisor: Ümit Cali
Co-supervisor: Magnus Korpås
June 2021

Norwegian University of Science and Technology
Faculty of Information Technology and Electrical Engineering
Department of Electric Power Engineering

NTNU
Norwegian University of
Science and Technology

Acknowledgements

This master's thesis has been written at the Department of Electrical Power Engineering at the Norwegian University of Science and Technology (NTNU) and it constitutes the completion of the MSc programme Energy and Environmental Engineering. The thesis was supervised by Associate Professor Ümit Cali and co-supervised by Professor Magnus Korpås, and concluded during the spring semester of 2021.

The thesis was done in collaboration with Statnett, who provided exiting topic and research discussions that helped determine the scope of the thesis. Additionally, good observations and local system data were provided by Nordkraft. As such, there are several persons to be acknowledged for their assistance with this thesis.

First of all, I would like to express my deep gratitude to my supervisor Ümit Cali for his strong commitment and interest in both this thesis and my experience of the process being as good and educational as possible. I have no doubt that his knowledge and guidance have improved the resulting thesis and my learning outcome. I would also like to thank my co-supervisor Magnus Korpås for excellent discussions and suggestions on the thesis topic. I would likewise express my gratitude to Associate Professor Hossein Farahmand for providing superior help and literature for my inquiries throughout the semester. In addition, I would like to thank PhD candidate Marthe Fogstad Dynge for great academic input and advice on the practicalities connected to writing a master thesis. Her sharing of her own experiences has undoubtedly helped facilitate this thesis. My gratitude also goes to Gjermund Sætermo and Ane Meisingset Elgsem from Statnett, who contributed with valuable insight into the power system, as well as inspiration for the determination of the thesis objective. Additionally, I would like to thank Tore Schjelderup and Matthew Homola from Nordkraft for providing relevant data and good advice regarding the studied area.

I would also like to thank my friends and family for their encouragement throughout the whole process. Among these I would like to mention and thank my parents for their unconditional support and patience, always showing interest and providing motivation during ups and downs. A special thanks also to Hilde Kiernan for thorough proofreading of a thesis far outside her scope of interest. And last but not least, I would like to express my gratitude to Jonas Sjong Forfot for invaluable support and collaboration, both professionally and personally, during our time as students.

Øvre Singsaker, 11.06.2021

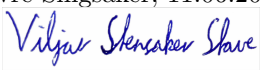

Viljar Stensaker Stave

Abstract

The increased awareness of climate change is causing an increased share of production based on Variable Renewable Energy Sources (VRES) in the power system. This introduces new challenges for system operators, as VRES generate intermittent production and are often located at remote areas with poor transmission capacity. As a means to solve these challenges, the Norwegian Ministry of Petroleum and Energy revised the Regulation on grid regulation and the energy market (NEM) in 2019. In NEM, the legislative conditions of newly connected VRES are regulated. Moreover, the revision in 2019 enabled power producers to acquire grid connection with terms of production restrictions, with the intention of increasing the utilisation of the existing grid.

In this thesis, both a simulation model and an optimisation model are devised and used in a local power system in Northern Norway in order to perform a techno-economic analysis of how the provisions in NEM affects grid utilisation and operational patterns. Moreover, a hybrid power system, comprising hydropower and wind power, is analysed with a local energy balance and an energy loss minimisation model in Python. A bilateral power agreement between producers is introduced along with Dynamic Line Rating (DLR), thereby providing both a political and technical complement to the provisions in NEM.

The simulation results indicate that NEM is able to increase grid utilisation. However, it is seen that the improved utilisation is at the expense of the new producer based on VRES, who experiences loss of potential production. By introducing a bilateral power agreement, the grid utilisation is seen to further improve with 1.01% as the activated flexibility of the reservoir hydropower is able to eliminate all energy loss from the VRES, which constituted $16.41GWh$. The resulting change in system cash flows are found to economically substantiate the use of a bilateral power agreement. Furthermore, the utilisation of DLR was found to reduce the amount of energy loss experienced in the simulation model by $11.89GWh$, inducing an increase in grid utilisation equal to 0.97%. The overall results demonstrate that NEM is able to increase grid utilisation and, combined with a bilateral power agreement or DLR, can provide higher social surplus.

Sammendrag

Det økende fokuset på klimaendringer forårsaker en stadig større andel av variable fornybare energikilder i kraftsystemet. Dette gir systemoperatører nye utfordringer, da slike energikilder har uforutsigbar produksjon og ofte befinner seg på avsidesliggende plasser hvor det er dårlig overføringskapasitet i nettet. For å løse disse utfordringene så reviderte det norske olje- og energidepartementet *Forskrift om nettregulering og energimarkedet* i 2019. Denne forskriften inneholder lovgivningsmessige forhold for tilknyttning til kraftnettet og revisjonen i 2019 åpner opp for at kraftprodusenter kan anskaffe nettilknyttning med vilkår om produksjonsbegrensning. Denne revisjonen har som hensikt å gi økt utnyttelse av eksisterende nett.

I denne oppgaven er både en simuleringsmodell og en optimaliseringsmodell utviklet og brukt i et lokalt kraftsystem i Nord-Norge for å utføre en tekno-økonomisk analyse av hvordan den reviderte forskriften påvirker nettutnyttelse og driftsmønstre. Videre analyseres et hybrid kraftsystem, bestående av vannkraft og vindkraft, med en lokal energibalanse og en modell som minimerer energitap i Python. I tillegg innføres en bilateral kraftavtale mellom produsenter og dynamisk linjekapasitet. Dette gir både et politisk og et teknisk supplement til bestemmelsene i den reviderte forskriften.

Simuleringsresultatene indikerer at revsjonen av forskriften er i stand til å øke nettutnyttelsen. Man ser imidlertid at den forbedrede utnyttelsen går på bekostning av den nye produsenten, basert på variabel fornybar produksjon, som opplever tap av potensiell produksjon. Ved å innføre en bilateral kraftavtale mellom produsentene i området, ser man at nettutnyttelsen forbedrer seg med $1,01\%$ da den aktiverte fleksibiliteten til vannkraften er i stand til å eliminere alt energitap energitap, tilsvarende $16.41GWh$. Den resulterende endringen i systemets kontantstrømmer viser at bruken av en bilateral kraftavtale er økonomisk gunstig. Videre ble det observert at bruken av dynamisk linjekapasitet reduserer mengden energitap som oppleves i simuleringsmodellen med $11,89GWh$, noe som gir en økning i nettutnyttelsen lik $0,97\%$. De samlede resultatene viser at revisjonen av *Forskrift om nettregulering og energimarkedet* er i stand til å øke nettutnyttelsen og, kombinert med en bilateral kraftavtale eller dynamisk linjekapasitet, kan gi høyere sosialt overskudd.

Table of Contents

Acknowledgements i

Abstract ii

Sammendrag iii

List of Figures vii

List of Tables ix

List of Acronyms x

1 Introduction 1

1.1 Motivation and Background . . . 1

1.1.1 Project Description . . . 2

1.2 Chosen Method . . . 2

1.3 Structure of the Thesis . . . 2

2 Theory and Literature Review 3

2.1 Regulation on Grid Regulation and the Energy Market . . . 3

2.2 Hydropower . . . 4

2.2.1 State of the Art of Hydropower . . . 4

2.2.2 Pumped Storage Hydropower . . . 8

2.3 Wind Power . . . 11

2.3.1 State of the Art of Wind Power . . . 11

2.3.2 Wind Potential in Norway . . . 14

2.3.3 Grid Impacts of Wind Power . . . 15

2.3.4 Facilitation of Wind Power Integration . . . 17

2.4 Dynamic Line Rating . . . 19

2.5 The Norwegian Power Market and Power Agreements . . . 21

2.5.1 The Norwegian Power Market . . . 21

2.5.2 Power Purchase Agreements . . . 22

2.5.3 Ancillary Services . . . 23

3 Methodology **24**

3.1 Data Collection . . . 24

3.2 Simulation of Grid Regulation . . . 25

3.3 Optimisation With a Bilateral Power Agreement . . . 29

3.4 Implementing Dynamic Line Rating . . . 33

3.5 Economic Analysis . . . 33

4 Case Study **34**

4.1 Reference Case . . . 34

4.1.1 Hydropower Plant . . . 34

4.1.2 Wind Farm . . . 35

4.1.3 Transmission Line . . . 36

4.2 Grid Regulation and Power Agreement . . . 36

5 Results **37**

5.1 Reference Case . . . 37

5.1.1 Simulation of Grid Regulation . . . 37

5.1.2 Optimisation With a Bilateral Power Agreement . . . 39

5.2 Dynamic Line Rating . . . 42

5.2.1 Simulation of Grid Regulation . . . 42

5.2.2 Optimisation With a Bilateral Power Agreement . . . 44

5.3 Sensitivity Analysis . . . 46

5.3.1 Increase in Wind Power Capacity . . . 46

5.3.2 Change in Inflow . . . 48

5.3.3 Including Dynamic Line Rating . . . 50

5.3.4 Dry Year and Increased Wind Power Capacity . . . 52

6 Discussion **53**

6.1 Grid Regulation . . . 53

6.1.1 Grid Utilisation and Energy Losses . . . 53

6.1.2 Cash Flows . . . 54

6.1.3 Sensitivity Analysis . . . 55

6.2 Bilateral Power Agreement . . . 56

6.2.1 Grid Utilisation and Energy Losses 56
6.2.2 Operational Impact on the Hydropower Producer 57
6.2.3 Cash Flows 58
6.2.4 Sensitivity Analysis 58
6.3 Dynamic Line Rating 61
6.3.1 Grid Utilisation and Energy Losses 61
6.3.2 Cash Flows 62
6.3.3 Sensitivity Analysis 63
6.4 Assumptions and Shortcomings 65

7 Conclusion and Further Work **67**
7.1 Conclusion 67
7.2 Further Work 68

References **70**

A Close-Up Plots of Power Production Scheduling **77**
A.1 Simulation Plots 77
A.2 Optimisation Plots 78

List of Figures

1 Schematic diagram of a pumped storage hydropower facility. The diagram is retrieved from [33, p.75] . . . 9

2 Predicted installed global power capacity of fuels and renewables from 2019 to 2025. The predictions and chart are made by IEA and found in [38]. . . . 11

3 Operational regions of a typical wind turbine during different wind speeds. The figure has been retrieved from [41]. . . . 14

4 Wind map for Norway. The wind speed is the annual average speed at an altitude of 80m, and increases from the blue to the red color. The map is made by Kjeller Vindteknikk, on behalf of NVE, and found in [43]. . . . 15

5 A schematic overview of the Norwegian power market and how the different partakers interact. Here, the blue arrows represent cash flows, the yellow arrows represent communication flows and the red arrows represent power agreements. . . . 22

6 Flow chart of the overall calculation flow in the methodology. The DLR is an expansion of the original models, which is indicated by orange frames. . . . 24

7 Flowchart of the simulation model's behaviour. The different parameters are explained in the nomenclature in Table 2. . . . 29

8 Flowchart illustrating the behaviour of the optimisation problem through one time step. Unlike the simulation model, the decision variables are chosen from a range, affected by how the energy losses are weighted. The different parameters are explained in the nomenclature in Table 2. . . . 32

9 Schematic diagram of the studied system in Northern Norway. . . . 34

10 Simulation results with time series of 2014, highlighting power production, reservoir levels, wind curtailment and available transmission capacity throughout the year. . . . 37

11 Wind power curtailment experienced in the reference system throughout the year when simulating with time series of 2011 to 2015. . . . 39

12 Optimisation results with time series of 2014, showing the scheduled power production, the reservoir level trajectory and the available transmission capacity throughout the year. . . . 40

13 The resulting DLR of the studied transmission line when utilising the ambient temperatures and wind speeds of 2014. . . . 42

14 Simulation results with time series of 2014 and DLR, highlighting power production, reservoir levels, wind curtailment and available transmission capacity throughout the year. The power production is plotted relative to the DLR in each time step. . . . 43

15 Optimisation results with time series of 2014 and DLR, highlighting power production, reservoir levels, wind curtailment and available transmission capacity throughout the year. The power production is plotted relative to the DLR in each time step. . . . 45

16 Annual wind power curtailment of the studied system for different amounts of installed wind power capacity. The blue line represents curtailment for the simulation model, while the orange line represents curtailment for the optimisation model. 46

17 Annual grid utilisation of the studied system for different amounts of installed wind power capacity. The blue lines represent transmission surplus and grid utilisation for the simulation model, while the orange lines represent transmission surplus and grid utilisation for the optimisation model. 47

18 Annual revenue of the different power producers and lost revenue in the studied system for different amounts of installed wind power capacity. The blue lines represent revenue of the wind power producer, the orange lines represent revenue of the hydropower producer and the red lines represent lost revenue due to wind power curtailment. The lines with a darker shade of colour are values from the simulation model, while the brighter lines are from the optimisation model. 48

19 Inflow when altering the time series of 2014. Both the dry and wet year is a scaling of the normal year, i.e., the original inflow of 2014, using scaling constants 0.9 and 1.3 respectively. 49

20 Close-up of the resulting production scheduling in May 2014 from the simulation of the reference case with SLR. Here, it is confirmed that there is hydropower production in the start of May, which substantiates the reservoir level trajectory shown in Figure 10 77

21 Close-up of the resulting production scheduling in May 2014 from the simulation of the reference case. Here, it is confirmed that there is hydropower production in the start of May, which substantiates the reservoir level trajectory shown in Figure 12 . 78

22 Close-up of the resulting production scheduling in June 2014 from the optimisation of the reference case. Here, it is confirmed that there is hydropower production in the end of June, which substantiates the reservoir level trajectory shown in Figure 12 78

23 Close-up of the resulting production scheduling in September 2014 from the optimisation of the reference case with SLR. Here, it is confirmed that there is hydropower production in the end of September, which substantiates the reservoir level trajectory shown in Figure 12 79

24 Close-up of the resulting production scheduling in May 2014 from the optimisation of the reference case with DLR. Here, it is confirmed that there is hydropower production in the end of May, which substantiates the reservoir level trajectory shown in Figure 15 79

25 Close-up of the resulting production scheduling in June 2014 from the optimisation of the reference case with DLR. Here, it is confirmed that there is hydropower production in the end of June, which substantiates the reservoir level trajectory shown in Figure 15 80

26 Close-up of the resulting production scheduling in June 2014 from the optimisation of the reference case with DLR. Here, it is confirmed that there is hydropower production in the end of September, which substantiates the reservoir level trajectory shown in Figure 15 80

List of Tables

1 Description of parameters used for power calculation in hydropower systems. 5

2 Nomenclature of the simulation and optimisation model. The left column presents the used symbol, the middle column presents an explanation and the right column presents the unit. 28

3 Technical data for the aggregated hydropower plant. 35

4 Average annual results from simulations with SLR and time series of 2011 to 2015. . 38

5 Average annual results from optimisations with SLR and time series of 2011 to 2015. 41

6 Average annual results from simulations with DLR and time series of 2011 to 2015. . 44

7 Average annual results from optimisations with DLR and time series of 2011 to 2015. 45

8 Resulting values for various hydrological scenarios in 2014, when a bilateral power agreement between the power producers are functioning. 50

9 Resulting values for $180MW$ installed wind power capacity with original inflow, and for various hydrological scenarios with original installed wind power capacity. All results are for time series from 2014, when the DLR of the transmission line is utilised. In the inflow scenarios, a bilateral power agreement between the producer is functioning. 51

10 Resulting values for various hydrological scenarios in 2014, having an installed wind power capacity of $180MW$ and a bilateral power agreement between the power producers. 52

List of Acronyms

AGC Automatic Generation Control.

BEP Best Efficiency Point.

DC OPF DC Optimal Power Flow.

DLR Dynamic Line Rating.

IEA International Energy Agency.

LP Linear Programming.

NCCS Norwegian Centre for Climate Services.

NEM Regulation on grid regulation and the energy market.

NVE Norwegian Water Resources and Energy Directorate.

PMU Phasor Measurement Unit.

PPA Power Purchase Agreement.

RME Norwegian Energy Regulatory Authority.

SLR Static Line Rating.

TSO Transmission System Operator.

TSR Tip Speed Ratio.

VRES Variable Renewable Energy Sources.

1 Introduction

1.1 Motivation and Background

Global power production is and has in recent years been pushing towards a higher share of the production coming from Variable Renewable Energy Sources (VRES) [1]. This development has received much acclaim and global commitment, culminating with the signing of the Paris Agreement in December 2015. Here it was agreed to reduce greenhouse gas emissions to avoid global temperatures exceeding two degrees Celsius above pre-industrial levels [2].

Although an increase in renewable energy production will help mitigate greenhouse gas emissions, and thus help resolving the climate challenge, other issues follow. A major concern is that the typical solar and wind VRES have intermittent production. The sudden fluctuations in generation can cause reliability issues and induce instability of the short-term operation of the power grid [3]. Consequently, the grid will experience a higher degree of uncertainty with the increase of VRES. Furthermore, VRES, and especially large-scale wind power facilities, are often located in remote areas with limited transmission capacity, due to better siting conditions and higher production potential. The combination of intermittent production and poor transmission capacity often results in a need for grid expansions, which are costly investments. This may in turn slow the desired increase of VRES, as the economic competitiveness is undermined.

The Norwegian power system today is dominated by flexible reservoir hydropower. However, the share of wind power is expected to increase and constitute a significant part of the power production in the coming decades. Predictions performed by the Norwegian Water Resources and Energy Directorate (NVE) expect the annual wind power production in Norway to increase with $11TWh$ by 2040 [4], which equals approximately 7.2% of the annual power production in Norway today [5]. Nevertheless, the most favourable wind power resources in Norway are located in areas with poor transmission capacity, which will cause an increase in congestion issues in the transmission system. These challenges connected to integration of wind power are a common problem, and several studies have been conducted to find a solution [3], [6], [7]. A common suggestion in such studies is to combine wind power and hydropower, using the regulated hydropower to counter the intermittent wind power [8]–[10].

As a means to face these challenges and maintain the economic incentives to invest in VRES, NVE revised the Regulation on grid regulation and the energy market (NEM)[1] in 2019. This revision enables new power producers to connect to the grid with terms on production restriction according to grid limitations, and intends to avoid costly grid investments and improve utilisation of existing capacity [11]. As new producers often are based on VRES, however, they might experience loss of power potential. Nevertheless, it is reasonable to believe based on the predicted increase in wind power production that there will be an increase in cases where VRES are connected according to the revised provisions in NEM. Therefore, the focus of this thesis is on how operational patterns, grid utilisation and cash flows in a local area can be affected by having a wind power producer connected with production restrictions. This thesis also endeavours to provide a techno-economic and political study of how to optimise grid utilisation, based on the opportunity brought about by the regulation revision.

[1] NEM is the official law abbreviation and is therefore used throughout this thesis. The abbreviation is based on the Norwegian name of the regulation, *Forskrift om nettregulering og energimarkedet* [11]

1.1.1 Project Description

This thesis aims to investigate and address the following questions:

- How does the connection of wind power with terms of production restrictions affect grid utilisation, wind power integration and operational patterns in a local part of the power system?
- Can a bilateral power agreement designed to activate the flexibility of neighbouring reservoir hydropower plants improve wind power integration and is it financially sound?
- How is wind power integration, operational production patterns and grid utilisation affected by the utilisation of Dynamic Line Rating (DLR)?

For this purpose, a case study of a suitable area in Northern Norway, consisting of wind power with production restrictions, hydropower and limited transmission, is performed. Furthermore, a simulation is conducted to identify the impacts of the revised provisions in NEM. Moreover, an optimisation model designed to replicate the operational pattern induced by a bilateral power agreement is derived to explore how the hydropower flexibility might enable optimal grid utilisation and ease wind power integration. Lastly, the DLR of the transmission line is estimated and added to the two models to comment on the third question.

1.2 Chosen Method

The main idea behind the chosen approach has been to replicate how the aforementioned political regulation and agreement affect the studied system. These operational patterns have been replicated by utilising a simulation model using a local energy balance and a Linear Programming (LP) optimisation model minimising energy loss. Both models illustrate power production in the studied system over a time period of one year, thus enabling an analysis of the parameters of interest. Python and excel have been used for adaptation and revision of input data, modelling and calculations.

1.3 Structure of the Thesis

Section 2, *Theory and Literature Review*, gives a brief introduction to the revised regulation, the different power production unit types in the studied system, the principles of DLR and how the Norwegian power market is structured.

Section 3, *Methodology*, presents how the simulation and optimisation models utilised for analyses are developed and function. In addition, explanations of the estimated DLR and the economic equations used in the economic part of the analyses are provided.

Section 4, *Case Study*, presents the different elements of the local power system that are used for the analyses in this thesis.

Section 5, *Results*, highlights the most important results from the different simulations and optimisations of the analysed system.

Section 6, *Discussion*, discusses and interprets the main findings presented in the results.

Section 7, *Conclusion and Further Work*, summarises the most important findings of the study, and presents relevant expansions and recommendations for further work on the subject.

2 Theory and Literature Review

This master's thesis is a continuation of the work done in [12], which is also conducted by the undersigned. It should therefore be noted that the following theoretical sections, along with the methodology, overlap with the previous work. Several expansions and revisions have been done, but there are still elements from [12] present. Consequently, some similarities should be expected.

2.1 Regulation on Grid Regulation and the Energy Market

The Norwegian energy system consists of several different sections, which require various regulatory bodies. One of the superior bodies is the Ministry of Petroleum and Energy, having the responsibility of coordinating and integrating a common energy policy [13]. This central coordination affects aspects like production, transmission, and consumption, providing direction to power producers and grid companies, among others. One of the laws set by the Ministry of Petroleum and Energy is the Energy Act [14]. The Energy Act was announced in 1990 and comprises production, transmission, distribution, and consumption of energy. It liberalised the power market, allowing grid subscribers to choose supplier among other things. Chapter three, paragraph four (§3-4) states that a grid company is obliged to connect new electrical installations located within their concession area to their grid. This includes making necessary investments in their grid, for instance grid expansions, to provide a sufficient and stable connection for the new installation [14].

When financing grid investments connected to new electrical installations, the grid company can issue a construction fee to the new grid customer. Such an arrangement are also practised in Great Britain [15] and Sweden [16]. Depending on the situation, the owner of the new installation can end up paying for the entire investment through this fee. Any disagreements regarding the construction fee is brought before the NVE. One possible outcome, which only occurs in the most severe cases, is that the operator's obligation lapses [17].

However, the grid obligation was revised by the Ministry of Petroleum and Energy in 2019 to include a middle ground. Through chapter three, paragraph three (§3-3), in NEM, it is established that a grid company and a producer can enter into an agreement of grid connection with conditions on production restrictions [11]. Such an arrangement cannot be demanded by only one of the parties, and the agreed connection must be operationally sound for all affected grid companies [18]. This involves clarifying with neighbouring and overlying grid companies, as well as the System Operator. Here it is controlled and checked if the specific agreement is feasible for grid operation.

After an agreement of production restrictions is issued, it is the grid company's responsibility to ensure that the agreement is complied with. Moreover, the criteria for when and how the production of the producer is to be downregulated or disconnected must be clearly specified between the grid company and producer. If the new producer has specific obligations from its production concession, then these must be considered and fulfilled even with the production restrictions. The motivation behind NEM is to enable an option that bypasses grid expansions and hopefully increases the utilisation of the existing grid. Furthermore, it is a faster and cheaper alternative than paying construction fees and waiting for the expansion of the grid. However, the producer loses some production flexibility and potential. For instance, if the current area consists of several producers, then a producer with production restrictions will be the last to be granted transmission capacity. In other words, the restricted producer receives the remaining capacity after the other production in the area has been accounted for. [18]

Consequently, a grid connection with terms of production restrictions is a compromise for the producer, motivated by having a higher possibility of receiving grid connection as well as a shorter time frame until connection. The grid company's motivation for such an agreement is that the agreement can increase the utilisation of the existing grid capacity. In addition, costs connected to grid expansions are completely avoided. Similar to the obligation to provide grid capacity, there is a body for addressing disagreements regarding the provisions in NEM. If affected parties disagree, then the issue is brought before the Norwegian Energy Regulatory Authority (RME). And just like disagreements regarding the obligation to provide grid capacity, a possible outcome is that the grid company gets an exemption from its obligation to provide grid connection. [18]

2.2 Hydropower

Hydropower is a form of electricity generation that utilises the energy in water. It is, with a global installed capacity of 1307 GW in 2019 [19] the world's largest renewable source of electricity generation. As such, hydropower plays a critical role in decarbonising the power system. In addition, hydropower plants with reservoirs and pump storage are very well suited to provide system flexibility, as they can generate on demand. Hydropower is expected to further increase in the coming years and remain the most installed renewable energy generation source [19]. In Norway, approximately 89% of the power production is generated from hydropower. In a normal hydrological year, hydropower is estimated to constitute an average annual production of 136.4 TWh [20]. As of January 1st 2021, the Norwegian hydropower system consists of 1682 hydropower facilities, ranging from micro hydropower plants below 1 MW to large facilities with capacity above 100 MW. Furthermore, thirty of the hydropower facilities are pumped storage facilities. Like the global expectations, the total hydropower production in Norway is expected to increase. A long-term power market analysis done by NVE predicts an increase in annual hydropower production of 10 TWh in the period 2020 to 2040 [4].

2.2.1 State of the Art of Hydropower

Electricity from water is generated by exploiting the three energy types potential energy, pressure energy and kinetic energy. These three energy types are converted into electricity by a generator, which is connected to a turbine being in contact with the water. The conventional type of hydropower facility uses dams to store water [21, p.539]. Here, the water in the hydropower system starts by containing potential energy, being stored in reservoirs high above the hydropower turbine. The height difference between the reservoir and the turbine is often called head. Furthermore, the water is transported to the turbine by a pipeline, called a penstock. When in the penstock, the water is pressurised. As such, it is able to perform work when released to the turbine, due to the change in pressure. The pressure energy is therefore associated with the penstock pressure. Lastly, water flows through the turbine, having kinetic energy, and rotates the turbine as it passes. [21, p.541]

When estimating the available energy from water, it is common to sum up the three different energy types found in a hydropower system. This energy equation is often formulated on a per unit of weight basis. Due to the resulting terms having the unit length, the estimated energy is called the energy head of the hydropower plant. It is formulated as follows [21, p.541]:

$$Energy\ head = z + \frac{p}{\gamma} + \frac{v^2}{2g} \tag{1}$$

The different expressions represent the potential head, pressure head and kinetic head, respectively. Explanations of the different parameters are presented in Table 1. By utilising Equation (1), the actual electrical power that is delivered from the hydropower plant to the power system, can be derived. When including losses in penstock and efficiency of turbine and generator, the final equation becomes [21, p.545]:

$$P_{hydropower} = \eta \cdot \rho \cdot g \cdot Q \cdot H_N \tag{2}$$

As the penstock of the hydropower system produces losses, one uses net head term, H_N, to take this into account. The net head is defined as the difference between the potential head in Equation (1) and the losses of transporting the water from the reservoir to the turbine. The parameters for Equation (2) are explained in Table 1. Hydropower systems can be found with various designs and configurations. The different configurations are dependent on the geographical properties of the area they are located in, and are often classified by how the power plant interacts with the water resource. The conventional hydropower facility is characterised by having storage capacity in the form of reservoirs. Here the water can be kept until there is need of power production. These facilities often rely on dams to provide storage and usually have a large altitude difference between the reservoir and turbine. The second main type is run-of-river plants. They have small to no storage capacity and are located along rivers. A run-of-river plant generates power by diverting a small portion of the river to the turbine, using a penstock. The intake to the penstock is often placed at an elevation, making the height difference to the turbine as high as possible. This maximises the utilisation of the energy potential in the water, in accordance with the energy head in Equation (1). [21, p.539]

Table 1: Description of parameters used for power calculation in hydropower systems.

Parameter	**Description [Unit]**
z	Altitude difference between reservoir and turbine, often called gross head [m]
p	Pressure in the penstock [N/m^2]
γ	Specific weight of water [N/m^3]
v	Average velocity of the water [m/s]
ρ	Volumetric mass density of water [kg/m^3]
g	Gravitational acceleration [m/s^2]
η	Efficiency of the turbine and generator [unitless]
Q	Flow rate of the water [m^3/s]
H_N	Net energy head [m]

A consistence difference between the two mentioned hydropower configurations is that hydropower plants with storage tend to have a larger installed power capacity than the run-of-river plants. Furthermore, hydropower with storage can serve more purposes than just being a power generation unit. This includes flood control, irrigation, recreation, and urban water supply. However, the most important aspect for the power system, other than the production itself, is the flexibility the hydropower reservoir provides. The available storage enables hydropower plants to go online and offline to adapt to the constant varying loads and demand in the power system. As such, reservoir hydropower facilities are one of few renewable power production units that are not VRES. In addition, hydropower plants with reservoirs can be cascaded, signifying that the outflow of one plant is the inflow of another plant. [21, p.539]

Another aspect of the reservoir hydropower system is that it can impact the local environment to a greater extent than the run-of-river facility. This is due to the reservoir often requiring a dam, which is a major encroachment on nature [21, p.539]. Moreover, the dam is often able to block the associated river completely, which can be harmful for the local environment. Consequently, NVE demands that all hydropower producers who receive production concession must have a minimum water flow through their facilities [22]. Similarly, there is a demand to always have a reservoir level above a minimum level, called the lowest regulated water level, in order to prevent damage to the hydrological ecosystem [23]. Furthermore, the flexibility of the hydropower plant is dependent on the measure degree of regulation. The degree of regulation is defined as the ratio between the average annual inflow to the reservoir and the storage capacity of the reservoir. A high degree of regulation gives high flexibility, as the probability of flood losses are low.

The third main category of hydropower systems is the pumped storage hydropower. This configuration is an expansion of the conventional reservoir hydropower, where a pump is utilised to actively refill the reservoir [21, p.540]. Pumped storage hydropower is elaborated upon further in Section 2.2.2. In addition to the mentioned main types, there are two less common hydropower configurations, namely the in stream hydropower system and the gravitational vortex hydropower system [24].

In line with the existence of several hydropower system designs, there are many different types of hydropower turbines. The turbines are divided into two main categories, based on how they interact with the water, namely impulse turbines and reaction turbines [24, p.83]. Impulse turbines capture the energy in water by having high speed jets of water shot onto buckets along the circumference of a wheel [21, p.543]. In general, impulse turbines are most appropriate in facilities with high head and low water flow and are mostly used in small systems. One of the main impulse turbines, which also is recognised as the first impulse turbine design, is the Pelton turbine. Here, water is shot out of nozzles onto sets of twin buckets attached to the turbine. The efficiency of Pelton turbines is usually in the range of $70\% - 90\%$. Two other common impulse turbines are the Turgo wheel and the crossflow turbine. The Turgo wheel is like a Pelton turbine, except for an altered bucket design that enables a higher turbine speed. In contrast to the Pelton and Turgo turbines, the crossflow turbine is most useful in low to medium head situations. It is also simple to fabricate, making it a popular choice for situations where the hydropower turbine is preferred to be built locally [21, p.544].

While the impulse turbines rely on jets of water with high velocity, reaction turbines mostly use the pressure difference across the turbine blades to create the desired torque. Instead of having the water shot onto the turbine blades, the reaction turbine has its blades completely immersed in water. When the mass of water moves through the turbine, torque is generated and power is produced [21, p.544]. Therefore, reaction turbines have a better performance in hydropower systems with low head and large water flow. For extensive hydropower systems with reaction turbines, there are two main designs. The first is the Kaplan turbine, which is widely used in low head situations [21, p.545]. A Kaplan turbine is formed as an outboard motor propeller and comes with anywhere from three to six blades. The turbine has mechanisms to adjust blades and pitch. This enables regulation of production and maintenance of operating conditions with high efficiency [24, p.88].

The second main reaction turbine design is the Francis turbine. This turbine design is characterised by having radial or axial flow blades that are mounted in a spiral with internal adjustable guide vanes [24, p.88]. Furthermore, a well-designed Francis turbine can reach an efficiency of $90\% - 95\%$ and can perform at both high and low head and water flow [25, p.43]. This combination of high

efficiency and wide applicability has made Francis turbines the most common hydropower turbine, both globally and in Norway [24, p.88], [25, p.39], [26, p.71-92]. Moreover, Francis turbines are the heavyweights of the turbine world. Some of the largest turbines, for instance at the Iaipu power plant on the Brazil-Paraguay border and at the Three Gorges Dam in China, have a capacity of $700MW$ [25, p.44].

As previously mentioned, hydropower systems have high efficiency and flexibility. However, due to an increasing amount of variable production from wind and solar energy, the hydropower plants are often required to counter production in order to maintain the grid stability. Consequently, hydropower plants are often operating far from the turbines' Best Efficiency Point (BEP). Such operation can lead to a residual swirl in the exit tube of the facility, which again can decrease the efficiency. This phenomenon is especially affecting turbines with fixed pitch blades, e.g., Francis and Kaplan turbines. When a turbine operates away from BEP, its lifetime is diminished. The turbine operates away from designed operation, for instance having an increased amount of start-up operation and load rejections. Such operation can over time induce instabilities that provoke fatigue damages. [27, p.2]

In [27], Kougias *et al.* review different emerging technologies that aim to solve the issues caused by operation away from BEP. Here, passive control techniques, such as installing stabiliser fins, are found to significantly improve the turbine operation at far off-design regimes. However, the passive components generate unnecessary hydraulic losses and pressure fluctuations, as they continue to compensate operation when the operational conditions are good [27, p.2]. Furthermore, active control methods, which generally use water or air injection, are found to reduce surges in the exit tube during wide range operation, but also generate volumetric losses [27, p.3]. Kougias *et al.* [27, p.3] also highlight the importance of a digitalisation of the hydropower industry, which is expected to revolutionise how new and existing hydropower plants operate. Digitalisation is estimated to increase the annual global hydropower production by $42TWh$, due to an increase in overall efficiency of existing power facilities [27, p.5]. Variable speed generation and generators with current controlled rotor segments are two other mentioned technologies that can reduce turbine fatigue. These are especially helpful against frequent start and stops, and improve the efficiency of operating away from BEP [27, p.7].

Besides control systems aiming to maximise the efficiency and therefore the amount of power produced, hydropower facilities have regulators tasked with maximising the quality of the power output. The turbine itself is often equipped with a speed regulator that controls inflow to the turbine. In addition, the generator is usually equipped with a voltage regulator that measures grid voltage and adjusts the magnetisation of the generator accordingly [28, p.26]. These regulators help to maintain the voltage quality of the produced power, as well as the power system frequency. However, hydropower facilities with long penstocks demand a more complex regulation function in order to achieve sufficient frequency regulation. A nonlinear governing system is found to give stable and conditionally stable frequency regulation during opening control mode and power control mode respectively [29, p.1].

An important feature of the regulators, especially when several production units are connected, is the ability to regulate automatically [28, p.27], [30, p.335]. Automatic Generation Control (AGC) is of fundamental importance when handling sudden load changes in the power system. Moreover, AGC deals with abrupt power demand changes and controls both the acquisition of the desired frequency, as well as the achievement of net power interchanges with neighbouring areas [30, p.336].

A controller that has been found to be a good choice to provide AGC is a PID controller. PID is a proportional-integral-derivative controller and usually provides small stationary deviation [28, p.347]. Moreover, a PID controller has been shown to enhance the damping of the power system during a small step change in load and gives a better performance than a conventional PI controller [31, p.7].

Even with the control challenges mentioned, hydropower has advantages compared to most renewable technologies with regard to flexibility and efficiency [21, p.539], [27, p.1], [24, p.83]. The hydropower plants can be used to cover both base load and peak load, having a wide range of operation. Especially hydropower plants with variable-speed operation are able to bring further flexibility [32, p.20]. In addition, hydropower facilities can provide spinning reserve and energy storage to the power system. Moreover, the reaction time of a hydropower plant allows it to meet minute-by-minute load fluctuations quickly over a large range. Such abilities are necessary in a complex power system, to secure reliable and flexible energy supply to consumers. As a result, hydropower plants are a favoured for providing ancillary services to the power system. This also enables hydropower, when the hydropower system holds storage capacity, to function as a complement to unpredictable VRES. Installing a hydropower facility with pumped storage can further increase the flexibility of hydropower, something that is elaborated upon in the following part. [21, p.539]

2.2.2 Pumped Storage Hydropower

Pumped storage hydropower is an energy storage system that builds on the principle of having a hydropower plant with a reservoir. The reservoir provides an element of energy storage, by enabling storage of water during periods with high water inflow. With a pumped storage reservoir, the water can be actively stored, which develops the original principle of reservoir storage from being a seasonal cycle to a daily cycle. This makes the hydropower plant less dependent on the natural flow of the water. In other words, the flexibility of the hydropower plant is increased as it now has a way to actively avoid both flooding and water shortage. [33, p.73]

The main idea of pumped storage hydropower is to have two reservoirs, one located above, and one located below the hydropower generator, and use a pumping system to enable water flow regulation both ways. When there is low electricity demand, the facility can use surplus energy from the grid to pump water from the lower reservoir back into the upper reservoir. This process can be seen as analogous to charging a battery. Furthermore, the upper reservoir can be drained to generate power during high demand periods, filling up the lower reservoir. A simple schematic diagram of a pumped storage hydropower plant is shown in Figure 1. As can be seen the pumped storage facility is having a similar configuration as a hydropower plant, only with the additional property of the water and power being able to flow both ways. [33, p.73]

The pumped storage configuration in Figure 1 is a fundamental configuration, and the basis of the various designs being used today [33, p.75]. One often has variations in configurations due to reservoir locations, inflow amount to the system and how the reservoir and pump are connected. In [34], Hunt *et al.* present a review of existing and new configurations of pumped storage facilities. Hunt *et al.* [34, p.4] emphasise that the most well-known pumped storage hydropower configurations are open-loop, closed-loop and pump-back storage. The different configurations are characterised by the water inflow and outflow of the system.

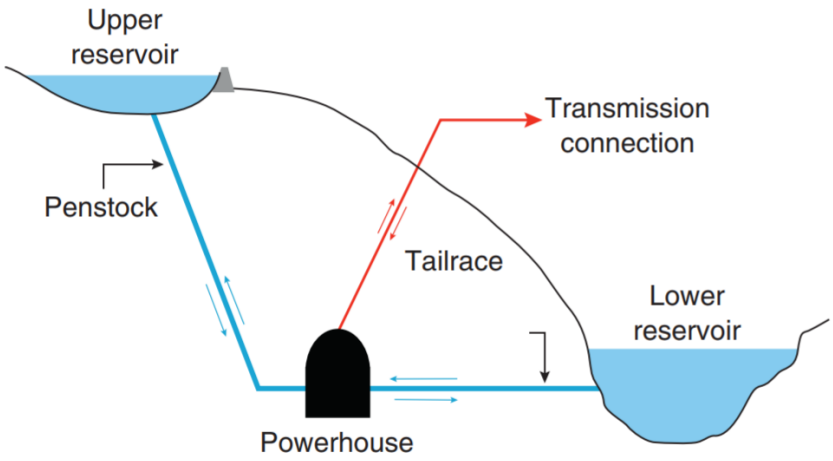

Figure 1: Schematic diagram of a pumped storage hydropower facility. The diagram is retrieved from [33, p.75]

Open-loop systems have a significant inflow to either one of their reservoirs and is often built with the lower reservoir being an existing hydropower dam. This reduces both costs and the impact on nearby environment and river flow [34, p.4]. Closed-loop systems consist of an upper and lower reservoir with limited water inflow. Consequently, the environmental impact of a closed-loop system is usually lower than for the open-loop. Moreover, the storage cycles are limited to weeks or days. Here water does not leave the system on the same scale as in open-loop systems, which makes the facility a closed loop for the water. The schematic in Figure 1 is an example of a closed-loop system. Neither the upper nor lower reservoirs have a visible source of inflow, indicating that the loop is closed.

Lastly, the pump-back storage configuration consists of two consecutive reservoirs being located immediately after each other. In other words, there is no penstock between the reservoirs as in Figure 1. This allows a flexible operation with water flowing back and forth between the two welded reservoirs [34, p.5]. The storage capacity of the pumped storage facilities is, similarly to hydropower, directly connected to the amount of water the upper reservoir can store. Furthermore, the round-trip efficiency in a pumped storage hydropower facility, which is the ratio between energy used to pumping water and energy retrieved from utilising the same water amount, is in the range of $70\% - 80\%$ [33, p.77].

In order to have a functioning pumped storage facility, one must be able to both generate and actively store energy from water. One solution is to install motors, dedicated to pumping water into the upper reservoir, in an existing reservoir hydropower system. Such a solution is usually found in high-head facilities with Pelton turbines, as this turbine cannot act as a pump itself. The Pelton turbine's inability to function as a pump causes high-head facilities to also need separate water shafts for pumping, which incurs extra costs [33, p.77]. Consequently, single-unit pump-turbines have become the standard for most pumped storage plants. Furthermore, pump-turbines based on a Francis turbine are favoured as they are applicable in a large range of head heights. However, the turbine risks low-head operation, due to the upper reservoir being depleted. Therefore, Francis

turbines with adjustable blades, often called Deriaz pump-turbines, are usually used. Such a turbine is able to maintain high generation efficiency during low-head operation by adjusting the blades to [33, p.78]. An alternative pump-turbine type is the Ternary, which combines a Pelton turbine and a Francis pump [34, p.3]. The main benefit of this pump-turbine is the fast transition between power consumption mode and generation mode, enabling the turbine to rapidly respond to fluctuating power production from wind and solar generation sources. This property is due to the configuration between the Pelton turbine and the Francis pump, enabling change of operation mode without needing to reverse the direction of rotation [34, p.3].

Another aspect regarding pumped storage turbines is the rotational speed of the turbine. Hunt *et al.* [34] mention in their review of pumped storage plants that a fixed-speed turbine will have fixed generation and pumping capacity. The fixed generation makes fixed-speed turbines improper, as pumped storage hydropower plants often are often intended to complement VRES and maintain the quality of the power system [34, p.3]. On the contrary, a variable-speed turbine allows the final generated power to vary. This gives an improved ability to control the frequency of the grid, an easier start up when synchronising to the grid, as well as a better ability to utilise variable surplus power from the grid. In addition, the efficiency is higher, since a variable-speed turbine is able to adapt the rotational speed to the water flow rate and therefore maintain optimum efficiency [33, p.78], [34, p.3]. Nevertheless, the fixed-speed turbine is more common, as it is cheaper than the variable-speed turbine [34, p.3]. Even so, it is expected that the variable-speed turbine will be used more frequently, in line with the anticipated increase of VRES in the power system [34, p.3][33, p.78].

Regardless of the turbine type, pumped storage hydropower plants are considered as power units that react quickly to variation in power demand [33, p.78]. The fastest configuration for providing grid services consists of separate pumps and turbines, which allows simultaneous pumping and generation. Moreover, it enables seamless switching between the two operation modes. The planned Gordon Butte facility, with a total pumping and generation capacity of $400MW$, is an example of this configuration. It is estimated that the facility will have a switching rate of over $20MW/sec$, including cold-start [34, p.4] [35]. Pumped storage hydropower, with its fast reaction properties, can quickly provide power to the grid, as well as absorb surplus power rapidly. Furthermore, it can provide reactive power supply, voltage stabilisation and spinning reserve, which helps the grid to repel sudden changes in the operational conditions [33, p.78], [21, p.550].

As mentioned in Section 2.2, Norway's energy production is mainly generated from hydropower. Consequently, Norway has good conditions for pumped storage facilities, which can be coupled to the existing hydropower plants. Nevertheless, only thirty pumped storage facilities exist in Norway per January 2021 [20]. Pitorac *et al.* [36] review in their study the existing pumped storage plants in Norway, investigating both technical properties and operation experiences of the plants. Here it is observed that the Norwegian hydropower reservoirs contain approximately 50% of the total reservoir capacity in Europe. Moreover, the low prevalence of pumped storage facilities in Norway is pointed out [36, p.2]. Pitorac *et al.* thus draw the observation, supported by data of Europe, that Norway has the largest pumped storage hydropower potential in Europe. In other words, Norway can play a pivotal role regarding integration of VRES in Europe [36, p.3].

Furthermore, the technical part of the review in [36] shows that the Norwegian pumped storage facilities are mostly constructed for seasonal storage, having an upper reservoir that is considerably larger than the lower reservoir in the system. This comes from the facilities being built for pumping

inflow to the upper reservoir during flood season, and not for pumping to the lower reservoir. In other words, the Norwegian systems are open-loop systems, having a considerable natural inflow to the reservoirs. On average, over 90 days of operation are needed to empty or fill the upper reservoirs, compared to just 22 days to fill the lower reservoirs [36, p.5]. The round-trip efficiencies of the Norwegian pumped storage facilities are found in [36] to be in the range $65\% - 80\%$, which is consistent with the efficiencies mentioned in [34] and [33]. Pitorac *et al.* [36] also highlight that the reaction time of the pumped storage facilities in Norway is high, due to being designed for seasonal storage. However, the possibility to upgrade the starting mechanisms and consequently reducing the reaction time is concluded to be present. In addition, the improved reaction time is observed to be increasingly attractive as the spread between high and low power prices is increasing. Such an upgrade will increase the potential earnings of the pumped storage hydropower plants, as price variations can be utilised better [36, p.18].

2.3 Wind Power

Wind power is generated by exploiting the energy of wind and transforming it into electricity. It is a renewable energy source and considered to be the second most important renewable energy source in the world, only surpassed by hydropower [37, p.223]. Furthermore, the International Energy Agency (IEA) predicts that the installed capacity of wind power and solar power will exceed any other energy source by 2025 [38]. The predicted development is shown in Figure 2.

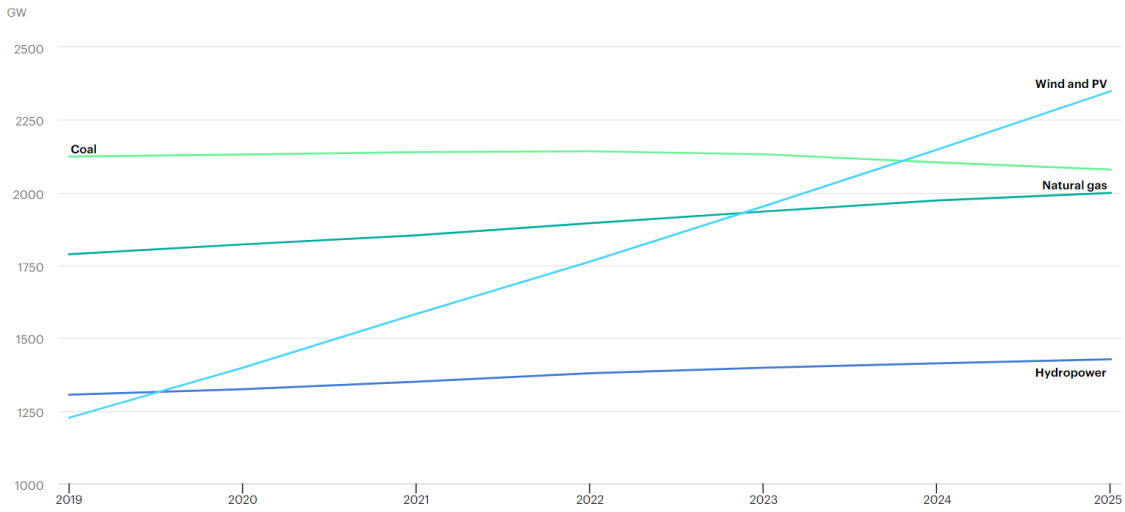

Figure 2: Predicted installed global power capacity of fuels and renewables from 2019 to 2025. The predictions and chart are made by IEA and found in [38].

2.3.1 State of the Art of Wind Power

A wind turbine is rotated when wind passes through. The mechanical movement is then converted to electricity by a generator, in the same way as hydropower generators convert mechanical movement from a hydro turbine. The amount of power a wind turbine can produce is usually derived by first

calculating the power in the wind itself, and then include how much power the turbine manages to extract. Unlike the water in hydropower systems, wind only contains kinetic energy. By considering the mass and speed of the wind that flows through the cross-sectional area of a wind turbine, the power in the wind itself can be derived. The resulting relation is as follows [21, p.425]:

$$P_W = \frac{Wind\ Energy}{time} = \frac{\frac{1}{2}mv^2}{t} = \frac{1}{2}\dot{m}v^2 = \frac{1}{2}\rho A v^3 \tag{3}$$

Here, P_W is the power in the wind, $\dot{m}$ is the mass flow rate of air through the turbine, A is the cross-sectional area of the wind turbine, ρ is the density of the air and v is the wind speed. When a wind turbine extracts the kinetic energy in wind, the wind speed is reduced. The rotor power will equal the difference between the power in the wind before and after it has passed the turbine, which is directly connected to the wind speed difference. Moreover, the wind turbine power will be the remainder of the rotor power after losses from converting from mechanical to electrical power have been considered. By using the relation in Equation (3), the final expression becomes [21, p.435]:

$$P_{wind\ power} = \frac{1}{2}\rho A v^3 \cdot C_p \cdot \eta \tag{4}$$

Rotor efficiency is denoted as C_p and has a theoretical limit of approximately 59.3%, often called the Betz efficiency. The Betz efficiency was conjectured by the German physicist Albert Betz in 1919, who found the optimal wind speed reduction in a wind turbine [21, p.433]. As mentioned, a wind turbine slows the wind when extracting the kinetic wind energy. An extraction rate of 100% would give a downwind velocity of zero, making the wind stop completely behind the wind turbine. This would prevent further wind from passing through the turbine and is why wind turbines has a maximum theoretical efficiency much lower than 100%. By taking the difference between upwind and downwind kinetic energy, and exploiting that the speed at the rotor is equal the average of upwind and downwind velocity, Betz found the following expression for rotor efficiency:

$$C_p = \frac{1}{2}(1+\lambda)(1-\lambda^2) \tag{5}$$

λ is here defined as the ratio of downstream to upstream wind velocity. By taking the derivative of Equation (5) with respect to λ, Betz found the ideal reduction of wind speed to be one-third of the initial upstream velocity. Modern wind turbine rotors can achieve 80% of the Betz efficiency, which gives around 48% efficiency in converting the power in the wind into the rotating generator shaft. Lastly, the generator's conversion efficiency is accounted, denoted as η in Equation (4), equivalent to the efficiency in the hydropower equations. [21, p.435]

The usual wind turbine configuration is a three-bladed rotor attached to the front of a horizontal-axis drive-train, and the rotor is always facing the wind [37, p.227]. Historically, wind farms have been located onshore, but a rapid development has happened in offshore technology over the last few years. One has seen in recent years that more offshore farms are being built and it is expected that the offshore share of wind power will further increase [37, p.233] [39]. The global onshore potential is estimated to be in the range $100TW$ to $1000TW$, while offshore even higher [37, p.225]. The size and capacity of a wind turbine are dependent on wind conditions as well as what is practically possible for each location. Usually, offshore wind turbines have a higher installed power capacity

than onshore turbines. This is due both to more optimal wind conditions offshore and to the fact that transportation onshore becomes impractical when the turbine reaches a certain size. The practical complications of large turbines are connected to wind turbines often being located at remote sites with poor infrastructure [37, p.229]. Average installed wind turbine size was $2.7MW$ onshore and $4.2MW$ offshore in 2015. However, manufacturers have issued products in the range $4MW - 6MW$, and it is expected that turbines above $4MW$ will be more common in the next decade. The wind turbine size expansion is driven by the need of decreasing the cost per kWh produced [40].

In line with the increase in wind turbine size, wind turbine control systems have evolved. Control systems are central for having a high efficiency level of production and making wind power cost efficient [41]. One of the main control objectives is the regulation of rotor speed. The wind turbine efficiency is highly affected by the rotational speed of the rotor, making it vital to have a system that maintains optimal rotor velocity at different wind speeds. Furthermore, speed control is a safety measure to prevent damage to the wind turbine during storms and other events where wind speeds are above rated speed. Optimal rotor speed is dependent on the rotor size; large rotors are most efficient at low wind speeds, and smaller rotors are efficient at sites with high wind speeds. When determining the optimal rotor speed, a parameter called Tip Speed Ratio (TSR) is often used. The TSR is defined as the ratio between the speed of the rotor blade tips through the air and the wind speed. For three-blade rotors, the optimum TSR is typically between six and seven. [37, p.229]

Figure 3 shows the typical relation between wind speed, power output and turbine operation for a wind turbine [41, p.2]. This correlation is often reffered to as the power curve of a wind turbine, and it is used to estimate expected output of a turbine, given wind data. The curve is divided into four regions, each having a specific characteristic. Regions one and four have zero power production, due to unfavourable wind conditions. In the former, the wind speed is too low to initiate rotation of the turbine, while in the latter the wind speed is too high, making production dangerous for the turbine. Region two starts where the wind speed is high enough to start rotating the turbine, often called the cut-in speed. Here the maximum rotor efficiency is prioritised, controlling the rotor speed to maintain optimal TSR. When the wind speed passes the rated speed of the turbine, region three is entered. The turbine now produces nominal power output until the wind reaches a velocity that makes it dangerous to operate, called cut-out speed. [41, p.3]

Rotor speed control is divided into passive and active speed control. In a passive speed control approach, the rotor blades are designed aerodynamically to stall when the wind reaches a certain speed, which is the cut-out speed in Figure 3. Due to only having a passive exploitation of stall, passive speed control is often called passive stall control. This technique does not, other than being a safety measure during very high wind speeds, help to vary the rotor speed. It is therefore unable to increase the efficiency of the turbine. In contrast, when employing active speed control one can control the speed and allow wind turbines with variable-speed generators to maintain optimal efficiency. Within the category of active speed control, there is a further subdivision between active stall control and pitch control [41, p.4]. Both techniques involve having an actuator connected to each blade at the rotor. The actuators are located where the blades join the hub of the tower. They enable the blades to be rotated about their long axis and by such regulating the pitch of the rotor. Therefore, a variable-speed generator with a pitch-regulated rotor can contain an optimal TSR and maximise the efficiency when operating at different wind speeds. Both active control techniques give a higher power production compared to passive control [41, p.4]. Consequently, most of the modern turbine designs have pitch-regulated active speed control of some kind. [37, p.229]

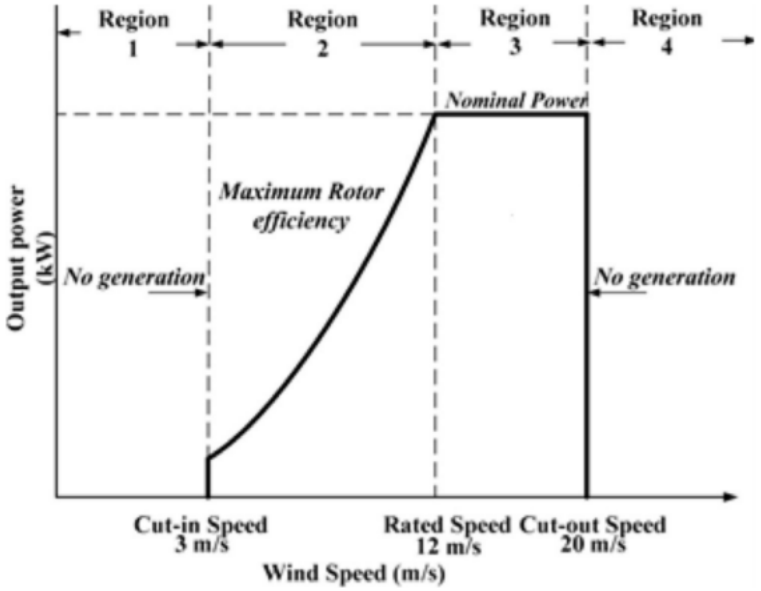

Figure 3: Operational regions of a typical wind turbine during different wind speeds. The figure has been retrieved from [41].

2.3.2 Wind Potential in Norway

As mentioned in Section 2.2, the Norwegian power production mainly consists of hydropower [5]. However, a possibility study done by Waagaard *et al.* [42] in 2008 showed that there is a wind power potential in Norway around $5800MW$ to $7150MW$ installed capacity by 2025. For a normal year, this is estimated to give between $17.4TWh$ and $21.5TWh$, which equals approximately 11 to 14 percent of the total power production in Norway in an average year today [5]. Moreover, NVE estimates in their long-term power market analysis for 2020-2040 an increase in annual wind power production equal to $11TWh$ by 2040 [4].

Furthermore, Byrkjedal *et al.* [43] showed with their generated wind map for Norway that there are large areas in the inner parts of Norway that may be suitable for wind power production. These areas are shown in Figure 4 as the yellow and red domestic regions, and substantiate the predicted Norwegian wind power potential. In addition, an increment in wind power is in accordance with the global energy mix predicted by IEA, mentioned in Section 2.3. This prediction is shown in Figure 2, and it is clear that wind, together with solar energy, will have a rapid growth over the next years. As such, it is reasonable to expect, based on the different analyses presented, that wind power will supply a larger part of the Norwegian power system in the future.

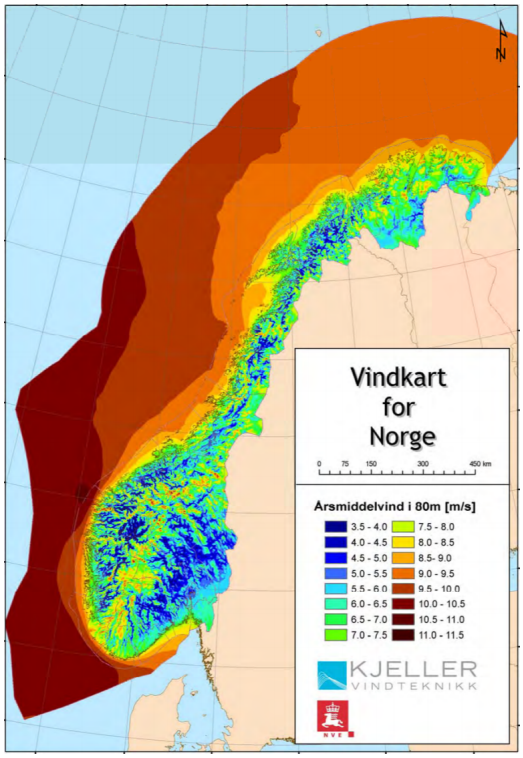

Figure 4: Wind map for Norway. The wind speed is the annual average speed at an altitude of 80m, and increases from the blue to the red color. The map is made by Kjeller Vindteknikk, on behalf of NVE, and found in [43].

2.3.3 Grid Impacts of Wind Power

Due to wind power being dependent on wind speed to generate energy, it is a highly inconsistent energy source. Even with state-of-the-art weather forecasting to predict wind speed and direction, the wind will remain somewhat unpredictable, hence the wind power production will be intermittent. This uncertainty will introduce new challenges in the Norwegian power system when the amount of wind power increases. A report published by the Norwegian Transmission System Operator (TSO), Statnett in 2018 highlights how the wind power affects the transmission grid [44]. In [44], Statnett gives an overview of estimated wind power capacity in the existing power grid. Here, existing grid and known grid expansions are integrated into their marked and grid model, *Samnett*, together with expected data for 2025. The report then simulates scenarios with this model, having different amounts of wind power installed in different areas of Norway. The simulations show that a local increase in wind power gives higher variation in local power prices, due to bottlenecks and the intermittent nature of wind power. This limits the grid capacity of wind power locally. The bottlenecks disable an even market price, making local prices drop and simultaneously decrease the economic profitability of wind projects. However, an increase in local consumption will counteract this phenomenon. [44, p.6]

In the book *Valuing Wind Generation on Integrated Power Systems* by Ken Dragoon [6] an overview of system impacts of wind generation in power systems is presented. Here, the effects wind power generation has on other generators are highlighted. One of the most significant economic factors mentioned is the low variable operating cost and the absence of fuel costs in wind power. Therefore, many analyses of system effects from wind power are modelling wind power as a must-run resource, due to the priority order of generator dispatch being based on using sources with low operational costs first [6, p.6]. Consequently, other generating types are adjusted to meet the net load in the system, after the wind generation has been subtracted. The primary savings from wind are derived from operating costs and emission reduction associated with decrease in generation based on peaking and intermediate load units. However, due to the intermittent nature of wind, the value of wind energy depends on the wind forecasting accuracy. If weather forecasting is precise, the amount of backup power needed in order to handle unexpected changes of the wind generation is reduced [6, p.8].

Another effect of the wind intermittency that is mentioned in [6], is how fast the generation from wind power can change. System operators need to calculate the ramp rate requirements that significant amounts of wind can bring. Although the amount of backup generation is sufficient, it must also have a response time fast enough to quickly compensate for sudden wind changes. Wind power can fall off relatively rapidly, e.g. during high wind speeds when the turbine is forced to shut down to avoid damage. If the generating units in reserve are not able to increase generation fast enough to compensate for the falling wind power, the wind power production may need to be limited. Further, a system containing high levels of wind might experience that the wind production becomes so high that the remaining need of production is less than the minimum generating requirements of the other generation units. Therefore, the wind generation may need to be limited, which increases wind curtailment. [6, p.12]

One measure that can increase the accuracy of wind generation prediction is to forecast several wind turbines in a wind farm collectively. In a wind farm, much of the individual randomness of each turbine is cancelled out. The power output is therefore more predictable when the farm is modelled as a whole. Moreover, the individual variability of a single wind turbine is unimportant when regarding the whole power system [6, p.14]. However, a great concern is how different wind farms in the same power system interact with each other. If wind farms increase or decrease their generation simultaneously, the impact on the power system is much more severe than if there is a random relationship among the wind farms [6, p.15]. Dragoon quantifies this effect by using a statistical correlation function. It is shown that the correlation between wind farms is highly dependent on the time scale of the calculations and the geographical distance between the wind farms. The longer the geographical distance and shorter the time scale, the more independent the wind farms are of each other [6, p.15].

Other studies that consider the impact of high wind power penetration in the power system are [7], [45], [46]. Similar to the sources mentioned earlier, it is in these studies highlighted that many of the challenges connected to wind integration originate from the stochastic nature of wind. In [45], Kabouris and Kanellos present load following as a key challenge in systems with high wind penetration. The frequency control is a major technical problem, and it is mentioned that the difficulty of maintaining balance between production and consumption increases when operating under light-load conditions. Consequently, it is argued that a combination of system flexibility, wind curtailment, wind ramp-rate mitigation, and reserve loads added in light-load periods will be needed in systems with high wind power penetration [45, p.113]. Similarly, Xie *et al.* [46]

call attention to the challenges wind integration introduces in scheduling, frequency regulation and system stabilisation methods. It is suggested that a multi-temporal model-based systematic approach will achieve a cost-effective and reliable integration of large amounts of wind power [46, p.228].

Where [45], [46] provide an analysis focusing on technical effects in the power system, Nicolosi [7] aims attention towards the power market. Similar to the findings in [44], it is stated that high penetration of wind power can cause a decrease in the electricity spot price. In times of low power demand and high wind power production, the market tends to react with bids below operational costs to avoid reduction of rigid base load power plants [7, p.1]. This phenomenon is particularly relevant in countries that have a high share of nuclear and fossil power plants in their power system. A solution to avoid low market prices and ensure market clearance is to increase the flexibility of the power system, both on demand side, supply side and in the grid itself. Nicolosi emphasizes demand-side management applications, grid enhancements, a flexible generation mix and power storages as good measures towards a healthier power market in a system with high wind penetration [7, p.12].

2.3.4 Facilitation of Wind Power Integration

As mentioned, one of the challenges with high wind power penetration is wind curtailment. The necessity of limiting the power production in wind farms is severely reducing the profitability of wind power, among other things [6]. Jorgenson *et al.* [47] identify insufficient transmission capacity to be a primary driver for wind curtailment, which is often caused by wind power being located at remote areas. As seen on the wind map in Figure 4, the wind conditions, and therefore the wind power in Norway, are also favourable in remote areas. Consequently, insufficient transmission capacity is a plausible scenario for new wind farms in the Norwegian power system.

Several studies have considered energy storage to be a possible solution to wind curtailment [37, p.238], [47]–[49]. In [47], Jorgenson *et al.* concludes that increased transmission capacity is a more effective measure than energy storage at reducing wind curtailment and generation costs. However, a limited synergy between storage and transmission is acknowledged. Furthermore, Abhinav and Pindoriya [48] highlight how battery energy storage systems can provide frequency support, mitigating power fluctuations and active and reactive power management when correlated with wind production. Moreover, batteries are stated as the most cost-effective for wind farm integration. In contrast, both Breeze [37] and Saber *et al.* [49] state that pumped hydro energy storage is the most promising and commercially suitable grid-scale energy storage due to large power capacity, low operation costs and a long lifetime. In addition, the current capital cost of energy storage is not found to be justified [37], [47]. Breeze [37] further elaborates that utilising existing reservoir hydropower plants to integrate wind power is a cheap and effective solution. The hydropower is favourable due to its ability to be rapidly taken offline and online. However, it does not have the full flexibility of pumped storage hydropower.

In-depth examinations of the possibility to coordinate wind power and hydropower can be found in [50] by Farahmand *et al.* and in [51] by Korpås. Both studies investigate how such a correlation can benefit the integration of high wind power penetration, although they go in slightly different directions. In [50], Farahmand *et al.* run power flow simulations on a future scenario with high wind penetration from the North Sea and increased pumped storage facilities in southern Norway. Here, it is concluded that the pump storage provides generation flexibility which compensates

for the variability of wind generation [50, p.26]. Moreover, sensitivity analyses of the results are conducted, having altering water inflow and installed wind power capacity. These analyses show that the Norwegian hydropower reservoir levels increase with increased wind capacity. In other words, the surplus production from wind energy is stored in the Norwegian hydropower reservoirs by the pumped storage facilities [50, p.26]. Furthermore, simulated pumping patterns highlight that the pumped storage facilities are in phase with the wind power production, running when the production is high and resting when the production is low. This corresponds well with the Norwegian hydropower system functioning as a green battery for the fluctuating energy generation of Northern Europe [50, p.18].

While Farahmand *et al.* [50] examine future scenarios of the power system in Northern Europe, Korpås [51] investigates the existing power system in Northern Norway. In [51], it is explored how a correlation between wind power and hydropower can increase the feasibility of increasing the amount of installed wind power in areas with scarce transfer capacity. By calculating a local energy balance for the power grid, both with the hydropower producer as an active and a passive component, the energy loss in the system is found. The results show that a regulation of hydropower in opposite phase to wind power gives reduced energy losses, due to less wind curtailment [51, p.14]. Established effects of the correlation between wind power and hydropower are increased power operation of the hydropower plant, faster power changes, more frequent production at full power and more often full stop. However, it is stated that the hydropower plant does not necessarily get a negative effect from this, due to hydropower being a technology with good properties for regulation. Korpås states that it is more likely that such regulation can increase the negative impact the hydropower plant has on the local environment [51, p.17].

Furthermore, Korpås [51] examines the effect of increasing the installed wind power capacity, as well as the installed hydropower capacity. The results show that there is a clear limit to how much one can expand the wind power capacity before substantial curtailment occurs. An influential parameter affecting this observed limit is the transfer capacity of the area. Having an installed wind power capacity larger than the transfer capacity of the transmission bottleneck in the area risks experiencing insufficient transmission capacity even when the hydropower production is absent. The solutions that are highlighted are investing in a pumped storage facility and to include more hydropower plants to correlate with the wind power production. Both measures can increase the sustainable wind power capacity limit in the area. Another demonstrated effect of the increased wind power capacity is increased flooding of the correlated hydropower facility. Sensitivity analyses of installed power in the hydropower plant demonstrate how a higher installed hydropower capacity reduces the flood losses and has an increased value for hydropower plants with low degree of regulation. In addition, the simulations show that the increased installed hydropower capacity can have more applications than avoiding wind curtailment. The main alternative application is to take advantage of the different spot prices in the market to a greater extent, thereby maximising profits. Being a large power reserve in case of errors in predicted wind power production or import power is also highlighted as an extra application for the increased hydropower capacity. [51, p. 30]

As wind-hydro coordination is frequently suggested as the solution to wind integration issues, several reliability and stability studies of correlating wind power and hydropower have been produced [8]–[10]. In [8], Tande and Vogstad use thirty years of wind speed data from five different locations, together with a power curve as seen in Figure 3, to achieve a normalised measure of expected supply from wind turbines along the Norwegian coastline. Through their calculations, they found that the annual supply from wind turbines can vary with 20%. However, this is less than the

annual variation of hydrological inflow, which can vary with up to 30%. Moreover, the seasonal variations in wind power production are seen to match the variations in demand, which is beneficial for system reliability [8, p.4]. While Tande and Vogstad [8] focus on estimating national production variations on an annual scale, Matevosyan *et al.* [10] develop a day-ahead planning algorithm for a multi-reservoir hydropower system coordinated with wind power in areas with limited transmission capacity. The algorithm highlights how wind power utility, hydropower utility and transmission grid utility can be increased. In addition, wind curtailment is seen to decrease and no negative economic impact for the producers is observed [10, p.10].

Of the three studies [8]–[10], [9] is probably the most comprehensive. Organised by IEA, [9] is a collaboration between several countries, focusing on wind integration in a variety of electrical system configurations, hydropower configurations and market and operational configurations. In particular, case studies analysing the benefits, feasibility and costs of specific wind-hydro projects have functioned as a driving force for the collaboration [9, p.2]. The results from the different projects show that incremental impacts of wind integration are usually best handled by utilising the entire power system, and not isolated to a single hydropower plant. Moreover, the impact of non-power constraints in the hydropower system, e.g. environmental regulation, is not found to impact wind integration substantially, due to these constraints often occurring on different system operation time scales than the wind integration. The collaboration concludes that the flexibility of hydropower generators and the potential energy storage in reservoirs make hydropower well suited to integrate wind power [9, p.14].

2.4 Dynamic Line Rating

Another technology that can provide an increment in grid utilisation and improve the wind power integration is DLR, also known as dynamic thermal rating and real time thermal rating. DLR is a technology that enables a dynamic increase of the ampacity in overhead transmission lines [52]–[55]. Ampacity, or ampere capacity, is defined as the maximum constant current that still meets the design, security, and safety criteria of the transmission line. Consequently, an increase in ampacity will give a higher allowed maximum current and therefore a higher transmission capacity. Since the ampacity is dependent on environmental conditions, e.g. ambient temperatures, DLR is based on online monitoring of several parameters employing sensors and weather forecasts [53, p.1713] [52, p.1]. Moreover, DLR adjusts the line rating to ensure that the current limit is adjusted to the ampacity, providing better utilisation as the operation is able to occur close to the maximum state. Furthermore, DLR can benefit the security and safety of the line, as one is able to detect periods where the ampacity should be reduced below the designed amount [52, p.13]. The applications and benefits of DLR are many, and ultimately they are believed to ultimately give lower consumer prices, postponement in grid expansions and rapid integration of distributed energy resources [55, p.9].

Even though DLR is believed to improve many aspects of the power grid, it is not very commonly used. The usual approach is to use the Static Line Rating (SLR), which is a transmission capacity based on worst-case combinations of environmental parameters [52, p.1]. SLR is used as it is a simple and applicable solution, but it does not fully utilise the grid capacity. Often, DLR can provide considerably higher capacity compared to SLR, due to environmental conditions usually being better than the conservative values used for estimating the SLR [52, p.2] [53, p.1713]. Nevertheless, DLR has been downgraded, as its variability and the need for accurate forecasting and real-time measurements makes DLR particularly difficult to exploit. This poses a challenge, as maintenance of

sufficient electrical safety margins, avoidance of premature conductor system aging and determination of DLR with high instrument reliability are all vital for public safety [54, p.921] . In addition to the operational procedures that are required, DLR can challenge existing legal framework, which then must be remedied [53, p.1729].

However, DLR operational issues are subject that have been thoroughly studied in recent years, as a means to facilitate the implementation of DLR [53, p.1713]. This has led to the advent of new sensor and measurement methods for the environmental parameters required to calculate the DLR. These are found to be accurate, reliable and relatively inexpensive; measuring weather, transmission-line sag tension and conductor temperature [54, p.921]. In addition to real-time sensors, forecasting comprises a central part of DLR. As the power market is organised in a day-ahead structure, see Section 2.5, the grid companies need to know the transmission capacity of their system in advance. Forecasting of DLR follows the same approach as forecasting of VRES, utilising a mix of statistical methods and meteorological forecasts [53, p.1714]. The forecasting will then enable the grid company to consider and offer transmission based onDLR. Still, forecasting provides an element of uncertainty, providing an additional need for real-time sensors as a foundation [54, p.927].

When the various environmental parameters are acquired, the ampacity and rating itself can be estimated. However, there are many different methods used for estimating the DLR [56], [57]. In [56], Black and Chisholm organise and describe a number of these approaches. The main difference is found to be what kind of environmental parameters the different approaches depend on. Here, it is seen that DLR calculations based on weather data and estimates from direct measurement of conductor temperature have similar performance as predictions of conductor-to-ground clearances for DLR systems [56, p.2160]. Furthermore, pole inclination, which is a monitoring method that establishes conductor conditions on the basis of the temperatures at the vertical hanging insulators at each line pole, is highlighted as a promising new approach for DLR [56, p.2161].

Where [56] gives an overview of different methods for estimating DLR, [57] provides an in-depth study of how a Phasor Measurement Unit (PMU) can be utilised to achieve on-line voltage and current phasors for estimating DLR. Here, Du and Liao [57] outline the procedure to obtain the required parameters from the PMU measurements. Firstly, the phasors are used to derive the line parameters series resistance, reactance, and shunt susceptance. This is shown for several different transmission network configurations. In all cases, the principles of Kirchhoff's voltage and current laws [58] are used on equivalent circuits of the transmission configurations to achieve a set of real equations that can be solved to obtain the wanted line parameters [57, p.41]. The average line temperature is then estimated by utilising the calculated series resistances. Next, conductor sag of the selected span can be calculated accordingly, exploiting known mechanical properties of the overhead line for different temperatures. Lastly, the obtained line temperature and conductor sag can then be used for DLR and other power system reliability and safety measures. Presented numerical cases studies indicate that the utilisation of PMU is a good method for DLR calculations [57, p.44].

2.5 The Norwegian Power Market and Power Agreements

As described in Section 2.1, the Norwegian power sector is regulated by the Energy Act [14]. Here a market-based power trading principle is incorporated. The Norwegian power market is today part of a common spot market for the Nordic countries, called Nord Pool [59]. In Nord Pool, power producers and consumers bid in a day-ahead spot market, Elspot, determining power prices through a double auction [60, p.103]. The central counter party is called Nord Pool Spot and guarantees settlement for trade. When the market price on Elspot is unconstrained it is called the System Price. The System Price is the ideal power price and it works as a reference price for the financial trade in the Nordic market [60, p.104]. Different partakers and cash flows in the Norwegian power market are further explained in Section 2.5.1.

In addition to partaking in the spot market, there can, for large participants, be traded directly between producers and consumers. Such an arrangement is often called a Power Purchase Agreement (PPA) [61, p.9], and is a bilateral agreement. PPAs are elaborated upon in Section 2.5.2. Furthermore, there is a market between the TSO, being Statnett in Norway, and the other participants in the power system. This market is called the Regulating power market and aims to provide the TSO with measures to keep the power system stable. Here, the TSO is the only buyer, while producers, consumers and grid companies can all sell services to help with stability issues [60, p.276]. These services are called ancillary services and is discussed further in Section 2.5.3.

2.5.1 The Norwegian Power Market

The Norwegian power market can be divided into three main actors who each corresponds to one of the main parts in the power system. These three actors, who correspond to production, transmission, and consumption respectively, are power producers, grid companies and end consumers. In addition to the three participants mentioned, there are actors who function as links between the different parts of the market. The two most notable amongst them are Nord Pool and electricity retailers. As mentioned in the previous section, Nord Pool is the power exchange for the Nordic countries, and the spot-price of electricity is settled here. Electricity retailers are the links between end consumers and the rest of the market, providing power to consumers and dealing with grid companies and power producers. [60, p.102]

Since there are many different parts and partakers in the power market, a variety of cash flows exists. Figure 5 shows a schematic overview of the main actors in the market and the cash flows that are going between them. At the consumer's end of the market there are two main flows. First, there is the electric bill a consumer pays to a retailer. The electric bill is usually divided into three main parts that are approximately of the same size [62]. These parts are payment to the electricity retailer, grid rent [63] and taxes. The retailer pays the grid rent directly to the grid company, while the price of power is paid indirectly to the power producer through the power exchange. Second, there are power purchase agreements, which go directly from consumer to producer. The power purchase agreement is not a cash flow in itself, but it generates a cash flow from consumer to producer according to the terms of the agreement. At the producer's end of the market there is a tariff called the feed-in tariff, which is what the power producers pay to the grid companies for having their production transferred to consumers [64]. The feed-in tariff consists of an energy term, which represents the marginal cost of losses in the grid connection, and a tariff term based on average annual production. Depending on the marginal cost of losses, the feed-in tariff can be both positive and negative. In other words, the power producers might end up being paid by the grid

company for sending power onto the grid if it reduces the grid losses. Lastly, there are ancillary services. Similar to the power purchase agreement, ancillary services are not cash flows as such. However, ancillary services generate cash flows from grid companies to power producers based on the service the producer provides.

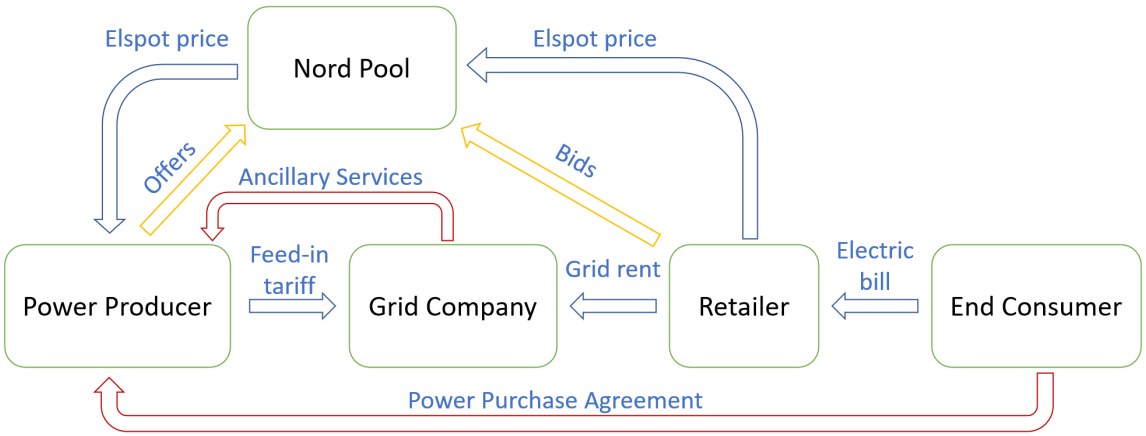

Figure 5: A schematic overview of the Norwegian power market and how the different partakers interact. Here, the blue arrows represent cash flows, the yellow arrows represent communication flows and the red arrows represent power agreements.

2.5.2 Power Purchase Agreements

As mentioned, a PPA is a bilateral agreement between a power producer and a power consumer. Traditionally, it has been an agreement that settles a fixed power price between producer and consumer over several years combined. Moreover, it is typically producers with large upfront investment costs, such as wind producers, that are motivated to sell a PPA, due to it providing a stable income stream over several years. In other words, selling a PPA secures a buyer for the production of the producer over a long time period. On the buyer side, large consumers, e.g., heavy aluminium industry and data centres, are located. These are often motivated by hedging of prices, having such a large consumption, as well as securing a renewable business profile. [61, p.9]

A PPA often contains contractual specifications regarding agreement type, price, duration, profile of volume, balancing responsibility and energy attribute certificate ownership [61, p.19]. They can vary significantly, due to market participants having different risk profiles. Typically, the main variations relate to the contract's duration and how power is delivered. Otherwise, the contract elements tend to be similar. Most PPAs in Norway have a fixed price and are physical contracts [61, p.10]. The fixed price usually has the future market price as a starting point, but ends up being less than the expected spot price, since it has a negative risk premium [61, p.20]. Physical agreements denote that the producer feeds its production into the grid while the corporate consumer covers its consumption from the power grid. In other words, it is an agreement involving a physical flow of power [61, p.19].

The use of PPAs has become increasingly popular in recent years, which has resulted in new variations of PPAs. These are often divided into two categories, namely new corporate PPAs and utility PPAs. The new corporate PPAs are specific agreements between a developer of a renewable

production project, typically wind or solar, and a corporate consumer. In contrast, utility PPAs are agreements between a producer and a grid company. Moreover, there is no direct connection to the consumer. Instead, the utility company is distributing the power and can therefore chose to sell the power retrieved from the producer at market spot price. Some of the utility PPAs can be used by utility companies to secure ancillary services [61, p.14].

2.5.3 Ancillary Services

Ancillary services are services that secure the power system quality. Moreover, it enables the System Operator to maintain security of supply, constant voltage levels, voltage stability and frequency stability [60, p.275]. As previously mentioned, the System Operator is normally the single buyer of ancillary services, while both producers, consumers and grid companies can sell services. In the Norwegian system, the ancillary services are divided into two main types, namely balancing reserves and system services. The balancing reserves are divided into primary, secondary, and tertiary reserves. Primary reserves have a time response of mere seconds and are based on automatic control. This is used to provide frequency control reserves and contingency reserves. In contrast, the secondary and tertiary reserves in the Norwegian system are activated manually. Here, secondary reserves comprise the fast portion, and tertiary reserves comprise the slow portion of the manually activated reserves [60, p.280]. The Norwegian System Operator has demand of secondary reserves being operational within 15 minutes, while the tertiary reserves are provided on the Balancing Market and Reserves Options Market [60, p.281]. Further, the system services are divided into load following, system protection and reactive power, which is also called voltage control. System protection is again divided into grid splitting, load shedding and production tripping. All system services are required to have a time response of minutes. Some are manually activated, while others have either automatic voltage or frequency control [60, p.280].

One of the most important aspects of ancillary services is how it provides flexibility to the power system, as it improves the power system's ability to handle fluctuations and unforeseen events. Boscan and Poudineh [65] review in their study how the operational flexibility and its associated business models, focusing on short-term flexibility services, have evolved and introduced new roles in the power market. They define flexibility as the ability of power systems to utilise their resources to manage net load variation and generation outage, over various time horizons. Here, net load is defined as the power load minus power production from intermittent sources, e.g. VRES [65, p.364]. Boscan and Pudineh [65] highlight that a new set of entrants are coming to participate in electricity markets, pushed by the flexibility demand from increasingly intermittent energy production. A concept that is underlined in [65] is prosumers. Prosumers are defined as consumers that play an active role on the supply side. This is a type of demand-side management and is highlighted together with storage, interconnection between power systems and distributed generation to be ways to manage intermittent power production and provide ancillary services to a power system [65, p.365].

3 Methodology

In order to analyse the wind curtailment of a wind power producer connected to the grid with terms of production restrictions, a local energy balance was simulated in Python [66]. The simulation model is based on the work of Korpås [51], with some changes to suit the scope and motivation of this thesis. Furthermore, an optimisation model, aimed to improve grid utilisation and minimise wind curtailment and reservoir flooding, is developed in the open-source Python-based software package Pyomo [67]. In addition, DLR is implemented in both models to achieve a technical perspective of grid utilisation. Lastly, economical equations are utilised to enable an economical analysis of the different operational patterns that are generated. Figure 6 shows the overall calculation flow of the methodology, highlighting the needed data, the resulting power production of producers in the studied system, as well as the different regulations that are functioning. The calculations in the simulation and optimisation models are elaborated upon in the following sections.

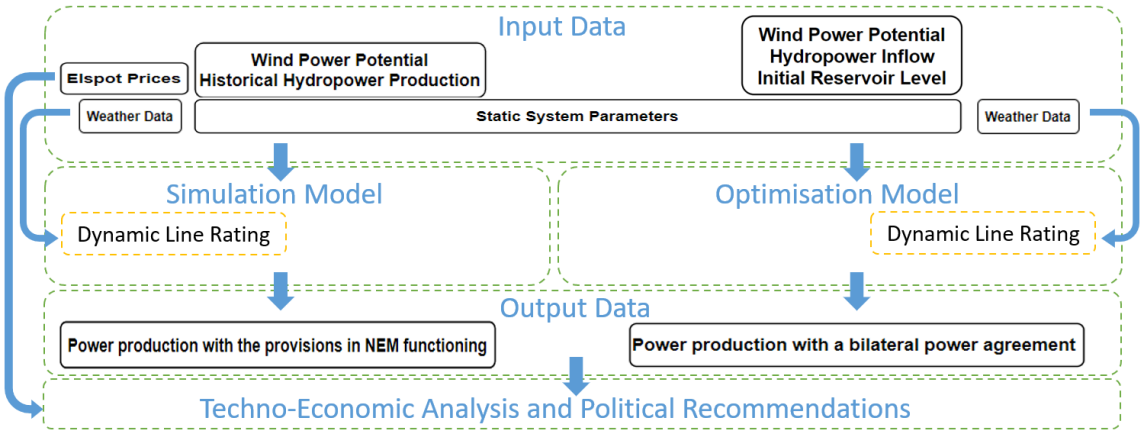

Figure 6: Flow chart of the overall calculation flow in the methodology. The DLR is an expansion of the original models, which is indicated by orange frames.

3.1 Data Collection

Both the simulation and the optimisation models require time series of wind power potential, in the area of interest, to function. Furthermore, Figure 6 underlines that both models need system parameters, which is a necessity to capture the physical properties of the system. System parameters refers to technical data of the different power plants as well as the transmission capacity of the limiting transmission line. All the remaining input data that is required is not shared by the models. The simulation model needs time series of historical hydropower production, while the optimisation model requires the initial reservoir level and the inflow to the reservoir throughout the analysed period.

All the required data of the system area and the input time series was provided by the Norwegian energy group Nordkraft [68]. The hydropower inflow and historical production are measured data from Nordkraft's own facilities for the years 2011 to 2015. However, some modifications and simplifications were done to highlight the focus of this thesis, as well as adapting to the case study.

An elaboration can be found in Section 4.1.1. Furthermore, measured reservoir levels were also provided by Nordkraft for the same period. This is not a necessity for the models, but it was decided to be utilised in order to get a reservoir trajectory in the simulation plot. Moreover, the measured reservoir levels increase the basis of comparison between the simulations and optimisations. Where the mentioned time series and most of the system parameters could be used directly, the data regarding the transmission line needed to be altered. Transmission capacity is sensitive information and therefore kept confidential.

Unlike the hydropower data, which are measurements, the wind power potential is based on estimations done by Nordkraft. When estimating potential wind power production of a wind farm, there are many different approaches. A common method used in several studies [69], [70], is to reduce the wind farm to an equivalent wind turbine and use a wind turbine model on the equivalent turbine to investigate the properties of interest. For example, Feijóo and Cidrás [69] highlight that a wind farm containing only one type of turbines can be combined to one machine. In addition, the power output, as function of wind speed, can be calculated in one iteration for constant wind speed. When having varying wind speed, due to wake effects, a wind speed estimation must be included. Moreover, Wu *et al.* [70] accounts for wake effects in their study, by using the average wind speed in the wind farm on a reduced equivalent representation of the farm. Another approach, used by Korpås [51], is to find the potential power output from one wind turbine by utilising the power curve of the wind turbine, like Figure 3, together with weather data. Afterwards, the power production is scaled according to the total installed power capacity of the wind farm. The wind power potential time series provided by Nordkraft were estimated in a similar manner as the method utilised by Korpås [51].

In order to calculate the DLR time series, several series of ambient temperatures and wind speeds in the area are needed. The ambient temperatures were provided by Nordkraft, who had aggregated the temperatures from a nearby weather station to be applicable at the altitude of the transmission line. The wind speeds were retrieved from the Norwegian Centre for Climate Services (NCCS), by choosing mean wind speed, with an hourly resolution, measured at the nearest weather station in the period between 2011 and 2015 [71]. NCCS is a collaboration between the Norwegian Meteorological Institute, NVE, the Norwegian Research Centre and the Bjerknes Centre that provides historical weather data from weather stations in Norway [72]. As such, NCCS is found to be a credible source.

Lastly, Elspot prices during the analysed period are needed in order to conduct the economic study of the simulation and optimisation results. This was retrieved from Nord Pool's historical area prices of Norway [73]. Here, a time series of hourly Elspot prices for 2011 to 2015 was found. Since the case study described in Section 4 is of an area in Northern Norway, the Elspot prices in Tromsø was found to be most applicable.

3.2 Simulation of Grid Regulation

As seen in Figure 6, the simulation is designed to replicate the operation pattern set by the grid regulation in NEM, mentioned in Section 2.1. Moreover, it replicates how grid utilisation and integration of VRES are affected in the studied area, further described in Section 4. Specifically, it is assumed that the system's hydropower plant has grid connection according to old regulations, while the wind power plant has connection on terms of production regulation, in accordance with NEM. Consequently, the wind power producer is obliged to downregulate its production for the benefit of the hydropower producer.

Several studies that focus on the simulation of wind integration and how unregulated wind power can lead to potential production losses, have been performed over the years. For example, Jorgenson *et al.* [47] simulate the impact different transmission grid and energy storages have on wind curtailment. They carried out the study by formulating an optimisation problem, which minimises the sum of fuel, start-up and shutdown, variable operation and maintenance cost, in the energy software PLEXOS [74]. Their model, like other studies investigating wind power complemented by energy storage [49], has a slightly different scope than the simulation in this thesis. The minimisation of cost is only indirectly highlighting wind curtailment, which is the purpose of the simulation model developed in this thesis. Moreover, a flow-based market model [44] is redundant, as the terms for connection with production regulation in NEM give all existing producers the first right to transmission capacity.

Two of the studies reviewed in Section 2.3.4, [50] by Farahmand *et al.* and [51] by Korpås, were found to be especially relevant for this thesis as they look closely at the correlation between wind power and hydropower, and how it can improve the utilisation of the power system. In [50], Farahmand *et al.* use an interconnection between a market model and a flow-based model to simulate the power flow in predicted scenarios of the power system in Northern Europe. Here, the result from the market model is used as a basis for the flow-based simulation, which uses DC Optimal Power Flow (DC OPF) to find an optimal generation dispatch and transmission flow. In [51], Korpås applies a local energy balance in an area of Northern Norway, finding the amount of lost power production that occurs with and without the utilisation of hydropower flexibility.

Based on the fact that the motivation and focus of this thesis deal with wind power curtailment in congested power systems, among other things, the model used by Korpås [51] was found to be an appropriate starting point. Moreover, the model used by Farahmand *et al.* [50] has a different approach than the intended method for this project, with regard to wind curtailment. Their use of optimal generation dispatch and operational cost minimisation is an indirect way of observing curtailed production, as it is more of an economic perspective. In contrast, [51] examines the production itself to then comes up with financial considerations. Consequently, the wind curtailment is observed explicitly.

The local energy balance used by Korpås [51] takes both wind power production, $P_{w,t}$, hydropower production, $P_{h,t}$, import, $P_{import,t}$, and export $P_{export,t}$ in the studied area into account, and controls that the transfer capacity in the limiting transmission line, P_{line}, is not exceeded. The studied area consists of two power producers, a hydropower plant and a wind farm, and a local load, $P_{local\ load,t}$. In addition, the system includes a transmission line for export and import abroad, other regional hydropower producers, $P_{regional\ hydro,t}$, and a transmission line for domestic power transfer. Furthermore, it is assumed that if the transmission line becomes congested, the wind power is downregulated. The amount of downregulated wind is then accounted as wind power curtailment, $P_{curtailed\ wind,t}$. Similarly, flood losses for the hydropower, $P_{flood\ loss,t}$, are also counted as lost energy. Korpås' model [51] has the following balance equation and curtailment equation:

$$P_{line} \geq P_{h,t} + P_{w,t} + P_{import,t} - P_{export,t} - P_{local\ load,t} + P_{regional\ hydro,t} \tag{6a}$$

$$P_{curtailment,t} = P_{curtailed\ wind,t} + P_{flood\ loss,t} \tag{6b}$$

Here, the curtailed wind power equals the difference between potential and produced wind power, while the flood loss is the amount of power the spilled water could have produced. All terms denoted

with the subscript t are time series of discrete values and are evaluated in time step t. The model assumes that AGC is used to keep the power flow within the maximum transmission capacity. As described in Section 2.2.1, AGC automatically downregulates the local power production when transmission capacity is reached [51, p.6].

When Korpås' model is adapted to fit the area studied in this thesis, the red terms in Equation (6) become irrelevant. Moreover, the red terms in Equation (6a) are removed as local loads in the case study are deemed negligible. Consequently, there is no power importation to the studied area. In addition, there is only one transmission line in the chosen system, making the export term superfluous according to the definition used in [51]. The flood losses in Equation (6b) are also excluded, due to the assumption that the hydropower plant is connected in accordance with old regulations. This implies that the hydropower plant always has sufficient grid capacity available and enables hydropower operation according to the historical production data. In other words, any flood losses will occur regardless of the wind production. Therefore, flood losses during simulation are peripheral to this thesis. The model then reduces to the following:

$$P_{line} \geq P_{h,t} + P_{w,t} \tag{7a}$$

$$P_{curtailment,t} = P_{curtailed\ wind,t} \tag{7b}$$

The set of Equations (7) can again be reduced to a single concentrated energy balance equation:

$$P_{curtailment,t} = max\left(0, P_{w\ pot,t} - [P_{line} - P_{h,t}]\right) \tag{8}$$

In the simulation model, one simulation spans over a year and has a time resolution of one hour. The input data to the model is time series of hourly production potential for the wind farm, along with historical hydropower production. Moreover, the historical hydropower data is the production the hydropower producer would have if all wind power production in the system is disregarded. This includes ignoring the occurrence of congestion in the transmission line. Furthermore, the historical hydropower data function as planned production for the hydropower plant. For the simulation, actual production, $P_{hydro,t}$, becomes equal to planned production, due to the grid connection regulations that are assumed to be functioning. In other words, the hydropower production becomes a parameter rather than a variable. In contrast, wind power production is a variable that depends on the input parameter wind power potential. Explanations of the different terms in the local energy balance can be found in the nomenclature in Table 2.

Furthermore, transmission capacity, installed wind power capacity and installed hydropower capacity are parameters that must be given to the model. Since the simulation is investigating the impact of having wind power connected on terms of production restriction, hydropower production is prioritised. Consequently, the wind power producer only has the opportunity to produce and transfer, at a maximum, an amount equalling the difference between the transmission limit and the hydropower production, as stated in Equation (8). A flowchart of the simulation model's behaviour is depicted in Figure 7, highlighting the logic being used. The model iterates through Equation (8) for a whole year and calculates the power production for the studied system when the provisions of NEM are functioning.

In [51], Korpås implements his simulation model in the software and language MATLAB. However, as previously mentioned, the programming language Python is chosen as the basic language in this thesis. Python is an open-source programming language which is becoming increasingly popular in both academia and industry. Due to its robust standard library and various open source tools,

Python is a good choice for this thesis [66]. The energy balance from Equation (8) in the simulation model is thus calculated with arithmetic operations in Python.

Table 2: Nomenclature of the simulation and optimisation model. The left column presents the used symbol, the middle column presents an explanation and the right column presents the unit.

Sets		
$t \in T$	Set of hours in a time horizon T	h
Variables		
$P_{curtailment,t}$	Amount of total power lost in time step t	MW
$P_{w\ loss,t}$	Amount of wind power lost in time step t	MW
$P_{h\ loss,t}$	Amount of hydropower lost in time step t	MW
P_{step}	Optimal hydropower production increment for a certain reservoir level	MW
$P_{h,t}$	Hydropower production in time step t	MW
$P_{w,t}$	Wind power production in time step t	MW
$E_{res,t}$	Amount of water in the hydropower reservoir in time step t	MWh
Parameters		
$P_{w\ pot,t}$	Wind power potential in time step t	MW
$P_{inflow,t}$	Amount of water flowing into the hydropower reservoir in time step t	MW
$P_{h\ planned,t}$	Historical hydropower production in time step t	MW
$E_{res\ init}$	Initial amount of water in the hydropower reservoir	MWh
$P_{h\ max}$	Total installed hydropower capacity	MW
$P_{w\ max}$	Total installed wind power capacity	MW
$P_{h\ loss,max}$	Maximum amount of water the hydropower plant can release	MW
$E_{res\ cap}$	Total capacity of the hydropower reservoir	MWh
P_{line}	Transmission capacity of limiting line	MW
$C_{el,t}$	Elspot price set by Nord Pool in time t	NOK/MWh
$r,\ q$	Weights for pricing the different types of energy loss	-

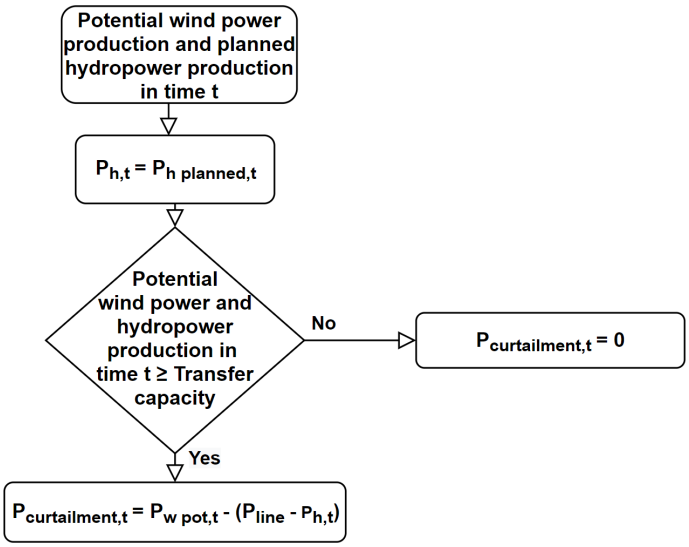

Figure 7: Flowchart of the simulation model's behaviour. The different parameters are explained in the nomenclature in Table 2.

3.3 Optimisation With a Bilateral Power Agreement

The optimisation model uses the simulation model as a starting point and optimises the production scheduling to minimise energy losses. Also, the losses that are considered are those connected to wind power curtailment and flooding of the hydropower reservoir. The flow chart in Figure 8 highlights the logic of the optimisation model throughout each iteration. As opposed to the simulation model, the wind power production is now prioritised for line capacity, and the model goes from losing excess energy, as wind power curtailment, to passively saving it in the hydropower reservoir.

To generate such an operational pattern in practice, power producers can enter into a power agreement. As opposed to the agreements mentioned in Section 2.5, this would be a direct agreement between producers. The outline of such an agreement could be that the hydropower producer agrees to downregulate its own production unless it generates unnecessary flooding of the reservoir. As a result, the optimisation model includes weights to enable regulation of how expensive the different types of energy loss are. In other words, the optimisation model is designed to enable different orders of transmission priority, which again enables a variety of solutions over the same time period.

Again, the study in [51] is found to be a natural starting point due to similarities in motivation and scope. Unlike the simulation model, which limited wind power, the optimisation model can decide to regulate hydropower production. Furthermore, having predetermined hydropower production in the simulation, Korpås now uses the historical hydropower time series as a basis and determines optimal hydropower production by including inflow to the system [51]. Consequently, the optimisation needs time series of inflow to the hydropower reservoir. Additionally, the optimisation model in [51] defines a hydropower increment parameter, P_{step}, to ensure optimal momentary change of hydropower production and avoid persistent high reservoir levels. This parameter is designed to increase hydropower production, when having extra transfer capacity available, if the total

hydropower production is less than the planned production based on historical data. The historical data is in [51] regarded as the optimal production scheduling for the hydropower plant, as it is production data prior to the inclusion of any wind power in the system. In other words, the historical production data is the unconstrained solution. Mathematically Korpås defines the use of the increment parameter as follows [51, p.6]:

$$\begin{aligned} &\textit{while } \sum_{i=1}^{t} P_{h,i} < \sum_{i=1}^{t} P_{h\ planned,i} \\ &\qquad P_{h,t} = max\left(P_{h\ planned,t} + P_{step},\ P_{h\ max}\right) \\ &\textit{end} \end{aligned}$$

Here, $P_{h,t}$ is the actual hydropower production in time t, $P_{h\ planned,t}$ is the historical hydropower production in time t and $P_{h\ max}$ is the total installed hydropower capacity. It should be noted that using a max function, as marked in red, is peculiar. Moreover, the current expression can potentially give a scheduled hydropower production that is larger than the installed capacity, which is not feasible. However, Korpås states later in the text that the installed capacity is the upper limit [51, p.7]. It is therefore found reasonable to believe that the max function should be a min function that chooses the smallest value.

Where Korpås [51] utilises an algorithm designed to determine optimal future power production, assessed on the basis of the past and present state of the system, it is here implemented an optimisation model that optimises the production over a historical time horizon. Consequently, only historical inflow data and wind power potential are needed. Moreover, it is the physical aspects of the system that are considered by the optimisation model in this thesis. The optimisation model will provide optimal power production scheduling over a time period where all input parameters are predetermined. In contrast, the optimisation model presented in [51] is applied to analyse the current state of the specified area and based on that determine the optimal future power production.

The resulting optimisation model in this thesis has only linear constraints and a linear objective function. It is therefore, per definition, a LP model [75, p.356]. LP is the most widely used optimisation concept, as it is suitable for use in many fields and possesses cutting edge software. Furthermore, the simplex method is the dominant method when solving LP models. A LP is usually written in its standard form, which is as follows [75]:

$$\begin{aligned} &\textit{Minimise} && z = c^T x \\ &\text{subject to} && Ax = b \text{ (linear constraints)} \\ &&& x \geq 0 \quad \text{(nonnegativity constraints)} \end{aligned}$$

Similarly to the standard form of LPs, the optimisation model used in this thesis is defined as stated below. Due to the local loads being neglected, the model does not include variables for import and export. Consequently, this model is only designed for power flowing out of the local area.

$$\textit{Minimise} \quad \sum_{t=0}^{T_{max}-1} (r \cdot P_{w\ loss,t} + q \cdot P_{h\ loss,t}) \cdot C_{el,t} \cdot \Delta t \tag{10a}$$

$$\text{subject to} \quad P_{w\ loss,t} + P_{w,t} - p_{w\ pot,t} = 0 \tag{10b}$$

$$E_{res,t} - P_{inflow,t-1} \cdot \Delta t - E_{res,t-1} + P_{h,t-1} \cdot \Delta t + P_{h\ loss,t-1} \cdot \Delta t = 0 \tag{10c}$$

$$P_{w,t} + P_{h,t} - P_{line} \leq 0 \tag{10d}$$

$$P_{h,t} - P_{h\ max} \leq 0 \tag{10e}$$

$$P_{w,t} - P_{w\ max} \leq 0 \tag{10f}$$

$$0.1 \cdot E_{res\ cap} \leq E_{res,t} \leq E_{res\ cap} \tag{10g}$$

$$P_{h\ loss,t} - P_{h\ loss,max} \leq 0 \tag{10h}$$

$$E_{res,0} = E_{res\ init} \tag{10i}$$

$$P_{h\ loss,t},\ \ P_{w\ loss,t},\ \ P_{h,t},\ P_{w,t},\ E_{res,t} \geq 0 \tag{10j}$$

It should be noted that some of the constraints are stated as inequality constraints, which is a deviation from the standard LP form. However, there are simple devices to transform such constraints to equality constraints. Furthermore, the model is still a valid LP, as linearity is not dependent on equality [75, p.356]. Additionally, a conversion of the inequality constraints was found unnecessary to perform, as the inequality constraints provide a more intuitive representation of the physical properties of the studied system.

As previously mentioned, energy loss minimisation is the objective of the model. This is given in the objective function represented by Equation (10a). The weights r and q are here included to enable pricing of the different energy loss types and thus provide a mean to implement the mechanics of a bilateral power agreement. An agreement will prioritise the production from one of the energy sources, which can be replicated by pricing the loss of the prioritised type to be more expansive than the other. Moreover, the LP model consists of equality constraints that define wind curtailment and the reservoir utilisation considering flooding and inflow. These constraints are represented by Equation (10b) and Equation (10c) respectively. Since $E_{res,t}$ has the energy unit MWh, the rest of the terms in Equation (10c), which have the power unit MW, are multiplied with the interval between each time step, Δt. Equation (10d) is the local energy balance used in the simulation model and is included to comply with the maximum transmission capacity. Furthermore, constraints regarding maximum power production and reservoir level limits are described with Equation (10e) to Equation (10g). The lower reservoir level limit is set to be equal 10% of the total reservoir capacity, as a measure to maintain the lowest regulated water level and thus sustain the local hydrological ecosystem. Equation(10h) represent the upper bound of the amount of flood losses that can occur in each time step. Without this constraint, the model could choose to release the entire amount of lost water in the time step with cheapest Elspot price, which is improbable. Lastly, the optimisation model consists of a condition determining the initial reservoir level, Equation (10i), and a non-negativity constraint, Equation (10j). Explanations of the different terms can be found in the Nomenclature in Table 2.

To solve the LP model developed in this thesis, the software package Pyomo was applied with the solver Gurobi. Pyomo is a Python software package that supports a diverse set of optimisation capabilities for formulating, solving and analysing optimisation problems [67]. Furthermore, Gurobi is a solver able to solve all major problem types, using different types of programming [76]. For LP, Gurobi applies a concurrent optimiser, exploiting multiple processors, to run primal and dual variants of the simplex method simultaneously [77]. The concurrent optimiser terminates when the first method completes, achieving a fast solution by pursuing different strategies simultaneously.

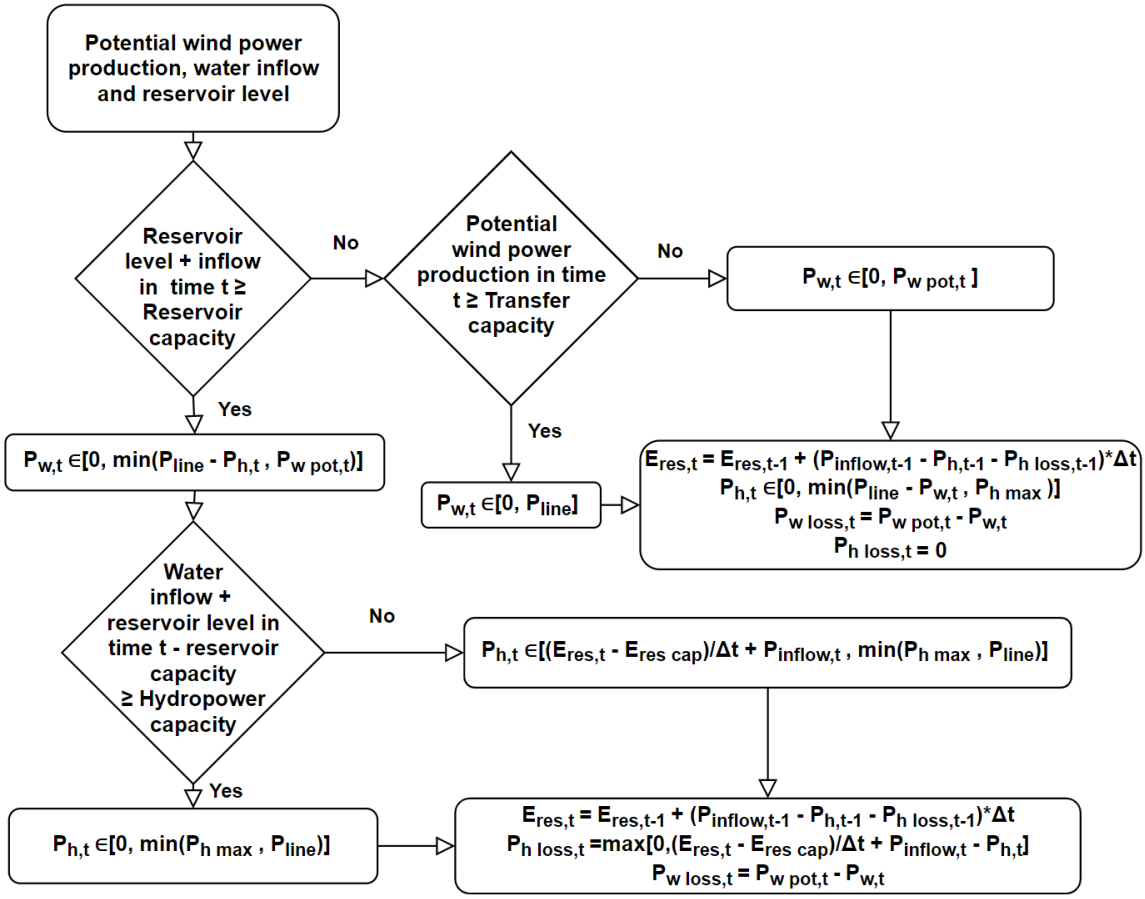

Figure 8: Flowchart illustrating the behaviour of the optimisation problem through one time step. Unlike the simulation model, the decision variables are chosen from a range, affected by how the energy losses are weighted. The different parameters are explained in the nomenclature in Table 2.

3.4 Implementing Dynamic Line Rating

The motivation of this thesis is to explore optimal grid utilisation. Therefore, a technical part is included, in addition to the studied regulations, to achieve a more complete perspective. This is done by running the simulation model and optimisation model with DLR. As mentioned in Section 2.4, DLR is a way to better operate and utilise transmission lines, making it a reasonable technical expansion for this thesis. The implementation is done by altering the transmission capacity, P_{line}, in Equation (8) and Equation (10d), from being the SLR to being the DLR of the transmission line in the studied system. In other words, the line rating goes from being a constant, P_{line}, in each time step to now being a time series, $P_{line,t}$, of different values in each time step.

There are several approaches calculating the DLR of a transmission line, as presented in Section 2.4. However, the technical part of the thesis is only intended to provide an overall view of another aspect of grid utilisation, as the main motivation and interest area is the revision of NEM. This, plus the available data, decided the chosen method for estimating DLR. The method is based on a given overview of the transmission line capacity, in the studied system, for different temperatures and wind speeds. By inserting ambient temperatures and wind speeds for the system, and interpolating with the different values in the overview, the time series of the DLR were estimated.

3.5 Economic Analysis

As seen in the overall flow chart, Figure 6, a techno-economic analysis is to be implemented on the output from the simulation and optimisation. In order to conduct such an analysis of the different regulations and their impact on the financial aspect of the system, some economic equations are needed. From the different cash flows in Figure 5, it is evident that the power producers' revenue is mostly generated from the Elspot price they receive on Nord Pool. The Elspot price is usually given on a money per energy amount basis, which is in NOK/MWh for the price zones in Norway. The revenue of power producers is therefore equal to their produced power times the Elspot price during production. Mathematically, this becomes as follows:

$$R_i = \sum_{t=0}^{T_{max}-1} P_{i,t} \cdot C_{el,t} \cdot \Delta t \tag{11}$$

Here, R_i is the revenue of power producer i, who produces the power $P_{i,t}$ in time step t. Since power has the unit W, the expression is multiplied with Δt in order to get the energy unit Wh, which corresponds to the Elspot price, $C_{el,t}$. The general subscript i is here used to highlight that this equation is applicable to all the different power producers in the studied system. Moreover, the equation can be used as a means to calculate lost revenue by inserting the amount of power lost in time step t.

4 Case Study

4.1 Reference Case

The system that is being used as a reference case in this thesis lies in the northern part of Norway and is a system scenario that is representative for many parts of the Norwegian power system. Figure 9 shows a schematic of the system with its, two generation units and a single transmission line. The first power unit, G1, is a hydropower plant with an installed capacity of $72MW$. Technical details of the hydropower plant is elaborated upon in Section 4.1.1. The second power unit, G2 is a wind farm. It has an installed capacity of $96.6MW$ and is further described in Section 4.1.2. As can be seen in the schematic, both generation units are connected to the same network bus. This is again connected to the external grid through a single transmission line. Furthermore, there are no noteworthy local loads. Therefore, power flow is assumed to only go in one direction, namely from the power producers to the external network.

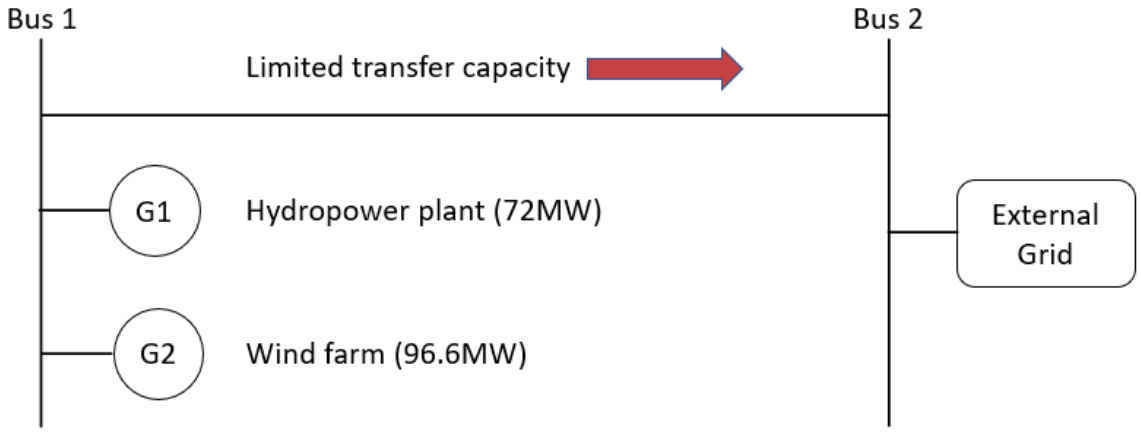

Figure 9: Schematic diagram of the studied system in Northern Norway.

4.1.1 Hydropower Plant

As shown in Figure 9, the area of interest contains a hydropower facility with an installed capacity of $72MW$. Moreover, the facility consists of a Francis turbine and reservoirs providing storage capacity. In addition, the hydropower plant has an intake for releasing water and avoid flooding, which bypasses the turbine. Specifications and technical data of the hydropower plant can be found in Table 3. The applied data are, as described in Section 3.1, provided from Nordkraft. However, some modifications and simplifications are done to the hydropower plant to achieve data in the form that is required by the different models in this thesis. Firstly, the original data, which were for a cascaded hydropower system, are aggregated to a single hydropower plant and reservoir. This is done by summing up the installed capacity of the hydropower turbines and scaling the historical production data accordingly. The turbine is assumed to be located at the same place as the largest original turbine. Furthermore, the reservoirs are combined into a single reservoir stationed at the location of the largest original reservoir. Both locations are found to be reasonable choices due to the largest entities of each type being considerably larger than the rest.

In order to find the equivalent reservoir capacity in amount of energy stored, the storage capacity of each reservoir is scaled to a value consistent with the height of the chosen location for the aggregated reservoir, namely at the height of the largest original reservoir. The constant used for the scaling is found by assuming that the only different property of the reservoirs is the net head, due to different altitude levels. From Equation (2), one sees that the net head is directly proportional to the power potential. As a result, the energy storage capacity contribution of the lesser reservoirs to the main reservoir, when aggregating the hydropower system, is calculated as follows:

$$E_{minor\ reservoir} = E_{major\ reservoir} \cdot \left(\frac{altitude\ minor\ reservoir}{altitude\ major\ reservoir}\right) \cdot \left(\frac{V_{minor\ reservoir}}{V_{major\ reservoir}}\right)$$

The last parameter that must be calculated is the maximum amount of water the aggregated hydropower can release through its bypass intake. This is done by utilising Equation (2). Consequently, the value that is derived will be the amount of power the released water represents. Similarly to the other calculated values in the aggregated facility, the maximum amount of released water is based on the properties of the largest plant in the cascaded system. By inserting the values given from Nordkraft into the calculations and adding up the different values, the aggregated hydropower plant receives an installed capacity of $72MW$ and a reservoir capacity of $97.02GWh$. Moreover, the maximum amount of released water the bypass intake can sustain becomes $67.74MW$. These values are utilised in both simulations and optimisations during the calculations.

Table 3: Technical data for the aggregated hydropower plant.

Parameter	**Value**
Installed power capacity	72MW
Total reservoir capacity	$97.02GWh$
Gross head	$486m$
Maximum absorption capacity	$15m^3/s$
Maximum bypass capacity	$67.74MW$

When simulating and optimising the aggregated hydropower plant, two time series are needed as input. First of all, historical hydropower production is required as a basis for the simulation. Secondly, inflow is needed for the optimisation model to determine the optimal scheduling of the hydropower plant. Both time series span over a whole year and have a resolution of one hour. The time series were acquired by Nordkraft and adapted to the aggregated hydropower plant by scaling with the ratios of installed power and reservoir capacity of the aggregated hydropower system compared with the original hydropower system. Furthermore, by assuming that the inflow is equal for each hour of a week, the inflow time series were enhanced from having a resolution in weeks to having a resolution in hours. In addition to the time series, physical parameters of the system, as described in Section 3, are required to constrain the models and ensure realistic results. These were again provided by Nordkraft.

4.1.2 Wind Farm

The studied wind farm consists of 23 wind turbines of the type Siemens Gamesa 4.2 DD 130. This constitutes a total installed capacity of $96.6MW$, and an expected annual production of $325GWh$. The Siemens Gamesa 4.2 DD 130 has a flexible power rating in the range $3.9 - 4.3MW$ and can

have heights of 85m, 115m, 135m or site-specific. Furthermore, the rotor has a diameter of 130m [78]. For the studied wind farm, the turbines are installed on towers with a height of 80 meters, indicating utilisation of site-specific towers.

In order to run the simulation and optimisation models, a time series of the wind power potential at the wind farm is needed. This was again provided by Nordkraft, who had estimated hourly power potential at the wind farm's location by combining local weather data with the power curve of the wind farm, similar to the curve in Figure 3.

4.1.3 Transmission Line

Another parameter required for the simulation and optimisation models is the transfer capacity of the transmission line between the generation units and the external grid. The line is a $19km$ three-phase overhead line with a line voltage of $132kV$. Due to transmission capacity being sensitive information regarding the power system, and therefore confidential, a general value was chosen. For the calculations in this thesis, a transmission capacity of $140MW$ was used. This is a value below the total installed power capacity in the system, giving rise to the risk of congestion. In other words, the transmission capacity is insufficient for maximum power production, which is the same scenario as NEM allows. Furthermore, it is assumed that the power system beyond bus 2, the external grid, always has enough demand to consume the power produced by the generation units in the local system. This assumption is motivated by the scope of this thesis, being an investigation into grid utilisation and wind power curtailment when having insufficient transmission capacity. Since there are no notable local loads in the system, the power flow is always going from the power plants at bus 1 to the external grid at bus 2.

4.2 Grid Regulation and Power Agreement

As mentioned in Section 3, the models in this thesis are designed to highlight the operational patterns imposed by NEM and a bilateral power agreement between power producers. For the simulation model, which completely adheres to the provisions for grid connection on terms of production restriction, the studied system is influenced to let the aggregated hydropower plant have transmission priority. Moreover, the wind farm is obliged to reduce its production when the transmission capacity is insufficient. In the optimisation model, the wind power producer has entered into a bilateral power agreement with the hydropower producer. Due to this, the situation has now been reversed as compared to the operational pattern in the simulation model. The bilateral power agreement enables the wind power producer to have transmission priority, while the hydropower utilises its reservoir for flexible operation. Furthermore, the agreement is assumed to include provisions for the hydropower producer to reacquire the transmission prioritisation when the risk of reservoir flooding is present. This assumption is based on the fact that the hydropower producer originally has the claim to transmission. As a result, the pricing weights in the optimisation model are set to $r = 1$ and $q = 10$, to encourage the model to prevent flood losses at the expense of wind curtailment.

5 Results

5.1 Reference Case

5.1.1 Simulation of Grid Regulation

Simulations of the system described in 4.1 were conducted to achieve the power production scheduling that occurs when only the provisions in NEM are active. By utilising the data from Nordkraft, simulations of the reference case were conducted for the years 2011 to 2015. The result of 2014 is shown in Figure 10, being a result that is representative for the whole analysed time period. Here one can see that with the reference data and the given measured time series, the sum of produced wind and hydropower exceeds the transmission capacity of the transmission line at several points in time. In other words, there are periods when the wind power producer is required to reduce production in order not to exceed the transmission capacity. When such congestion occurs, wind curtailment appears.

Furthermore, it is evident from the reservoir level trajectory in Figure 10 that the occurring losses are only affecting the wind power producer, due to the reservoir levels not breaching 100 percent. It should be noted that the seemingly odd pattern of the reservoir level trajectory at the beginning of May, is due to insufficient plot resolution. The power production vacillates at such a high frequency that the hydropower production is not visible from the plotted perspective. However, a plot specifically zoomed in on the beginning of May shows that there is hydropower production present, which justifies the trajectory of the reservoir level. The mentioned close-up plot can be seen in Appendix A.1.

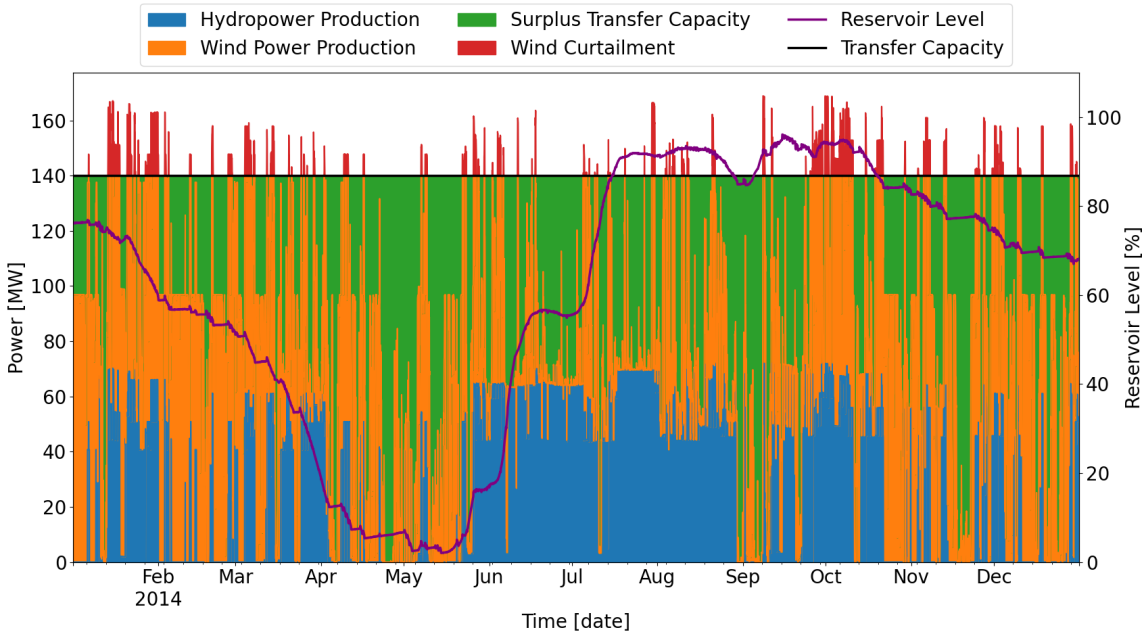

Figure 10: Simulation results with time series of 2014, highlighting power production, reservoir levels, wind curtailment and available transmission capacity throughout the year.

As previously mentioned, the result shown in Figure 10 is an operational pattern that is representative for all the simulated years of the system. However, to display the utilisation of all data acquired from Nordkraft, different parameters and values from each simulation were derived. The average of these values can be found in Table 4. It is evident from both the plot and the table that a major part of the transmission capacity is left unexploited. Furthermore, even though 45.79% of the transmission capacity is unused, the wind producer still experiences an annual energy loss of $16.41GWh$ in average. This comprises 4.20% of the total wind power potential of the studied wind farm. By utilising Equation (11) on the different variables in the simulation, the listed cash flows in Table 4 are found. As such, it can be seen that the wind power producer experiences an annual revenue loss of $4.67MNOK$ on average due to wind curtailment. This equals approximately 4.59% of the total annual revenue of the wind power producer. In contrast, the hydropower producer does not have any power loss and therefore no revenue loss.

Table 4: Average annual results from simulations with SLR and time series of 2011 to 2015.

Parameter	Value
Energy loss	16.41 GWh
Wind curtailment	16.41 GWh
Revenue loss from curtailment	4.67 MNOK
Revenue from wind power	101.72 MNOK
Revenue from hydropower	76.87 MNOK
Wind power potential	389.61 GWh
Hydropower production	292.01 GWh
Wind power production	373.20 GWh
Transmission Surplus (SLR)	561.58 GWh [45.79%]
Amount of lost wind potential	4.20 %
Curtailment frequency	1137.2 times per year
Grid utilisation (SLR)	54.24 %

Since integration of VRES is one of the major focus areas of this thesis, a separate plot for the wind power curtailment is shown in Figure 11. As described in Section 2.3.4, wind power curtailment is a frequent challenge in systems trying to integrate large amounts of wind power. Furthermore, it is evident in Figure 11, that the studied system experiences wind power curtailment every year. It can also be seen that the wind power curtailment follows a seasonal pattern, occurring more frequently in the autumn and winter months in Norway.

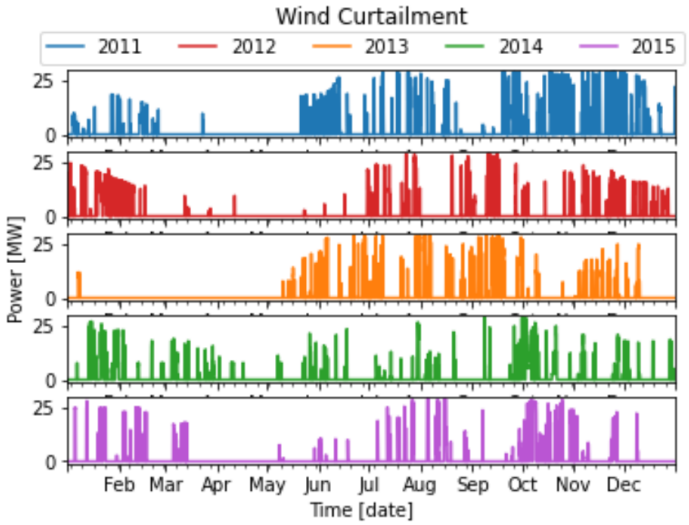

Figure 11: Wind power curtailment experienced in the reference system throughout the year when simulating with time series of 2011 to 2015.

5.1.2 Optimisation With a Bilateral Power Agreement

After the simulations were conducted, the reference system was optimised using the same time series in the optimisation model as in the simulation model. Here the system is regulated with a view to replicate an operational pattern induced by having a bilateral power agreement between the power producers in the area. The optimisation result of 2014 is shown in Figure 12 and it is representative for the whole analysed time period. Now all wind power curtailment has been eliminated, having shifted the hydropower production to time periods in which the wind power potential is low. Furthermore, the low levels of the reservoir level trajectory indicate that there is no flooding throughout the year. It is also evident that the transmission surplus, the green area of Figure 12, has decreased compared to Figure 10. In other words, the grid utilisation has increased for the optimised power schedule. It should be noted that the seemingly odd pattern of the reservoir level trajectory at the end of June is due to insufficient plot resolution, like the trajectory in Figure 10. The same is evident for the start of May and the end September. However, close-up plots of the mentioned periods substantiate the reservoir level trajectory. They can be found in Appendix A.2.

As with the simulations, several parameters and values from the optimisations were extracted in order to highlight the utilisation of the whole data set and result from the whole time period. These values are shown in Table 5, being the average values of the five optimised years 2011 to 2015. Both Table 5 and Figure 12 exhibit an increment in grid utilisation. The transmission surplus has decreased from comprising 45.79% of the total transmission capacity to now comprising 44.78%. However, the grid utilisation increment does not equal the lost wind power production in the simulation. The hydropower producer has a decrease in annual production of $4.05GWh$, which reduces the effect the $16.41GWh$ increment in annual wind power production has on grid utilisation.

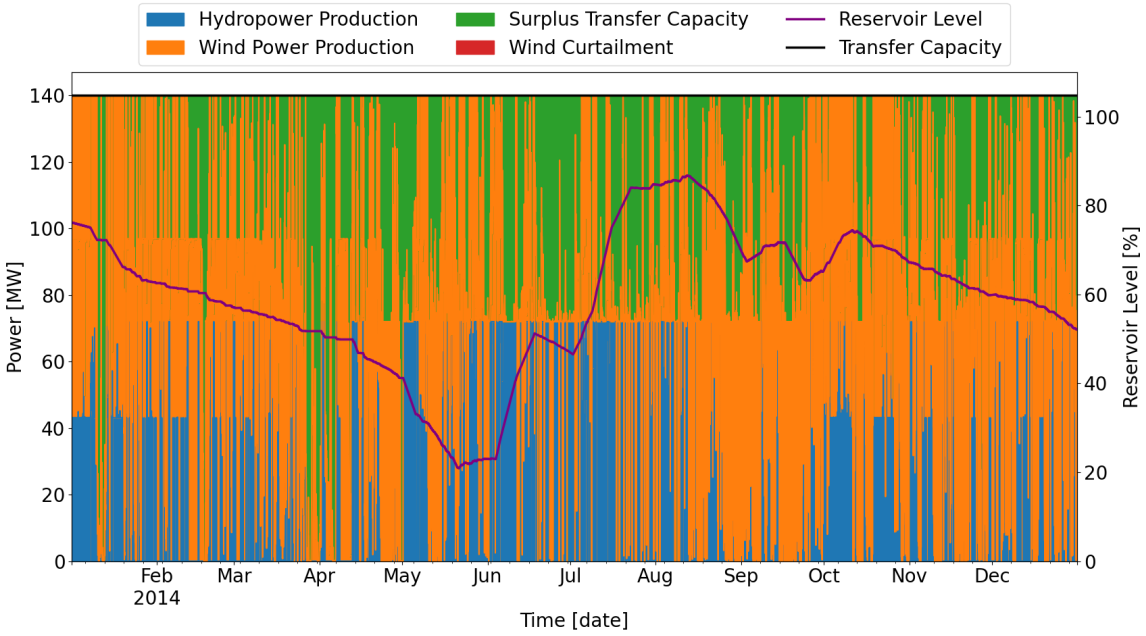

Figure 12: Optimisation results with time series of 2014, showing the scheduled power production, the reservoir level trajectory and the available transmission capacity throughout the year.

Furthermore, the different cash flows in Table 5 are calculated by utilising Equation (11) as in the simulation results. One can see that the wind power producer has increased its revenue by an amount approximately equal to the previous revenue loss. However, the revenue increment deviates somewhat from the revenue loss, due to rounding inaccuracy. Moreover, the hydropower producer has a decline in annual revenue, which is related to the reduced annual hydropower production. In addition, the shifting of hydropower production to different time periods will affect the revenue, due to variations in the Elspot price for each time step. Since none of the analysed years experienced wind power curtailment during the optimisation of the reference case, a wind curtailment plot similar to Figure 11 is deemed unnecessary.

Table 5: Average annual results from optimisations with SLR and time series of 2011 to 2015.

Parameter	Value
Energy loss	0 GWh
Wind curtailment	0 GWh
Flood losses	0 GWh
Revenue loss from curtailment	0 MNOK
Revenue loss from flooding	0 MNOK
Revenue from wind power	106.39 MNOK
Revenue from hydropower	74.05 MNOK
Wind power potential	389.61 GWh
Hydropower production	287.96 GWh
Wind power production	389.61 GWh
Transmission Surplus (SLR)	549.22 GWh [44.78%]
Amount of lost wind potential	0 %
Grid Utilisation (SLR)	55.25 %

5.2 Dynamic Line Rating

As presented in Figure 6 and described in Section 2.4, the simulation and optimisation models are further expanded with DLR to attain a technical perspective on grid utilisation. Figure 13 shows the resulting DLR for the transmission line in 2014. Some variations were registered in the analysed years of 2011 to 2015, but the overall trend of having a drop in capacity during the summer was evident in all years. In other words, Figure 13 gives a perception that is representative for each year. The average mean value of the DLR for the five years in total was found to be 189.91MW.

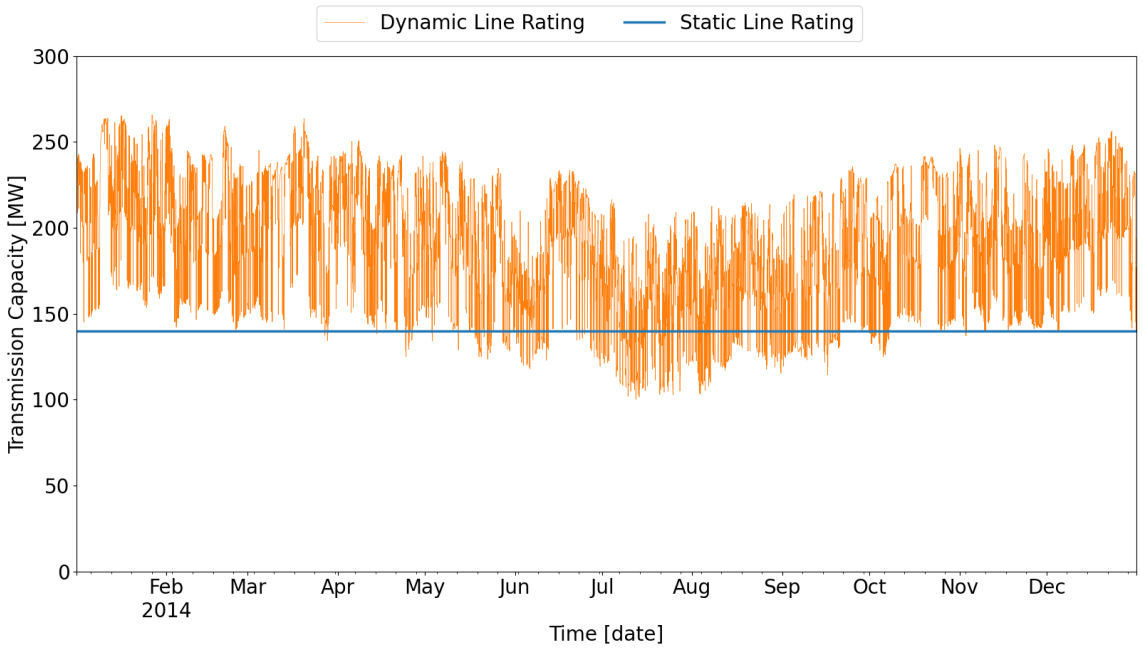

Figure 13: The resulting DLR of the studied transmission line when utilising the ambient temperatures and wind speeds of 2014.

5.2.1 Simulation of Grid Regulation

By replacing the previously used SLR with the estimated DLR shown in Figure 13, the studied system is again simulated with the provisions of NEM functioning. The resulting power scheduling and reservoir trajectory of 2014 can be seen in Figure 14. Here, the different power terms are plotted relative to the size of the transmission capacity in each time step. In other words, each term is divided by the size of the DLR, achieving a percentage distribution of the total transmission capacity and therefore a transmission capacity presented by a constant line. This is done to obtain a plot with similar arrangement as the previous power production plots, which improves the basis of comparison. However, the transmission capacity is still has the pattern in Figure 13 throughout the calculations in the simulation.

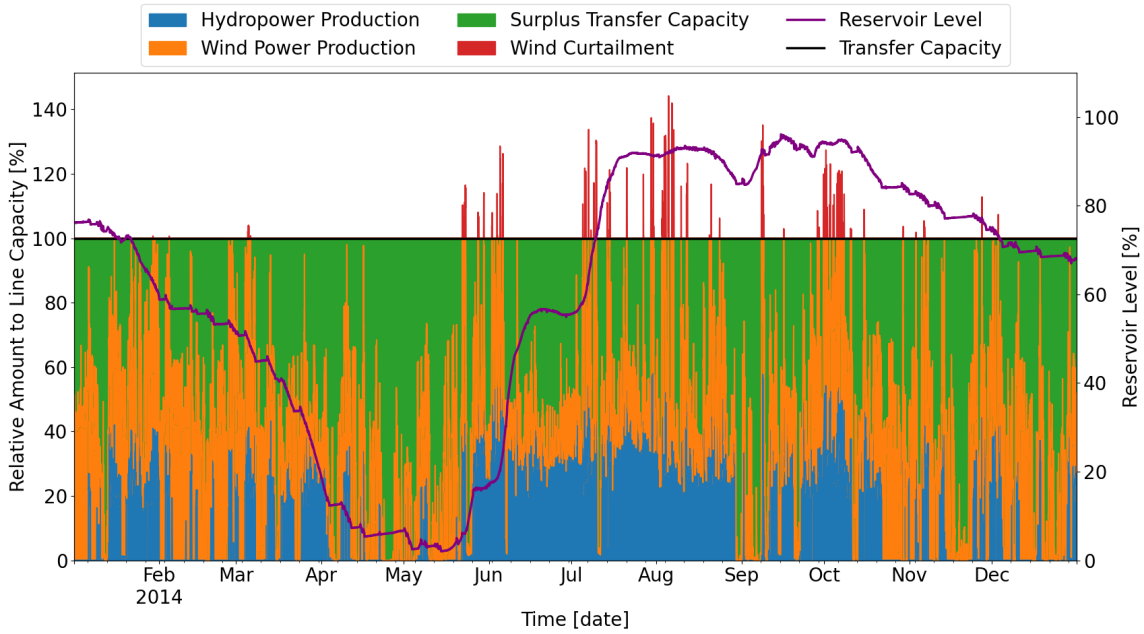

Figure 14: Simulation results with time series of 2014 and DLR, highlighting power production, reservoir levels, wind curtailment and available transmission capacity throughout the year. The power production is plotted relative to the DLR in each time step.

Similar to the previous simulation results, several parameters and values from the simulations with DLR were extracted in order to highlight the utilisation of the whole data set and provide a more precise result. These values are shown in Table 6, being the average annual values of the five simulated years 2011 to 2015. Both Table 6 and Figure 14 show that the wind curtailment has decreased compared to the simulation results in Section 4.1. The wind power curtailment is seen to occur primarily during the autumn and has a frequency that is reduced from 1137.2 times per year to 243.8 times per year. The amount of lost wind power potential has also decreased with 3.05 percentage points to 1.15%. Accordingly, the grid utilisation, based on the SLR, has increased with 0.99 percentage points to 55.21%. Furthermore, it can be seen that the wind power producer's annual revenue loss has been reduced to $1.17MNOK$, resulting in an average annual revenue equal $105.23MNOK$. The hydropower revenue is unchanged, due to the hydropower production not being affected by transmission capacity in the simulation model.

Table 6: Average annual results from simulations with DLR and time series of 2011 to 2015.

Parameter	Value
Energy loss	4.52 GWh
Wind curtailment	4.52 GWh
Revenue loss from curtailment	1.17 MNOK
Revenue from wind power	105.23 MNOK
Revenue from hydropower	76.87 MNOK
Wind power potential	389.61 GWh
Hydropower production	292.01 GWh
Wind power production	385.10 GWh
Transmission Surplus (DLR)	987.10 GWh
Transmission Surplus (SLR)	549.30 GWh [44.79%]
Curtailment frequency	243.8 times per year
Amount of lost wind potential	1.15 %
Grid Utilisation (SLR)	55.21 %

5.2.2 Optimisation With a Bilateral Power Agreement

After the simulation of the studied system with DLR was done, optimisation with DLR was carried out. The resulting power scheduling and reservoir levels for 2014 is shown in Figure 15, where the system now has a bilateral power agreement functioning between the power producers. Again, the different terms in the power scheduling are plotted relative to the size of the DLR in each time step. The choice of specifically highlighting 2014 in Figure 14 and Figure 15 was found to be reasonable as both plots are representative for all five years and it enables comparisons with the previous results with SLR. Furthermore, it can be seen that the reservoir level trajectory in Figure 15 has a similar weakness from resolution as discussed for Figure 12. Close-up plots that substantiate the trajectory during May, June and September, being the periods where the reservoir level apparently behave peculiar, can be found in Appendix A.2.

Table 7 shows average annual values of several parameters retrieved from the optimisation results with DLR for the years 2011 to 2015. Here it can be seen that the values concerning the wind power producer are equal to the values found in the optimisation of the reference case, see Table 5. Furthermore, since wind power curtailment in the simulation with DLR is highly subdued, the reduction in wind power curtailment is not as extensive here as for the reference case. The average annual hydropower production equates to $286.41GWh$, which is less than both the value in the original optimisation and the simulation with DLR, as well as less than the increase in wind power production compared to the simulation. Consequently, grid utilisation is lower than previous results, having an average annual value equal 55.12%. Moreover, the hydropower producer's revenue is seen to decrease, while the wind power producer experiences an increase.

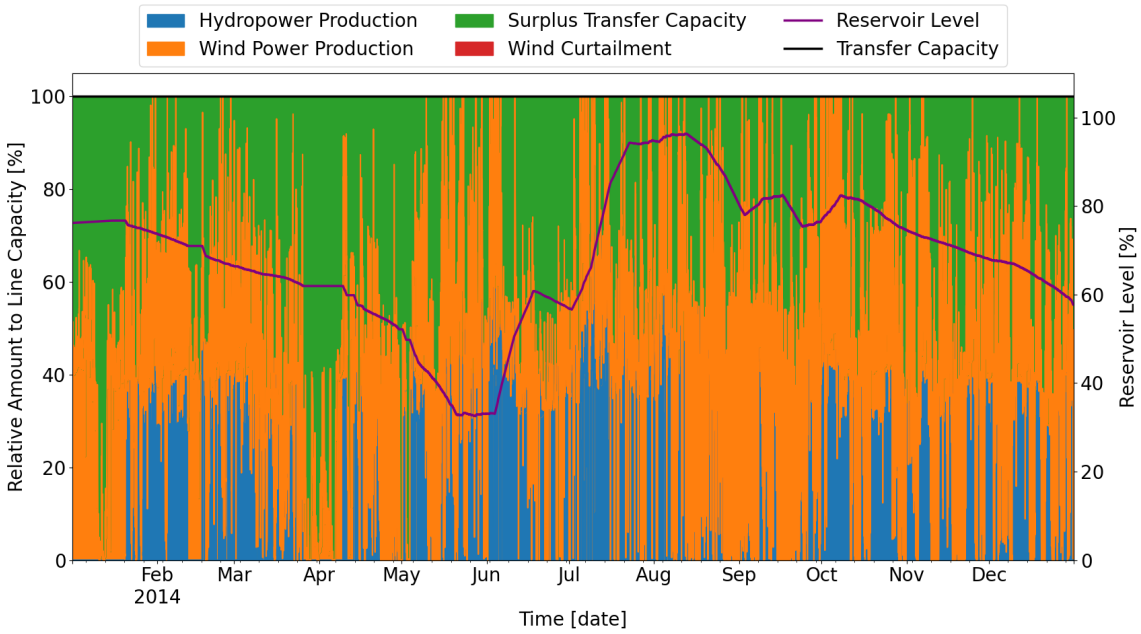

Figure 15: Optimisation results with time series of 2014 and DLR, highlighting power production, reservoir levels, wind curtailment and available transmission capacity throughout the year. The power production is plotted relative to the DLR in each time step.

Table 7: Average annual results from optimisations with DLR and time series of 2011 to 2015.

Parameter	Value
Energy loss	0 GWh
Wind curtailment	0 GWh
Flood losses	0 GWh
Revenue loss from curtailment	0 MNOK
Revenue loss from flooding	0 MNOK
Revenue from wind power	106.39 MNOK
Revenue from hydropower	72.80 MNOK
Wind power potential	389.61 GWh
Hydropower production	286.41 GWh
Wind power production	389.61 GWh
Transmission Surplus (DLR)	988.17 GWh
Transmission Surplus (SLR)	550.37 GWh [44.88%]
Amount of lost wind potential	0 %
Grid Utilisation (SLR)	55.12 %

5.3 Sensitivity Analysis

In order to achieve a more complete and thorough overview of the different power regulations and the potential of utilising hydropower flexibility for integration of VRES, a sensitivity analysis is conducted. Here, different parameters are altered to observe how the power grid utilisation and energy loss are affected. How the cash flows change is another factor of interest in the sensitivity analysis. The economic perspective is a natural aspect of interest for the different partakers. Moreover, measures that improve the economy are vital for the effectiveness of incentives aimed at increasing the share of VRES, which is a major part of the motivation behind NEM. The sensitivity analysis is done with the time series of 2014, being a representative year for the whole period. Additionally, it was found reasonable to investigate the same year as the one highlighted in Section 5.1 and Section 5.2.

5.3.1 Increase in Wind Power Capacity

Since the connection of new renewable power plants, and especially VRES, is the main focus area of this thesis, a natural parameter to explore is the installed wind power capacity. Moreover, the global focus of maximising the share of renewable power production, as well as the fact that the optimisation of the reference case yielded zero wind curtailment, makes it reasonable to only increase the wind power capacity. Therefore, the installed wind power capacity is increased from $110MW$ to $180MW$ with an increment of $10MW$. This is done by scaling the installed wind power capacity and the associated wind power potential time series. Figure 16 shows how the annual wind power curtailment is affected by the installed wind power capacity. Both the system results with only NEM active, i.e. simulation results, and with a bilateral power agreement between the producers, i.e. optimisation results, are included.

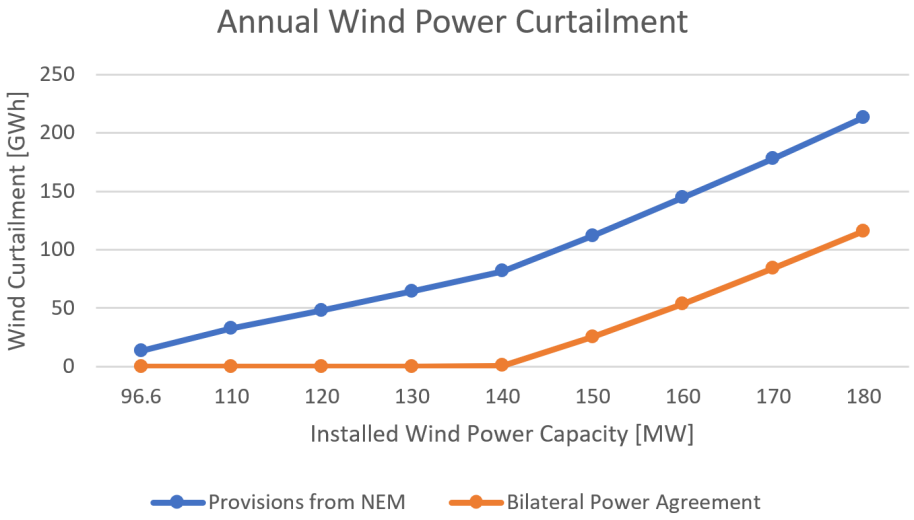

Figure 16: Annual wind power curtailment of the studied system for different amounts of installed wind power capacity. The blue line represents curtailment for the simulation model, while the orange line represents curtailment for the optimisation model.

Another parameter of interest is grid utilisation. Grid utilisation is directly connected to power production and therefore the amount of installed wind power capacity. In other words, grid utilisation is a reasonable parameter to highlight when varying the installed wind power capacity. Figure 17 shows the annual utilisation of the limiting transmission line. The figure is organised in a similar manner as Figure 16, containing the results from both variants of power regulations replicated through the thesis' models. Furthermore, Figure 17 includes both the annual transmission surplus and the corresponding amount of the grid that is utilised.

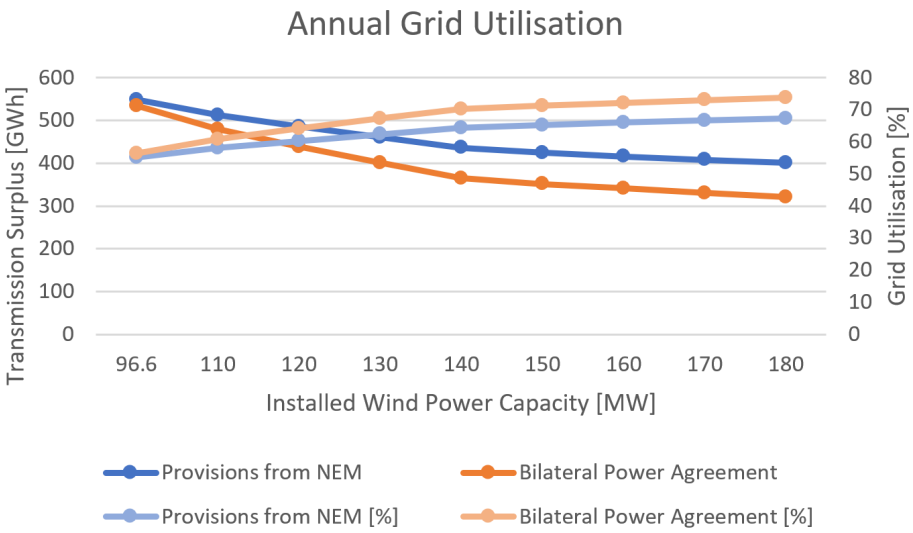

Figure 17: Annual grid utilisation of the studied system for different amounts of installed wind power capacity. The blue lines represent transmission surplus and grid utilisation for the simulation model, while the orange lines represent transmission surplus and grid utilisation for the optimisation model.

Lastly, the change in revenues and loss of potential revenue for the different power producers are highlighted in Figure 18. Economy is a central factor when deciding to invest in power plants, and it is therefore sensible to underline how the revenue of the producers are affected. Furthermore, the financial performance of each of the power regulations is of interest, as it will indicate if there are good incentives for utilising NEM individually or in a bilateral power agreement, compared to conventional grid connection with transmission capacity expansions. Moreover, the financial performance of each producer as well as the total social profit of the system are good indicators of the success of each regulation. As such, Figure 18 includes revenues of each producer and loss of revenue, during both NEM, i.e. simulation, and with a bilateral power agreement, i.e. optimisation.

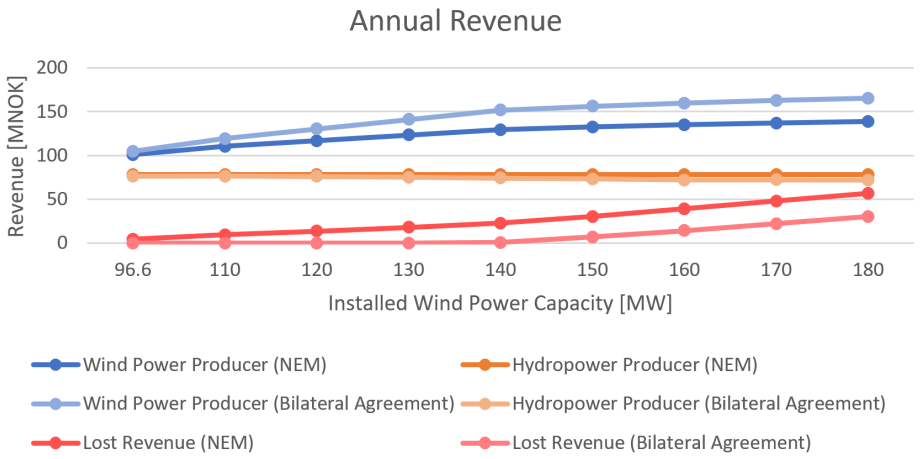

Figure 18: Annual revenue of the different power producers and lost revenue in the studied system for different amounts of installed wind power capacity. The blue lines represent revenue of the wind power producer, the orange lines represent revenue of the hydropower producer and the red lines represent lost revenue due to wind power curtailment. The lines with a darker shade of colour are values from the simulation model, while the brighter lines are from the optimisation model.

5.3.2 Change in Inflow

The second parameter that is altered in the sensitivity analysis is the inflow. Inflow is a stochastic amount that can vary greatly from year to year. In Northern Norway, there has been hydrological years where the inflow has been 80% above the average of the last 30 years, and years where the inflow has been 60% below average [79]. Moreover, the inflow time series of the studied system varies from $232.74GWh$ to $341.51GWh$, making varying inflow highly relevant for this study as well. Since the time series of 2014 had a total inflow between the two extreme points, it is here chosen to have a wet and dry scenario, compared to the original 2014 inflow. Based on the extreme points of the original data for 2011 to 2015, the wet scenario is chosen to be 30% above the 2014 inflow, while the dry scenario is chosen to be 10% below the 2014 inflow. This is achieved by scaling the inflow time series of 2014. Consequently, it is assumed that the seasonal pattern is the same in wet years as in dry years and that it is only the amount that changes. The different inflow scenarios are shown in Figure 19. The jagged shape is a consequence of the expanded resolution from the original weekly inflow to the hourly resolution used in the models. Furthermore, all other parameters are kept at their original value for 2014.

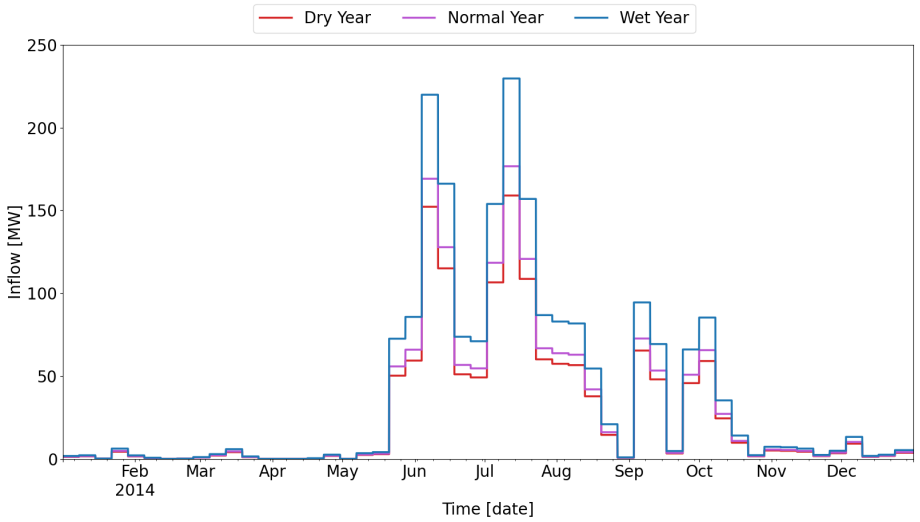

Figure 19: Inflow when altering the time series of 2014. Both the dry and wet year is a scaling of the normal year, i.e., the original inflow of 2014, using scaling constants 0.9 and 1.3 respectively.

Inflow is directly connected to hydropower production and the operational scheduling of hydropower facilities. Since the hydropower production in the simulation model is set by historical time series for production, and is therefore unaffected by any changes in inflow input, to include simulations in this part of the sensitivity analysis is considered to be redundant. Another argument is that the optimisation model is the only model which utilises the flexibility of the hydropower plant. Moreover, the flexibility can be affected by the inflow, due to it being a factor for the hydropower's ability to function as a passive storage and enable the wind power producer to obtain transmission priority. For these reasons, the following figures does only include the impact of altering the inflow in the system when there is a bilateral power agreement between the power producers.

Table 8 gives a summary of the resulting values from the different hydrological years when a bilateral power agreement between the producers is in place. Here, it can be seen that the energy loss has a positive correlation with the amount of inflow, being more comprehensive during the wet year. Moreover, part of the lost energy is flood losses, giving the hydropower producer some loss in revenue. However, one can also observe an increase in hydropower revenue when the inflow increases, which is reasonable as the hydropower production is increasing. The increment in hydropower production also provides a higher grid utilisation, even though there is a slight decrease in wind power production.

Table 8: Resulting values for various hydrological scenarios in 2014, when a bilateral power agreement between the power producers are functioning.

Parameters	Dry Year	Normal Year	Wet Year
Energy loss	0 GWh	0 GWh	23.00 GWh
Wind curtailment	0 GWh	0 GWh	6.68 GWh
Flood losses	0 GWh	0 GWh	16.32 GWh
Revenue loss from curtailment	0 MNOK	0 MNOK	1.71 MNOK
Revenue loss from flooding	0 MNOK	0 MNOK	2.99 MNOK
Revenue from wind power	104.82 MNOK	104.82 MNOK	103.11 MNOK
Revenue from hydropower	70.01 MNOK	76.19 MNOK	103.44 MNOK
Wind power potential	402.41 GWh	402.41 GWh	402.41 GWh
Hydropower production	264.90 GWh	288.41 GWh	386.32 GWh
Wind power production	402.41 GWh	402.41 GWh	395.73 GWh
Transmission Surplus	558.81 GWh	535.31 GWh	444.08 GWh
Amount of lost wind potential	0 %	0 %	1.66 %
Grid utilisation	54.44 %	56.35 %	63.79 %

5.3.3 Including Dynamic Line Rating

From the results found in Section 5.2, there seems to be a positive correlation between the DLR and wind power potential. Consequently, the DLR enables a reduction in wind curtailment that the SLR omits. As such, it is here included a section where DLR is implemented in the sensitivity analysis. The first variation that is explored is how much of the wind power curtailment, both with and without a bilateral power agreement, the DLR is able to prevent when the wind power capacity is increased to the previous maximum value, $180MW$. Next, the impact of DLR during different hydrological years is examined. Similar to Section 5.3.2, the inflow is reduced with 10% and increased by 30% to represent a dry and wet hydrological year respectively. The most significant results for the different variations are highlighted in Table 9. It should be noted that two different parameters for transmission surplus are included. The first is how much surplus capacity the line has according to the DLR ratings throughout the year, while the second is the surplus capacity of the line according to the SLR. Furthermore, only the grid utilisation of the SLR is included, i.e. the ratio between total power production and total transmission capacity with SLR, as it is the parameter that is comparable to the original grid utilisation.

Table 9: Resulting values for $180MW$ installed wind power capacity with original inflow, and for various hydrological scenarios with original installed wind power capacity. All results are for time series from 2014, when the DLR of the transmission line is utilised. In the inflow scenarios, a bilateral power agreement between the producer is functioning.

Parameters	NEM	Bilateral Agreement	Dry Year	Wet Year
Energy loss	63.46 GWh	16.61 GWh	0 GWh	20.99 GWh
Wind curtailment	63.46 GWh	16.61 GWh	0 GWh	4.67 GWh
Flood losses	0 GWh	0 GWh	0 GWh	16.32 GWh
Revenue loss from curtailment	16.99 MNOK	4.24 MNOK	0 MNOK	1.14 MNOK
Revenue loss from flooding	0 MNOK	0 MNOK	0 MNOK	2.99 MNOK
Revenue from wind power	178.33 MNOK	191.09 MNOK	104.82 MNOK	103.68 MNOK
Revenue from hydropower	77.94 MNOK	76.24 MNOK	79.93 MNOK	103.41 MNOK
Wind power potential	749.83 GWh	749.83 GWh	402.41 GWh	402.41 GWh
Hydropower production	287.93 GWh	286.41 GWh	298.50 GWh	386.31 GWh
Wind power production	686.37 GWh	733.22 GWh	402.41 GWh	397.74 GWh
Transmission Surplus (DLR)	691.10 GWh	645.77 GWh	964.49 GWh	881.35 GWh
Transmission Surplus (SLR)	252.10 GWh	206.76 GWh	525.49 GWh	442.35 GWh
Amount of lost wind potential	8.46 %	2.21 %	0 %	1.16 %
Grid Utilisation (SLR)	79.44 %	83.14 %	57.15 %	63.93 %

5.3.4 Dry Year and Increased Wind Power Capacity

Based on the findings in Table 8 and Table 9, which indicate a positive correlation between energy loss and inflow amount, it is found reasonable to include a scenario that includes two extreme points from the previous alternations. As such, a scenario having inflow equal a dry hydrological year and installed wind power capacity equal the greatest analysed amount, $180MW$, is here analysed. Moreover, it is only analysed for the scenario when there is a bilateral power agreement between the power producers, i.e., with the optimisation model. In addition, the scenario is analysed for both SLR and DLR. Table 10 highlights the resulting values from the analysed variations.

Table 10: Resulting values for various hydrological scenarios in 2014, having an installed wind power capacity of $180MW$ and a bilateral power agreement between the power producers.

Parameter	Dry Year(SLR)	Dry Year(DLR)	Normal Year(SLR)	Normal Year(DLR)
Energy loss	115.76 GWh	16.61 GWh	115.76 GWh	16.61 GWh
Wind curtailment	115.76 GWh	16.61 GWh	115.76 GWh	16.61 GWh
Flood losses	0 GWh	0 GWh	0 GWh	0 GWh
Revenue loss from curtailment	30.08 MNOK	4.24 MNOK	30.08 MNOK	4.24 MNOK
Revenue loss from flooding	0 MNOK	0 MNOK	0 MNOK	0 MNOK
Revenue from wind power	165.24 MNOK	191.09 MNOK	165.24 MNOK	191.09 MNOK
Revenue from hydropower	65.84 MNOK	68.92 MNOK	71.73 MNOK	76.24 MNOK
Wind power potential	749.83 GWh	749.83 GWh	749.83 GWh	749.83 GWh
Hydropower production	249.41 GWh	260.09 GWh	271.40 GWh	286.41 GWh
Wind power production	634.07 GWh	733.22 GWh	634.07 GWh	733.22 GWh
Transmission Surplus (DLR)	-	672.09 GWh	-	645.77 GWh
Transmission Surplus (SLR)	342.64 GWh	233.09 GWh	320.65 GWh	206.76 GWh
Amount of lost wind potential	15.44 %	2.21 %	15.44 %	2.21 %
Grid Utilisation (SLR)	72.06 %	80.99 %	73.85 %	83.14 %

6 Discussion

6.1 Grid Regulation

One of the main areas of interest in this thesis is the optimal utilisation of existing grid capacity. The reason behind and motivation for this angle of research was generated by the revision of grid regulation NEM in 2019. Chapter three, paragraph three (§3-3), enables grid connection with terms of production restrictions, which facilitates for increasing the installed power production of an area without improving existing transmission lines. In other words, the Norwegian Ministry of Petroleum and Energy provides a new way to improve grid utilisation, surpassing the old grid connection regulation's demand for sufficient transmission capacity.

6.1.1 Grid Utilisation and Energy Losses

In order to observe the impact of the revised power regulation, one must look at the simulation model, which replicates the operational pattern NEM creates. From the simulations results presented in Table 4 in Section 5.1, it is clear that the studied area had an average annual transmission capacity surplus of $561.58GWh$. This constitutes 45.79% of the total transmission capacity, meaning that the studied system on average utilised 54.24% of the existing grid over the time period of 2011 to 2015 when only NEM was active. The low grid utilisation is also evident in the power production scheduling of 2014, shown in Figure 10, as a large portion of the year has a production below the transmission limit. Nevertheless, the wind power producer still experiences an average annual loss of $16.41GWh$, which comprise 4.20% of the wind power potential of the wind farm.

Another notable operational pattern in the power scheduling caused by the provisions of NEM is the way in which transmission capacity is distributed among the power producers. As described in Section 2.1, the provisions of NEM put the new power producer last with regard to transmission priority. In exchange, the power producer achieves a grid connection faster for a cheaper price. This downgrading of the new power producer, being the wind power producer in this thesis, is evident in Figure 10. Here, the hydropower producer has production in high wind periods, even though the reservoir trajectory shows that there are low enough reservoir levels for the hydropower producer to shift its production to periods with reduced wind production. In other words, there seems to be possible for the studied system to reduce and prevent much of its energy loss by utilising the flexibility of the hydropower facility. At the same time, the system can increase the grid utilisation.

The resulting energy losses that are accounted for and found in the simulations are only consisting of wind power curtailment. All wind curtailment for the five analysed years are highlighted in Figure 11. Here, it can be seen that the studied system is experiencing wind power curtailment each year when only NEM is active. Furthermore, there are clear similarities between the different years. The curtailment, with the exception of 2013, occurs frequently in the Norwegian winter months of January, February, and March. In addition, all years have a high amount of curtailment in the late summer and autumn. These months traditionally have high demand in Norway, due to low outdoor temperatures causing need of electricity for heating [80, p.17]. As such, it is found reasonable to believe that lack of demand is not a cause for the wind power curtailment. A more plausible factor is congestion in the transmission line, which forces the wind power producer to restrict its production in accordance with NEM.

However, a trend can also be seen in Figure 11 that indicates the existence of periods where the

curtailment is less frequent. During the Norwegian spring and early summer there are long periods with zero curtailment for all the simulated years. Consequently, it might seem like the curtailment is mainly happening during periods where the demand is high. Furthermore, the spring and early summer does typically provide a large amount of inflow, due to snow melting. It might therefore be possible for the hydropower producer to shift its production to the months where the wind curtailment and wind power potential is low, giving the wind power producer more transmission capacity during high wind periods. A bilateral power agreement that shifts the transmission priority to the wind producer is believed to be a suitable approach to achieve such operational scheduling and is the suggested solution in this thesis.

6.1.2 Cash Flows

As described in Section 2.5.1, the power producers' revenue is mainly from the sale of power at Elspot prices. Energy losses and unredeemed production potential therefore constitute an alternative cost for the producers, being loss of revenue. Table 4 highlights the average annual revenues and loss of revenue for the different power producers during simulations of the reference system for the years 2011 to 2015. The hydropower producer has an annual revenue of $76.87MNOK$, while the wind power producer has an annual revenue of $101.72MNOK$. This difference in revenue is plausible due the difference in power production, being $292.01GWh$ and $373.20GWh$ respectively, which is directly connected to the amount of revenue. However, it should be noted that the Elspot price varies in each time step, making the correlation between revenue difference and production difference skewed. Furthermore, the wind power producer experiences an annual revenue loss equalling $4.67MNOK$ on average. In contrast, the hydropower producer does not have any loss of revenue, due to the traditional grid connection regulations and the provisions in NEM giving the hydropower producer transmission priority. Consequently, the energy loss is solely made up of wind power curtailment.

The annual loss of revenue the wind power producer is experiencing will likely provide an interest in measures that improve wind power integration in the system. Such measures will have an economic limitation determined by the annual revenue loss. It would serve no purpose to invest in the power grid, e.g., storage or transmission expansions, if the increase in revenue is less than the annual cost of the investment. Moreover, the lost revenue is a measure of whether the power producer benefits from NEM compared to conventional regulations with grid expansions and construction fees. In a report done by NVE in 2015, estimates of the cost of different overhead lines are presented. The cheapest $132kV$ line, which is the voltage of the transmission line in the studied system, is estimated to cost $1.4MNOK/km$ [81, p.208]. This gives a rough cost estimate of possible grid expansions to be $26.6MNOK$. As such, it seems plausible that the power producer, by avoiding the expansion cost, benefits from NEM. Furthermore, NEM also provides a quicker connection, which gives the power producer revenues earlier. However, it should be noted that this investment analysis is a brief estimation, only providing an overall perspective.

A different approach to investing in physical expansions of the power grid, is to utilise the existing system in an optimal way. As already suggested, the approach proposed in this thesis comprises a bilateral power agreement.In such an agreement, it is reasonable to assume that the wind power producer will compensate the hydropower producer for claiming transmission priority. As with grid investments, such an agreement will be limited as the compensation cost should not exceed the revenue increment. However, from a social perspective, the total surplus will increase, as the total amount of power from the system is likely to increase.

6.1.3 Sensitivity Analysis

In the sensitivity analysis in Section 5.3.1, the impact of the amount of installed wind power capacity is highlighted. This is highly relevant as a central part of the motivation of NEM is to increase production in existing grid systems. In other words, there is a strong similarity between this part of the sensitivity analysis and situations that are believed to occur due to NEM. Figure 16 shows that wind curtailment is steadily increasing until the installed wind power capacity reaches the transmission limit. After the installed wind power capacity surpasses transmission capacity, the annual wind curtailment has a steeper slope. The larger increment is reasonable, as the wind power producer now has enough installed power capacity to exceed transmission capacity by itself. Since the wind power potential is scaled together with the increased power capacity, there will be periods where curtailment of the wind power production is unavoidable.

As wind curtailment increases with increased installed wind power capacity, grid utilisation increases simultaneously. However, Figure 17 shows that this increase in grid utilisation is almost brought to a standstill when the transmission capacity is surpassed. In other words, the correlation between grid utilisation and installed wind power capacity is weakened. An explanation of this link can be that the time series used as input for the wind power is scaled by multiplying each element with the ratio between the original and new wind power capacity. Consequently, the biggest values get the largest increment, similar to the inflow in Figure 19. This causes the periods with already high wind and possible curtailment to give significantly more wind curtailment, while the periods with low wind only give a small increase in grid utilisation. It might therefore be necessary to improve the approach used to adapt the wind power potential time series in order to achieve a more realistic trend. Nevertheless, a decreased increment in grid utilisation, after the transmission capacity is surpassed, seems to be reasonable. Again, it boils down to the wind power potential exceeding the transmission capacity, giving periods where wind curtailment will occur in any case.

The last part of Section 5.3.1 focuses on the impact of the different installed wind power capacities on the cash flows of the studied system. In Figure 18 one can see that the revenue of the wind power producer has a slight increase until the wind power capacity reaches the transmission limit, where it then stabilises at an almost constant level. A mirrored pattern is observed for the lost revenue of the system. Here, the increment is small until the transmission limit is reached, where it then increases to a higher constant level. Since the lost revenue only stems from wind curtailment, the pattern is found to be reasonable and in accord with the pattern in Figure 16. In contrast, the hydropower producer's revenue is seen to be independent of the amount of installed wind power, remaining constant. This comes from the provisions in NEM, which gives the wind power producer access to the power grid, but only secondary to existing power producers. In other words, the hydropower production is not affected, indicating that NEM itself does not facilitate optimal grid utilisation.

Even though the provisions in NEM is found to not give incentives for optimal grid utilisation, it was still seen to increase utilisation by enabling more installed power production, see Figure 17. Furthermore, the simulation results show that for a VRES, such as wind power, the energy loss can be high. NEM gives no economic guidance, resulting in the alternative cost, consisting of lost revenue from lost production potential, only affecting the new producer. The regulation therefore provides, in principle, advantages to the grid companies. An interesting aspect here is the increased revenue the grid company receives from NEM. As mentioned in Section 2.5.1, the feed-in tariff the power producers pay to the grid companies has a term that is based on annual power production. Consequently, the feed-in tariff and correspondingly the revenue of the grid

company will increase along with grid utilisation. This does, however, not provide an additional contribution to the social surplus in the system, as the cash flows from the partakers neutralise each other. Rather, it demonstrates the grid companies' interest in NEM.

To sum up, the simulation results indicate that NEM provides the grid companies with improved utilisation of their existing grid, while producers based on VRES receive a disadvantage through lost energy potential. However, grid connection with production restrictions can still be a better option than paying construction fees for grid expansions, as both connection time and costs are considerably reduced. Still, NEM could possibly have been revised to include an economic guidance that motivates a socio-economic distribution of lost income. Another solution is to have bilateral power agreements between producers, which can activate the flexibility in the system thus reducing wind power curtailment.

6.2 Bilateral Power Agreement

Since the provisions in NEM are seen to give a disadvantage to VRES with regard to energy loss, an incentive for utilising the flexibility in the power system was introduced. This incentive is in the form of a bilateral power agreement between the power producers, which in the studied area motivates a rescheduling of the regulated hydropower production, in favour of wind power production. Moreover, the bilateral power agreement was designed to complement NEM and tested in a case area that is considered representative for many parts in Norway, due to the existing power system, the geographical location of sites with good wind conditions and the provisions in NEM.

6.2.1 Grid Utilisation and Energy Losses

A plausible operational pattern generated through a bilateral power agreement was implemented by expanding the principle behind the simulation model to the final LP optimisation model. From the resulting power scheduling in Figure 12 it can be seen that the system did not experience any wind power curtailment with the input data of 2014. This is also the case in the rest of the analysed years. As presented in Table 5, the average annual wind curtailment is found to be $0GWh$. This is a considerable difference from the average annual wind curtailment the system experienced when only NEM was functioning, which is presented in Table 4 to be $16.41GWh$. The bilateral power agreement thus enables the system to capture the missing 4.20% of the wind power potential that the system lost with solely the provisions in NEM functioning.

Based on the eliminated wind power curtailment, it is reasonable to assume that the overall power production and therefore grid utilisation has increased with the bilateral power agreement functioning. This is confirmed by both the reduced green area in Figure 12 and the reduced transmission surplus in Table 5. The average annual transmission surplus has been reduced by $12.36GWh$, giving a resulting average grid utilisation of 55.25%. The bilateral power agreement has therefore provided an increase in the utilisation of the existing grid equalling 1.01 percentage points. However, this increment comprises less than the captured wind power curtailment. This is due to a decrease in average annual hydropower production, which counteracts the increment in grid utilisation provided by the increased wind power production. Therefore, it could be interesting to expand the optimisation model with a constraint demanding equal hydropower production as in the simulation model. This might improve the basis of comparison between the simulation and optimisation models.

6.2.2 Operational Impact on the Hydropower Producer

A key element of the idea of using a bilateral power agreement was that it could exploit the reservoir capacity, and therefore the flexibility of hydropower by scheduling the production in counter phase with wind power. By comparing the resulting power scheduling in Figure 10 with Figure 12, it is evident that the hydropower production has been shifted to periods with low wind power potential, preventing all previous wind power curtailment. However, the changed hydropower production schedule might affect the hydropower plant and its environment, something that should be studied further.

Even though hydropower was found in the literature review to be a robust technology for variable operation, the rapid production changes might still increase wear on the facility [27, p.2]. Moreover, the average number of occasions with wind power curtailment was found to be 1137 times per year, which will be the number of hours where the hydropower production is required to differ from its original schedule. As mentioned in section 2.2.1, a hydropower turbine risks diminishing its lifetime when operating away from BEP. Furthermore, with the frequent starts and stops in production, stricter generator requirements may follow. For instance, a variable speed generator for the hydropower plant might be necessary. In addition, plants with outflow to rivers might have a severe impact on the local environment, as stated by Korpås [51]. All these factors should be considered when the economic details of a bilateral power agreement between the producers are decided.

Another relevant aspect regarding the change in operation of the hydropower facility, is how the reservoir levels are altered form the simulation to the optimisation. Looking at Figure 10 and Figure 12, it is evident that both the reservoir level trajectories generated by the provisions in NEM and the bilateral power agreement follow a similar pattern. Both trajectories are seen to decrease to their lowest annual value in late spring, and then increase to a maximum by the end of July. Nevertheless, the trajectory in the simulation has both a lower minimum and a higher maximum than the optimisation trajectory. This might be connected to the simulation being based on historical measured values. Since there is uncertainty to predicted inflow amount in real systems, it might be that the reservoir was deliberately emptied in order to have a safety margin during periods with high expected inflow. Such a measure is not necessary in the optimisation, as the inflow is known for the whole period. Another observed characteristic is that the simulation reservoir trajectory has a more rapid decrease and increase than the optimisation reservoir trajectory. Again, it might be connected to the nature of the models and how they derive the reservoir trajectory.

Finally, the final reservoir level is seen to be higher in the resulting reservoir trajectory in the simulation than in the optimisation trajectory. This appears unlikely, as the observed decrease in average annual hydropower production in the optimisation results indicates that it should be otherwise. However, the total hydropower production amount for 2014, which is the year that is plotted, is slightly larger in the optimisation than in the simulation. Still, the difference in hydropower production for 2014 during simulation and optimisation is not enough to justify the final reservoir level being almost 10 percentage points lower in the optimisation compared to the simulation. Moreover, none of the results in the reference case have any flood losses, meaning that the hydropower production is the only variable affecting the reservoir level trajectories. There are some plausible explanations for the difference between the final reservoir levels. For instance, the simulation model is plotting measured reservoir levels that are scaled to fit the aggregated hydropower plant, while the optimisation model is calculating the reservoir level based on inflow,

production, losses, and the initial reservoir level. Consequently, a natural inaccuracy is generated, as the two trajectories are based on two different measurements, as well as there being inaccuracy in the measurements themselves.

6.2.3 Cash Flows

As mentioned in Section 6.1.2, the bilateral power agreement is a solution for the energy loss, which will be limited by the difference between the cost of such an agreement and the increment in revenue it can provide. In Table 5, which highlights the average annual revenues and loss of revenue for the producers when a bilateral power agreement is in place, it can be seen that the wind power producer has an annual revenue of $106.35 MNOK$ on average from 2011 to 2015. This gives a revenue increment equalling the earlier revenue loss, $4.67 MNOK$, something that is reasonable as all the previous wind curtailment is exploited. Furthermore, the average annual revenue of the hydropower producer has now been reduced to $74.05 MNOK$, which corresponds to the observed decrease in annual hydropower production.

The financial design of a bilateral power agreement is difficult to envisage, as the literature review conducted for this thesis did not reveal any existing agreements of this nature. Still, it seems reasonable that the hydropower producer will demand a fee from the wind power producer, to compensate its deviation from optimal production schedule. Any increase in flood loss, which especially hydropower facilities with a low degree of regulation might experience, also needs to be compensated. This is reasonable as the hydropower producer originally has sufficient transfer capacity. Another aspect is whether the grid company, which increases the utilisation of its grid, should take part in covering the expenses.

By assuming that the hydropower producer will demand compensation for its revenue decrement, namely $2.82 MNOK$, the wind power producer will still be left with $1.85 MNOK$ in annual profit from the bilateral power agreement. In other words, the power agreement seems to provide the wind power producer with a financial advantage, making it an attractive alternative to grid expansions and energy storage. This also indicates a healthy synergy between the provisions from NEM and the bilateral power agreement, as the wind power producer is able to exploit all its production potential as well as bypassing construction fees and delays connected to grid expansions. However, a more extensive investment analysis is needed to determine whether conventional grid connection regulation or investing in energy storage would be the better financial alternative. In addition, the hydropower producer might demand compensation for their changed operational pattern, reducing the wind power producer's annual profit. On the other hand, from a grid utilisation perspective it is evident that there is unused transmission capacity in the studied system, which speaks in favour of avoiding grid expansions.

6.2.4 Sensitivity Analysis

From the sensitivity analysis presented in Section 5.3.1, it is evident that the bilateral power agreement is able to improve wind power integration better than NEM. Figure 16 in particular highlights this fact, showing that the bilateral power agreement, i.e. the optimisation model, only experiences losses when the installed wind power capacity is equal to or larger than the maximum transmission line capacity. Moreover, the gap in wind power curtailment between the two models increases steadily to around $90 GWh$ at $140 MW$ installed wind power capacity, where the gap stabilises. When the installed wind power capacity is increased further, the wind power curtailment

is seen to approximately increase equally in simulation and the optimisation. This indicates that even the flexibility of the hydropower facility is unable to prevent wind power curtailment when the wind power potential is greater than the transfer limit itself. Since the hydropower only provides passive storage, i.e., can shift its production in favour of the wind power, it is reasonable that the bilateral power agreement does not prevent curtailment as the wind power potential surpasses the transmission limit.

A possible solution could be energy storages that enable active charging, e.g. pumped storage hydropower or batteries. As presented in Section 2.3.4, a pumped storage works well with wind power fluctuations. Furthermore, it is a natural choice for the case area, since both the upper and lower hydropower plant in the cascaded configuration have the potential to become a pumped storage hydropower facility. Still, a more extensive economic analysis is needed to conclude whether pump storage is a better option than grid expansions or not. In addition, it is evident from Figure 16 that pumped storage most likely will not be beneficial before the original wind farm in the reference case is expanded to a size that surpasses transmission capacity. However, the pumped storage might provide the hydropower producer with a means to increase its revenues by enabling an improved way in which to exploit variations in the Elspot price. Consequently, the hydropower producer might be interested in covering some of the expenses connected to a pumped storage expansion. The pumped storage alternative might thus become more favourable for the wind power producer.

The annual grid utilisation for the different amounts of installed wind power is highlighted in Figure 17. Similar to the simulation model, the transmission surplus has a steep decline until transmission capacity is reached, and then decreases at a lower rate. Moreover, the decrease in surplus is, before the transmission capacity is surpassed, larger for the optimisation model than for the simulation model. Based on the development in wind power curtailment observed in Figure 16, this is deemed reasonable. Accordingly, the difference in grid utilisation increases until the line capacity is surpassed, and then stabilises at a difference of approximately five percentage points. Final grid utilisation is seen to be around 74% and 69% for the optimisation and simulation, respectively. The slow increase in grid utilisation after the transmission capacity is exceeded substantiates the belief that hydropower flexibility cannot cover wind potential above the transmission limit.

Another change caused by the change in wind power capacity is the annual revenues of the power producers. As can be seen in Figure 18, the wind power producer's revenue has a similar development as the observed grid utilisation. The difference in revenue between having a bilateral power agreement and solely having NEM increases steadily until the transmission limit, and then stabilises. The same development is evident for the lost revenue. A bilateral power agreement can prevent revenue loss until the installed wind power capacity reaches maximum transmission capacity. A different interesting feature is how the hydropower producer's revenue develops. For the bilateral power agreement, the hydropower revenue decreases slightly, which is consistent with the observed reduction in hydropower production in the optimisation results. Furthermore, the revenue loss from wind curtailment is seen to increase more than the revenue gained from increased wind power capacity after the farm size has surpassed transmission line capacity. In other words, the wind power producer loses more potential revenue than it gains.

The other parameter that was altered in the sensitivity analysis was the inflow amount. It was done by scaling the original time series, resulting in the inflow seen in Figure 19. It might be that the inflow time series should have been historical data of different hydrological years. However, the simplifications done to aggregate the hydropower system itself are deemed to provide a higher level of inaccuracy, making the direct scaling of the original inflow data a sensible approach for the purpose of the sensitivity analysis.

As hydropower production is highly dependent on inflow and is predetermined in the simulation model, this part of the sensitivity analysis was only carried out for the optimisation model. In Table 8 it can be seen that the energy and revenue loss increase with the increase in inflow. Furthermore, the wet year scenario is the first instance where the hydropower producer experiences losses. In addition, the wind power producer is only experiencing curtailment during the wet scenario, which indicates that the increased inflow is reducing the hydropower flexibility. Since the bilateral power agreement is designed to prioritise minimisation of flood losses before minimisation of wind power curtailment, the reduced flexibility leads to curtailment.

Even though the energy loss increases with inflow, the grid utilisation is also seen to increase. Table 8 shows that the wind power production decreases with $6.68GWh$ when the inflow is increased. In contrast, the annual hydropower production increases with $97.91GWh$, which is why the grid utilisation still improves. This development seems reasonable, as hydropower production is regulated and highly controllable. Consequently, more inflow will give the hydropower producer the potential to produce more, and it will be able to mostly produce during favourable periods. As seen in Figure 17, the increase in grid utilisation is almost brought to a standstill after the installed wind power capacity surpasses the transmission line capacity. Such a development is less likely to happen as the inflow amount increases, due to the hydropower being flexible and able to store the energy. Therefore, inflow might be a better parameter for increasing grid utilisation than the size of the wind farm, in the context of analyses. Nevertheless, inflow is a highly stochastic parameter and should be further analysed to ensure a valid conclusion.

By looking at the financial aspect of the system, the resulting flood losses are observed to cause an annual revenue loss for the hydropower producer amounting to $2.99MNOK$. Regarding the compensation the wind power producer is likely to pay the hydropower producer through the bilateral power agreement, flood losses might constitute some of it. Consequently, hydrological wet years might make the bilateral power agreement less attractive for the wind power producer. However, the optimisation model was designed based on the assumption that the agreement prioritises flood loss minimisation. In other words, the flood losses that occur should then be losses that are unavoidable and arguably would occur regardless of the agreement. In that case, the wind power producer should not have to cover the lost revenue due to flooding. Still, there are large variations in the Elspot prices that can make it cheaper for the objective function of the optimisation model to have flood losses at a low price instead of wind power curtailment at a high price. This will be dependent on the weights, r and q, which determine the price of each type of energy loss. A sensitivity analysis of the weights should therefore be conducted in order to achieve a more precise conclusion regarding the necessity of compensating flood losses.

6.3 Dynamic Line Rating

Where the simulation and optimisation strive to highlight how the power regulation and power agreement affect the studied system, the inclusion of DLR provides a look at how a technical solution can improve grid utilisation. In order to expand the models with DLR, the rating itself had to be estimated for the studied period. As mentioned in Section 2.4, there are many different approaches and parameters used to estimate DLR. The resulting rating shown in Figure 13 is based on a chart of estimated line ratings of the studied transmission, at different wind speeds and temperatures, provided by Nordkraft.

The estimated DLR time series were derived by finding temperature and wind speeds for the analysed period and interpolate with the values in the line rating chart. The temperature values are measurements done by Nordkraft around the studied line, while the wind speeds are measurements from a nearby weather station. These values represent uncertainties, especially the wind speeds that are not measured in near proximity to the line. Moreover, there is likely a variation in temperature and wind speed along the line, causing a risk of the estimated DLR not to be applicable for the whole line. Another source of inaccuracy is the calculation method itself. Even though DLR based on weather data was found in the literature review to be a good method, more parameters are usually needed. The utilised DLR is therefore likely to have errors and should be improved in more technical studies. Nevertheless, the derived DLR is believed to be sufficient for highlighting overall effects, which is its purpose in this thesis. Furthermore, the general pattern of the DLR, with for instance a drop during the summer months, is observed to coincide with more extensive estimations given by Nordkraft.

6.3.1 Grid Utilisation and Energy Losses

From the resulting power production schedule shown in Figure 14, it is evident that the wind power producer still experiences wind power curtailment when only the provisions in NEM are active. However, the amount and frequency of wind power curtailment has been heavily reduced compared to the schedule shown in Figure 10, which indicates that the DLR is advantageous for the integration of wind power. This corresponds well with the findings of the literature review in Section 2.4. Moreover, in Table 6 it can be seen that the average annual wind power curtailment equals $4.52GWh$, which is a decrease of $11.89GWh$ compared to utilising SLR. The wind curtailment frequency is observed to be 243.8 times per year on average, providing a reduction of 893.4 times per year. Consequently, the change in operational pattern for the hydropower producer, when the system goes from only following NEM to also having a bilateral power agreement, is not as comprehensive for DLR as for the SLR scenario.

The power production schedule induced by a bilateral power agreement and DLR, as seen in figure 15, has many similarities with the equivalent variant with SLR. Firstly, there is no wind power curtailment throughout the plotted year. This is substantiated by the average annual value presented in Table 7. Secondly, it is evident that the reservoir level trajectories of these two instances follow an equal pattern. The final reservoir level, however, is seen to be higher in the case using DLR than the case using SLR. Consequently, it is reasonable to believe that there is less annual hydropower production with DLR with SLR.

The impact on power production can be seen by comparing Table 5 with Table 7. Here, the optimisation with DLR has a lower hydropower production than the optimisation with SLR. This is

found to be a bit odd, as the increase in line capacity from DLR should diminish occasions of line congestions. Consequently, the hydropower producer should be able to produce more with DLR. However, as mentioned in Section 6.2 the optimisation model does not specify how the hydropower should operate beyond facilitating wind power production and minimising losses. Since neither the optimisation with SLR nor the one with DLR experience losses, and are seen to have a high transmission capacity surplus, there are reasons to believe that there exist several possible solutions. This missing specification of the hydropower production during periods without energy loss is a natural expansion and improvement of the existing model. A possible expansion is to have the hydropower producer maximise its own profit.

The average annual grid utilisation for the studied area with DLR, and only NEM in place, is seen in Table 6 to be 55.21%. This is an increase of 0.97 percentage points compared to the equivalent case with SLR, and comprises $11.89GWh$ in increased annual power production in the system on average. Furthermore, the average annual grid utilisation for the studied area with DLR and a bilateral power agreement between the power producers, is seen in Table 7 to be 55.21%. As such, grid utilisation has decreased in the optimisation, something that is unexpected. However, this again stems from the fact that the hydropower producer does not have any constraints regarding production in periods without risk of line congestion. Another interesting parameter is the transmission capacity surplus of the line based on the DLR. In both Table 6 and Table 7, it is seen that the transmission surplus for the DLR is almost twice the amount of the transmission surplus for the SLR. In other words, it is clear that the DLR increases the total transmission capacity of the line over a year.

6.3.2 Cash Flows

How the implementation of DLR affects the economy in the system is highlighted through Table 6 and Table 7. It can be seen that the wind power producer's average annual revenue with production restrictions is $105.23MNOK$ when DLR is active. This gives an increase of $3.51MNOK$, compared to the average annual revenue from the simulation with SLR. Furthermore, the hydropower revenue is observed to be equal in the simulation results, which is due to the fact that the hydropower production is predetermined. The increase in wind power production, and the corresponding revenue, also provides the grid company with an increased income. There might therefore exist financial incentives to implement DLR into the system. However, the question regarding who should cover the cost of such an implementation then arises. Sensors for determining the DLR as well as new operating methods are both likely needed. Nevertheless, the literature review presented in Section 2.4 showed that relatively cheap and efficient sensor equipment is emerging. In other words, implementation of DLR might be financially justified even with the extra requirements.

Furthermore, in Table 7, the average annual revenues for the studied system with DLR and an active bilateral power agreement is seen to be altered compared to the revenues just mentioned. First, the wind power producer's annual revenue increases as a result of the captured wind power curtailment. However, the $1.17MNOK$ increment is significantly lower than the corresponding increment in the calculations with SLR. Second, the hydropower producer's annual revenue is seen to decrease with $4.1MNOK$ compared to the revenue in Table 6. As a result, the total revenue decreases when the bilateral power agreement is operational, making it an unfavourable choice for the system. In other words, when the DLR is utilised there is no financial incentive to introduce a bilateral power agreement in the studied system. The compensation due to the hydropower producer will likely be more expensive than the profit such an agreement gives the wind power producer. Nevertheless,

this result will most likely change if the scheduling of the hydropower in the optimisation model is expanded, as discussed previously. It should also be noted that this result is highly system specific. If the line is more constrained, thus giving a large amount of wind power curtailment with DLR, the bilateral power agreement will most likely still be advantageous.

6.3.3 Sensitivity Analysis

As presented in Section 5.3.3, a sensitivity analysis which includes DLR is carried out. Here the system is studied with a $180MW$ installed wind power capacity and with an equal change in inflow as previously seen. These scenarios are generated separately, and the results are highlighted in Table 9. First, it can be seen that the only loss the system experiences, when having $180MW$ installed wind power, is wind power curtailment. Both simulation and optimisation are experiencing curtailment, equalling $63.46GWh$ and $16.61GWh$ respectively. This comprises 8.46% and 2.21% of the total wind power potential. As seen in Figure 16, this is considerably less than the curtailment encountered in the sensitivity analysis with SLR. In conclusion, the advantage of DLR is arguably more evident for higher installed wind power capacity. Moreover, it is evident that DLR has a positive correlation with wind power potential, giving easier integration of the wind power. Still, the sensitivity analysis with DLR should be expanded in a similar manner as the analysis with SLR, in order to achieve a better understanding and basis of comparison with SLR.

Due to the considerable decrease in wind power curtailment, the grid utilisation for the $180MW$ wind power scenarios with DLR is significantly higher than for similar scenarios with SLR. In Table 9 the grid utilisation based on the SLR capacity is found to be 79.44% with NEM and 83.14% with a bilateral power agreement. However, the transmission surplus for the DLR still comprise $691.10GWh$ and $645.77GWh$ respectively, which indicate that there should be enough transmission capacity to eliminate the wind power curtailment completely. The occurring wind power curtailment is therefore likely to be solely a result of the wind power potential being higher than the transmission capacity itself. This issue was also evident when using SLR, but to a greater extent as the DLR correlates with the wind power potential.

By comparing Figure 18 with Table 9 it can be seen that the wind power producer's annual revenue is considerably higher when DLR is utilised compared to utilising SLR. As previously stated, this is due to the wind power curtailment the DLR is able to eliminate. Moreover, the wind power producer's revenue is greatly improved with DLR when there is a bilateral power agreement in place. The revenue increases from $178.33MNOK$ to $191.09MNOK$ annually, which gives an increment of $12.76MNOK$. Furthermore, the hydropower producer's revenue is seen to have the same tendency as in the sensitivity analysis with SLR, namely having a slight decrease when going from utilising the provisions in NEM to having a bilateral power agreement. As such, it seems like there is a greater financial basis for the power agreement when the installed wind power capacity is increased.

For the scenarios with altered inflow and DLR, it seems like the development when going from NEM to a bilateral power agreement has a similar pattern as in the sensitivity analysis with SLR, which was discussed in Section 6.2.4. The main difference is the specific amount of production and corresponding grid utilisation and revenues. For instance, hydropower production in Table 9 is seen to be $298.50GWh$ during the dry hydrological year, that is $33.6GWh$ more than the dry hydrological year when using SLR. This provides a grid utilisation and hydropower revenue equal 57.15% and $79.93MNOK$, which are higher than the corresponding values in Table 8.

During the wet hydrological year the major difference between DLR and SLR seems to be connected to the wind power producer. With DLR, the system is able to reduce the wind power curtailment with $2.01GWh$, which gives a slightly higher grid utilisation and wind power revenue. Otherwise, the values in Table 9 and Table 8 coincide when one disregards rounding errors. The fact that the system only manages to decrease wind power curtailment and not flood losses indicates that the increased inflow congests the flexibility of the hydropower producer. With the increased inflow, the hydropower producer needs to produce power to avoid flooding of the reservoir, and thereby regaining the transmission capacity from the wind power producer. However, the total hydropower production is not near the maximum annual production the hydropower plant size indicates it could have. Moreover, the transmission capacity is not a constraint either, as the grid utilisation is approximately 64% in both tables. In other words, the flood losses could have been avoided. The reason why they are not avoided is probably connected to the weighting of the different types of energy loss in the model and the variations in Elspot prices, as discussed in Section 6.2.4.

The last part of the conducted sensitivity analysis, presented in Section 5.3.4, combines the different variations in order to explore how the system is performing in a dry hydrological year with $180MW$ installed wind power. This scenario is chosen with the purpose of capturing the possible correlation between inflow amount and energy loss. From Table 10 it can be seen that the only difference between the normal and dry hydrological years for DLR and SLR is hydropower production and the parameters it affects. In other words, the dry year with DLR and wet year with DLR are only different from each other as regards hydropower production and connected parameters, which also applies to the SLR results.

Since the wind power curtailment in Table 10 remains constant for the different inflow amounts when the line rating is unaltered, it seems reasonable to believe that the occurring curtailment is due to the wind potential being larger than maximum transmission capacity. Therefore, the increased flexibility the hydropower producer receives from reduced inflow does not matter, as to the hydropower plant only provides passive storage. In contrast, the utilisation of DLR is able to reduce the curtailment with $99.15GWh$, which comprises an increase in the wind power producer's revenue equal to $25.85MNOK$. In conclusion, the DLR provides a greater benefit for the system when there is more installed wind power capacity, in the same manner as having a bilateral power agreement is found to give a larger impact with more installed wind power.

Even though the results in Table 10 indicate that the inflow does not affect the energy loss in the studied system, Table 8 and Table 9 indicate otherwise. A possible solution is that the system for both normal and dry years has enough flexibility to cope with the prioritisation of wind power. Therefore, it is only the optimisation of a wet year that shows the effect of altering the inflow. However, further scenarios with altered inflow are believed to be necessary to fully determine the effect of inflow and how it correlates with the energy loss.

In summary, the sensitivity analysis shows that with regard to high installed wind power capacity, an improved transmission capacity, i.e. DLR, is able to reduce wind power curtailment to the largest extent. Furthermore, an increase in inflow is seen to generate both flood losses and wind curtailment, highlighting how the hydropower producer's ability to provide flexibility decreases with higher inflow. Finally, the sensitivity analysis shows that grid utilisation is increased by more inflow and more wind power capacity, despite increased losses, due to providing a significant increase in power production potential.

6.4 Assumptions and Shortcomings

Due to the complexity of the power system and the studied case area, several assumptions have been made during the development of the models and the calculations in this thesis. Moreover, the motivation and purpose of the thesis made it appropriate to simplify the studied system to better highlight and cover the thesis' scope. Consequently, there are some shortcomings to be found. Both assumptions and shortcomings can affect results and perceptions found in this thesis, which should be addressed. A summary of the most important assumptions and shortcomings are therefore listed below.

- The aggregation of the original cascaded hydropower system gives another type of operation and scheduling of the hydropower system. However, the inaccuracy induced by this premise is believed to be rather small, as the cascaded plants in the original hydropower system is owned by the same company and has a drain hatch that enables bypassing of the upper station. This results in a operational pattern that partly resembles a single hydropower plant.
- Both location and installed power capacity, as well as the reservoir size of the aggregated system, are simplifications. The reservoir size is believed to induce the largest amount of uncertainty, as the hydropower producer's flexibility, and therefore the efficiency of the bilateral power agreement, is highly dependent on storage capacity.
- In the case study, the external grid is assumed always to have enough demand to consume the power produced by the local system. This treatment of the external grid as a black box makes the simulation and optimisation results less transferable to the real power grid. However, the assumption is justified by the scope of the thesis.
- The simplification of assuming no local loads is found to be suitable for the studied system. However, this affects the design of the optimisation model, resulting in a model only applicable for systems without local loads.
- Losses in transformers, transmission lines and power stations are not taken into account. Moreover, it is assumed that the transmission line is the component setting the transmission capacity. However, both transformers and power station switches might have a lower maximum current than the transmission line. These shortcomings are considered to cause some result inaccuracies, but only have minor impacts on the overall results.
- Due to the aggregation of the hydropower plant, all input data for the hydropower plant are scaled according to the new plant properties. This is believed to be of little importance with regard to the overall results. However, specific details, like the pattern of the calculated reservoir level trajectory, could be affected.
- In the sensitivity analysis, both time series of inflow and wind power potential are scaled according to new values. In particular, the scaling of wind power potential is believed to be an inaccurate approach, due to the correlation between neighbouring wind turbines and wind farms observed in the literature review [6, p.15]. However, this is deemed to be acceptable, as it overall trends and developments that are studied in the sensitivity analysis.
- The optimisation model gives the ideal production scheduling, as it utilises historical time series and therefore knows all physical properties of the system throughout the time horizon, in advance. This is a good theoretical approach to highlight the project issue, but the stochastic nature of prices, inflow, demand and wind power potential is not captured. Consequently,

the optimisation model will not be very applicable in a practical context, unlike the model developed by Korpås [51].

- The maximum flood loss is determined by assuming that the hydropower producer will release water through a drain hatch. Since the optimisation model knows everything in advance it is reasonable that the hydropower plant will plan to release water during low Elspot prices, instead of the reservoir being flooded during high prices. This operational pattern is plausible in reality as well, since hydropower producers will choose to release water in advance if the prices are low and the future inflow is expected to be high.
- The optimisation model assumes that the regulation time of the hydropower plant is as fast as the wind power. Even though hydropower has a fast reaction time, the literature review indicates that it is slower than wind power. This weakens the practical accuracy of the results. However, the overall operational patterns should not be affected much since the optimisation model operates with historical data and therefore knows everything in advance.
- When estimating the DLR, a linear relationship between wind speed and rating is assumed to enable interpolation between the values in the given DLR chart of the actual line. Combined with the highest wind speed in the chart being $5m/s$, which is less than the highest wind speed in the time series, this approach is believed to induce inaccuracies to the estimated DLR. However, it is not found to deteriorate the DLR enough not to be used for a technical perspective.
- The wind speed time series used for estimating DLR is from a different source than the one the wind power potential is based on. Consequently, the found correlation between DLR and wind power potential, which was also recognised in the literature review, might therefore be stronger than what could be observed in the results.

7 Conclusion and Further Work

7.1 Conclusion

Throughout this thesis, the impact and possibilities induced from the revision of NEM have been explored in a local power system in Northern Norway. Both a political expansion, through a bilateral power agreement, and a technical expansion, by implementing DLR, have been investigated. The study has been carried out by utilising a local energy balance and an energy loss minimisation model to replicate the operational patterns caused by provision in these political regulations.

The overall result from the simulations showed that the wind power producer with production restrictions according to NEM experienced an average annual amount of wind power curtailment equal to $16.41GWh$. This constituted 4.20% of the annual wind power potential and induced an average revenue loss of $4.67MNOK$ each year. However, utilisation of grid capacity was found to be only 54.24% on average, indicating that there should be sufficient capacity to capture the wind power curtailment. In other words, a grid expansion appears to be unnecessary. Combined with financial estimates, the overall simulation result therefore implies that NEM might be a better alternative than conventional connection regulations. Moreover, grid expansion costs and building delays are avoided. Still, a more extensive investment analysis is deemed necessary to obtain a precise assessment of this matter.

Furthermore, the sensitivity analysis of the simulation model highlighted that the revision of NEM provided an increase in grid utilisation. Nevertheless, the provisions in NEM were not found to regulate the system thereby maximising maximise social surplus, as VRES, being wind power in this case, experienced a loss of power production potential. In other words, NEM was seen to improve grid utilisation, but not provide an optimal utilisation.

From the optimisation results it could be seen that a bilateral power agreement between the power producers was able to capture the $16.41GWh$ average wind power curtailment experienced in the simulations, thereby eliminating all curtailment. Thus, the grid utilisation was increased by 1.01 percentage points. The generated operational pattern also revealed that the hydropower production was shifted to periods with low wind potential, utilising the flexibility of the reservoir. Furthermore, the observed changes in cash flows indicate that a bilateral power agreement provides a financial advantage to the wind power producer and the overall system.

When the installed wind power capacity was increased above the transmission limit, it could be seen that the bilateral power agreement was no longer able to prevent wind power curtailment, due to the resulting wind power potential being greater than the limit itself. Consequently, the hydropower flexibility utilised by the agreement was unable to capture all the wind power potential, as it is a passive storage. This was substantiated by an observed drop in the grid utilisation increment as seen previously in the sensitivity analysis. In addition, it was seen that an increase in inflow diminished the advantage of entering into a bilateral power agreement. However, the accuracy of this observation is reduced by the optimisation model lacking a more specific requirement for the hydropower production and the energy loss weights being unexplored.

Implementation of DLR was found to reduce the amount and frequency of wind power curtailment experienced in the simulations by $11.89GWh$ and 893.4 times per year, respectively. This observation, combined with the results from the sensitivity analysis, indicates an advantageous positive correlation between DLR and wind power potential. Consequently, grid utilisation was seen to increase by

0.97 percentage points in the simulations compared to utilising SLR. Moreover, the bilateral power agreement's impact on the original hydropower production scheduling is significantly reduced with the reduced curtailment frequency. As such, the DLR might provide a decrease in possible wear and tear inflicted on the hydropower plant by the agreement. Furthermore, the DLR is seen to reduce the financial integrity of the bilateral power agreement, as the reduction of the previous wind power curtailment weakens the incentive of having the agreement. However, the estimated DLR is believed to capture only the overall characteristics of the real transmission line. Further improvements to the DLR calculations are therefore found necessary for a more precise outcome.

7.2 Further Work

The results presented in this thesis are found to be applicable for highlighting the overall effect of the revision of NEM and how a technical and political solution can complement the regulation. However, the study has implemented simplifications and assumptions, and does therefore not provide an in-depth analysis of the power system impacts. In the following list, expansions and enhancements that are considered to be logical next steps for further work on the topic, are presented. The recommendations presented in the list are based on the discussion in Section 6.

- **Further investigate grid impacts and expand the studied power system:** The power system presented in the case study in Section 4 is a simplification suitable for providing overall results that highlight the thesis' objectives. However, a future in-depth study could include more grid elements, such as transformers, power stations etc., to achieve a more precise and realistic outcome. Nevertheless, the exclusion of these grid elements is not considered to induce as much inaccuracy as the aggregation of the studied hydropower system. Consequently, further work should strive to utilise the original hydropower configuration.
- **Include pumped storage hydropower:** From the sensitivity analysis in Section 5.3, it is evident that an energy storage enabling active charging is needed to capture wind power potential exceeding the transmission limit. As seen in the literature review, pumped storage hydropower is found to be a good alternative, which also makes sense based on the existing hydropower facility. Therefore, further studies should include a pumped storage facility in their investigations.
- **Investigate the impact of the external grid:** The external grid was treated as a black box in this thesis and assumed to have the ability to consume all power produced in the local area. This is a reasonable simplification based on the scope of this thesis. However, the external grid is deemed to be a relevant expansion, which will increase how relatable future results are to the real power system.
- **Run power flow simulations:** A power flow simulation can provide a better understanding of the operational patterns in the power system, and therefore contribute to the verification of accuracy and feasibility in further studies.
- **Conduct a more extensive investment analysis:** As discussed in Section 6.1.2, a more extensive investment analysis should be conducted to further assess the performance of grid connection with production restrictions compared to grid expansions.
- **Evaluate different economic configurations for a bilateral power agreement:** From the discussion in Section 6.2.3 it is evident that the financial sustainability of the bilateral

power agreement is dependent on the economic conditions agreed between the producers. Consequently, an evaluation of different economic configurations is considered a logical next step together with a long-term cost-benefit analysis of the impacts of NEM.

- **Improve the estimation of DLR:** Even though the DLR used in this thesis was sufficient for highlighting overall properties, it is deemed reasonable that a future study utilises a more extensive estimation method to gain a more precise DLR.
- **Include more constraints in the optimisation model:** As mentioned in Section 6.2.4, the optimisation model does not specify how the hydropower should produce when there is no risk of energy losses. This enables several optimal solutions and operational patterns that might be counterintuitive and have a weak basis of comparison to the simulation model. A constraint specifying the hydropower producer's behaviour in periods without risk of losses should therefore be included. An interesting constraint could be to require the annual hydropower production to be equal to the production in the simulation. This would probably improve the basis of comparison. Another compelling constraint is to demand that the hydropower producer maximise its own profit, something that is common from a business perspective.
- **Improve the optimisation model to become more applicable for real power system operation:** As described in Section 3.3 and Section 6.4, the optimisation model does not include the ability to use the current state of the power system to optimise future production. This is an interesting expansion for further studies, as it will make the model more applicable to real production scheduling. A solution could be to implement a decision algorithm similar to the one used by Korpås [51]. Another relevant expansion connected to future scheduling is to include weather forecasting in order to estimate the future DLR of the transmission line.
- **Expand the sensitivity analysis:** The sensitivity analysis conducted in this thesis improves the understanding and better highlights the impact of NEM and the suggested complementary expansions. However, it is found reasonable to expand the analysis to include a higher resolution of the alternation of the already analysed parameters. Moreover, the reservoir size and installed hydropower capacity, which is connected to hydropower flexibility, would be interesting to alter. In addition, the weights used to determine the cost of each type of energy loss should be investigated. In particular, the flood losses during the wet hydrological year should be removed with a higher weight on flooding, as it was deemed to be avoidable. Different transmission line capacities should also be included, to investigate how the degree of limitation in the system affects the economic incentive of having a bilateral power agreement combined with DLR.
- **Investigate the environmental effects of altering the hydropower production:** The hydropower scheduling is altered drastically when the bilateral power agreement is implemented in the case study, which might impact the local environment. Consequently, a future study should investigate how the local ecosystem are affected and consider if a bilateral power agreement is environmentally sustainable.

References

[1] International Energy Agency, *Data and Statistics*, [Last accessed: 09 Jun 2021], Nov. 2020. [Online]. Available: https://www.iea.org/data-and-statistics?country=WORLD&fuel=Energy%5C%20supply&indicator=TPESbySource.

[2] The United Nations Framework Convention on Climate Change, *The Paris Agreement*, [Last accessed: 09 Jun 2021], Nov. 2016. [Online]. Available: https://unfccc.int/process-and-meetings/the-paris-agreement/the-paris-agreement.

[3] E. Nycander, L. Söder, R. Eriksson, and C. Hamon, "Minimising wind power curtailments using opf considering voltage stability," *The Journal of Engineering*, vol. 2019, no. 18, pp. 5064–5068, 2019. DOI: https://doi.org/10.1049/joe.2018.9371.

[4] K. Lund and A. V. Skrivarhaug, "Langsiktig kraftmarkedsanalyse 2020-2040," NVE, Tech. Rep., Oct. 2020, [Last accessed: 09 Jun 2021]. [Online]. Available: http://publikasjoner.nve.no/rapport/2020/rapport2020_37.pdf.

[5] The Norwegian Water Resources and Energy Directorate, *Kraftproduksjon*, [Last accessed: 11 Jun 2021], Apr. 2021. [Online]. Available: https://www.nve.no/energiforsyning/kraftproduksjon/?ref=mainmenu.

[6] K. Dragoon, "Overview of system impacts of wind generation on power systems," in *Valuing Wind Generation on Integrated Power Systems*, 1st ed., Elsevier Inc., Dec. 2010, ch. 2, pp. 5–20, ISBN: 9780815520474. DOI: 10.1016/B978-0-8155-2047-4.10002-X.

[7] M. Nicolosi, "Wind power integration and power system flexibility–an empirical analysis of extreme events in germany under the new negative price regime," *Energy Policy*, vol. 38, no. 11, pp. 7257–7268, Nov. 2010, ISSN: 0301-4215. DOI: https://doi.org/10.1016/j.enpol.2010.08.002.

[8] J. Tande and K. Vogstad, "Operational implications of wind power in a hydro based power system," in *European Wind Energy Conference and Exhibition (EWEC)*, Mar. 1999, pp. 425–428.

[9] T. Acker, A. Robitaille, H. Holttinen, M. Piekutowski, and J. Tande, "Integration of wind and hydropower systems: Results of iea wind task 24," *Wind Engineering*, vol. 36, pp. 1–18, Feb. 2012. DOI: 10.1260/0309-524X.36.1.1.

[10] J. Matevosyan, M. Olsson, and L. Söder, "Hydropower planning coordinated with wind power in areas with congestion problems for trading on the spot and the regulating market," *Electric Power Systems Research*, vol. 79, no. 1, pp. 39–48, Jul. 2009. DOI: https://doi.org/10.1016/j.epsr.2008.05.019.

[11] Ministry of Petroleum and Energy, *Forskrift om nettregulering og energimarkedet (FOR-2019-10-24-1413)*, [Last accessed: 09 Jun 2021], Oct. 2019. [Online]. Available: https://lovdata.no/dokument/SF/forskrift/2019-10-24-1413.

[12] V. S. Stave, "Optimal utilization of grid capacity for connection of new renewable power plants," Department of Electric Power Engineering, NTNU – Norwegian University of Science and Technology, Project report in TET4520, Dec. 2020.

[13] The Norwegian Government, *Ministry of Petroleum and Energy*, [Last accessed: 09 Jun 2021], Feb. 2020. [Online]. Available: https://www.regjeringen.no/en/dep/oed/id750/.

[14] Ministry of Petroleum and Energy, *Lov om produksjon, omforming, overføring, omsetning, fordeling og bruk av energi m.m. (LOV-1990-06-29-50)*, [Last accessed: 09 Jun 2021], Nov. 2019. [Online]. Available: https://lovdata.no/dokument/NL/lov/1990-06-29-50#KAPITTEL_3.

[15] UK Legislation, *Electricity Act 1989 c. 29 Part I Duties of electricity distributors*, [Last accessed: 09 Jun 2021], Apr. 2017. [Online]. Available: https://www.legislation.gov.uk/ukpga/1989/29/part/I/crossheading/supply-by-public-electricity-suppliers.

[16] Sveriges Riksdag, *Ellag (1997:857)*, [Last accessed: 09 Jun 2021], Nov. 2020. [Online]. Available: http://www.riksdagen.se/sv/dokument-lagar/dokument/svensk-forfattningssamling/ellag-1997857_sfs-1997-857.

[17] The Norwegian Energy Regulatory Authority, *Tilknytningsplikt*, [Last accessed: 09 Jun 2021], Dec. 2019. [Online]. Available: https://www.nve.no/reguleringsmyndigheten/nettjenester/nettilknytning/tilknytningsplikt/.

[18] ——, *Tilknytning av produksjon med vilkår*, [Last accessed: 09 Jun 2021], Dec. 2019. [Online]. Available: https://www.nve.no/reguleringsmyndigheten/nettjenester/nettilknytning/tilknytningsplikt/tilknytning-av-produksjon-med-vilkar/.

[19] International Energy Agency, *Hydropower*, [Last accessed: 09 Jun 2021], Nov. 2020. [Online]. Available: https://www.iea.org/fuels-and-technologies/hydropower.

[20] The Norwegian Water Resources and Energy Directorate, *Vannkraft*, [Last accessed: 11 Jun 2021], Jun. 2021. [Online]. Available: https://www.nve.no/energiforsyning/kraftproduksjon/vannkraft/?ref=mainmenu.

[21] G. M. Masters, *Renewable and Efficient Electric Power Systems Second Edition*. John Wiley Sons Inc, Jun. 2013, ISBN: 9780471668824. DOI: 10.1002/0471668826.

[22] S. B. Rawcliffe, A. G. Berthling, H. A. Grønsten, P. D. Bruun, E. V. Dalen, L. Midttun, and F. T. Kvernhaugen, "Slipp, måling og dokumentasjon av minstevannføring," NVE, Tech. Rep., Apr. 2020, [Last accessed: 09 Jun 2021]. [Online]. Available: http://publikasjoner.nve.no/veileder/2020/veileder2020_03.pdf.

[23] Skagerak kraft, *Water level*, [Last accessed: 09 Jun 2021], Apr. 2021. [Online]. Available: https://www.skagerakkraft.no/water-level/category2406.html.

[24] A. Elbatran (A. H. Elbatran), M. Walid, O. Yaakob, Y. Ahmed, and M. Ismail, "Hydro power and turbine systems reviews," *Jurnal Teknologi (Sciences & Engineering)*, vol. 74, pp. 83–90, May 2015. DOI: 10.11113/jt.v74.4646.

[25] P. Breeze, "Chapter 4 - Hydropower Turbines," in *Hydropower*, P. Breeze, Ed., Academic Press, Mar. 2018, pp. 35–46, ISBN: 9780128129067. DOI: https://doi.org/10.1016/B978-0-12-812906-7.00004-1.

[26] Norges vassdrags- og energiverk, *Kulturminner i norsk kraftproduksjon: - en evaluering av bevaringsverdige kraftverk (KINK)*. Norges vassdrags- og energidirektrorat, 2006, ISBN: 9788241005473. [Online]. Available: https://books.google.no/books?id=TYO9DAEACAAJ.

[27] I. Kougias, G. Aggidis, F. Avellan, S. Deniz, U. Lundin, A. Moro, S. Muntean, D. Novara, J. I. Pérez-Díaz, E. Quaranta, P. Schild, and N. Theodossiou, "Analysis of emerging technologies in the hydropower sector," *Renewable and Sustainable Energy Reviews*, vol. 113, p. 109 257, Oct. 2019, ISSN: 1364-0321. DOI: https://doi.org/10.1016/j.rser.2019.109257.

[28] J. G. Balchen, T. Andresen, and B. A. Foss, *Reguleringsteknikk 6. utgave*. Institutt for teknisk kybernetikk NTNU, Jan. 2016, ISBN: 9788278422021.

[29] W. Guo and J. Yang, "Stability performance for primary frequency regulation of hydro-turbine governing system with surge tank," *Applied Mathematical Modelling*, vol. 54, pp. 446–466, 2018, ISSN: 0307-904X. DOI: https://doi.org/10.1016/j.apm.2017.09.056.

[30] J. R. B. Jan Machowski Janusz W. Bialek, *Power System Dynamics: Stability and Control*. John Wiley & Sons, Aug. 2011, ISBN: 978-1-119-96505-3.

[31] A. Khodabakhshian and R. Hooshmand, "A new pid controller design for automatic generation control of hydro power systems," *International Journal of Electrical Power & Energy Systems*, vol. 32, no. 5, pp. 375–382, 2010, ISSN: 0142-0615. DOI: https://doi.org/10.1016/j.ijepes.2009.11.006.

[32] W. Guo and D. Zhu, "A review of the transient process and control for a hydropower station with a super long headrace tunnel," *Energies*, vol. 11, no. 11, 2018, ISSN: 1996-1073. DOI: 10.3390/en11112994.

[33] P. Breeze, "Chapter 8 - Pumped Storage Hydropower," in *Hydropower*, P. Breeze, Ed., Academic Press, Mar. 2018, pp. 73–78, ISBN: 978-0-12-812906-7. DOI: https://doi.org/10.1016/B978-0-12-812906-7.00008-9.

[34] J. D. Hunt, B. Zakeri, R. Lopes, P. S. F. Barbosa, A. Nascimento, N. J. de Castro, R. Brandão, P. S. Schneider, and Y. Wada, "Existing and new arrangements of pumped-hydro storage plants," *Renewable and Sustainable Energy Reviews*, vol. 129, p. 109 914, Sep. 2020, ISSN: 1364-0321. DOI: https://doi.org/10.1016/j.rser.2020.109914.

[35] Gordon Butte Energy Park, *Gordon Butte Pumped Storage Hydro Overview*, [Last accessed: 09 Jun 2021], 2020. [Online]. Available: https://www.gordonbuttepumpedstorage.com/about-the-project.

[36] L. Pitorac, K. Vereide, and L. Lia, "Technical Review of Existing Norwegian Pumped Storage Plants," *Energies*, vol. 13, 18 Sep. 2020, ISSN: 1996-1073. DOI: https://doi.org/10.3390/en13184918.

[37] P. Breeze, *Power Generation Technologies 2nd Edition*. Elsevier, Mar. 2014, ISBN: 9780080983301. DOI: https://doi.org/10.1016/C2012-0-00136-6.

[38] International Energy Agency, *Total installed power capacity by fuel and technology 2019-2025, main case*, [Last accessed: 09 Jun 2021], Nov. 2020. [Online]. Available: https://www.iea.org/data-and-statistics/charts/total-installed-power-capacity-by-fuel-and-technology-2019-2025-main-case#.

[39] ——, *Renewables 2020, Wind*, [Last accessed: 11 Jun 2021], Nov. 2020. [Online]. Available: https://www.iea.org/reports/renewables-2020/wind#abstract.

[40] F. Blaabjerg and K. Ma, "Wind energy systems," *Proceedings of the IEEE*, vol. 105, no. 11, pp. 2116–2131, May 2017. DOI: 10.1109/JPROC.2017.2695485.

[41] O. Apata and D. Oyedokun, "An overview of control techniques for wind turbine systems," *Scientific African*, vol. 10, e00566, 2020, ISSN: 2468-2276. DOI: https://doi.org/10.1016/j.sciaf.2020.e00566.

[42] I. H. Waagaard, E. B. Christophersen, and I. Slungård, "Mulighetsstudie for landbasert vindkraft 2015 og 2025," NVE and Enova, Tech. Rep., Dec. 2008, [Last accessed: 09 Jun 2021]. [Online]. Available: https://publikasjoner.nve.no/rapport/2008/rapport2008_18.pdf.

[43] Ø. Byrkjedal, E. Åkervik, and K. Vindteknikk, "Vindkart for Norge," NVE, Tech. Rep., Oct. 2009, [Last accessed: 09 Jun 2021]. [Online]. Available: https://www.nve.no/media/2470/vindkart_for_norge_oppdragsrapporta10-09.pdf.

[44] A. Kringstad, M. M. Winsnes, K. L. Västermark, and E. T. Bøhnsdalen, "Økt vindkraftproduksjon og virkninger i transmisjonsnettet," Statnett, Tech. Rep., Oct. 2018, [Last accessed: 09 Jun 2021]. [Online]. Available: https://www.nve.no/Media/7352/%5C%C3%5C%B8kt-vindkraftproduksjon-og-virkninger-i-transmisjonsnettet.pdf.

[45] J. Kabouris and F. D. Kanellos, "Impacts of large-scale wind penetration on designing and operation of electric power systems," *IEEE Transactions on Sustainable Energy*, vol. 1, no. 2, pp. 107–114, May 2010. DOI: 10.1109/TSTE.2010.2050348.

[46] L. Xie, P. M. S. Carvalho, L. A. F. M. Ferreira, J. Liu, B. H. Krogh, N. Popli, and M. D. Ilić, "Wind integration in power systems: Operational challenges and possible solutions," *Proceedings of the IEEE*, vol. 99, no. 1, pp. 214–232, Jan. 2011. DOI: 10.1109/JPROC.2010.2070051.

[47] J. Jorgenson, P. Denholm, and T. Mai, "Analyzing storage for wind integration in a transmission-constrained power system," *Applied Energy*, vol. 228, pp. 122–129, Oct. 2018, ISSN: 0306-2619. DOI: https://doi.org/10.1016/j.apenergy.2018.06.046.

[48] R. Abhinav and N. M. Pindoriya, "Grid integration of wind turbine and battery energy storage system: Review and key challenges," in *2016 IEEE 6th International Conference on Power Systems (ICPS)*, Mar. 2016, pp. 1–6. DOI: 10.1109/ICPES.2016.7583998.

[49] H. Saber, M. Moeini-Aghtaie, M. Ehsan, and M. Fotuhi-Firuzabad, "A scenario-based planning framework for energy storage systems with the main goal of mitigating wind curtailment issue," *International Journal of Electrical Power & Energy Systems*, vol. 104, pp. 414–422, Jan. 2019, ISSN: 0142-0615. DOI: https://doi.org/10.1016/j.ijepes.2018.07.020.

[50] H. Farahmand, S. Jaehnert, T. Aigner, and D. Huertas Hernando, "Nordic hydropower flexibility and transmission expansion to support integration of north european wind power," *Wind Energy*, vol. 18, Apr. 2014. DOI: 10.1002/we.1749.

[51] M. Korpås, "Effektøkning i vannkraftverk for bedre utnyttelse av vindkraft og nettkapasistet," Aug. 2010, [Last accessed at: 09 Jun 2021]. [Online]. Available: https://publikasjoner.nve.no/rapport/2011/rapport2011_01.pdf.

[52] L. Rácz and B. Németh, "Dynamic line rating—an effective method to increase the safety of power lines," *Applied Sciences*, vol. 11, no. 2, 2021, ISSN: 2076-3417. DOI: 10.3390/app11020492.

[53] A. Michiorri, H.-M. Nguyen, S. Alessandrini, J. B. Bremnes, S. Dierer, E. Ferrero, B.-E. Nygaard, P. Pinson, N. Thomaidis, and S. Uski, "Forecasting for dynamic line rating," *Renewable and Sustainable Energy Reviews*, vol. 52, pp. 1713–1730, 2015, ISSN: 1364-0321. DOI: https://doi.org/10.1016/j.rser.2015.07.134.

[54] D. Douglass, W. Chisholm, G. Davidson, I. Grant, K. Lindsey, M. Lancaster, D. Lawry, T. McCarthy, C. Nascimento, M. Pasha, J. Reding, T. Seppa, J. Toth, and P. Waltz, "Real-time overhead transmission-line monitoring for dynamic rating," *IEEE Transactions on Power Delivery*, vol. 31, no. 3, pp. 921–927, 2016. DOI: 10.1109/TPWRD.2014.2383915.

[55] IRENA, "Innovation landscape brief: Dynamic line rating," International Renewable Energy Agency, Tech. Rep., 2020, [Last accessed: 09 Jun 2021]. [Online]. Available: https://www.irena.org/-/media/Files/IRENA/Agency/Publication/2020/Jul/IRENA_Dynamic_line_rating_2020.pdf?la=en&hash=A8129CE4C516895E7749FD495C32C8B818112D7C.

[56] C. R. Black and W. A. Chisholm, "Key considerations for the selection of dynamic thermal line rating systems," *IEEE Transactions on Power Delivery*, vol. 30, no. 5, pp. 2154–2162, 2015. DOI: 10.1109/TPWRD.2014.2376275.

[57] Y. Du and Y. Liao, "On-line estimation of transmission line parameters, temperature and sag using pmu measurements," *Electric Power Systems Research*, vol. 93, pp. 39–45, 2012, ISSN: 0378-7796. DOI: https://doi.org/10.1016/j.epsr.2012.07.007.

[58] J. W. Nilsson and S. A. Riedel, *Electric Circuits 10th edition*. Pearson, Dec. 2015, ISBN: 978-1-292-06054-5.

[59] Nord Pool, *About us*, [Last accessed: 09 Jun 2021], Jun. 2021. [Online]. Available: https://www.nordpoolgroup.com/About-us/.

[60] I. Wangensteen, *Power System Economics - the Nordic Electricity Market*. Fagbokforlaget, Feb. 2012, ISBN: 9788251928632.

[61] Copenhagen Economics, "Changed trading behaviour in longterm power trading," Jan. 2020, ISBN: 978-82-410-2999-8.

[62] The Norwegian Energy Regulatory Authority, *Strømavtaler, strømpriser og faktura*, [Last accessed: 11 Jun 2021], Oct. 2020. [Online]. Available: https://www.nve.no/reguleringsmyndigheten/stromkunde/stromavtaler-strompriser-og-faktura/.

[63] ——, *Nettleie*, [Last accessed: 11 Jun 2021], Dec. 2019. [Online]. Available: https://www.nve.no/stromkunde/nettleie/.

[64] ——, *Innmatingstariffer*, [Last accessed: 11 Jun 2021], Mar. 2020. [Online]. Available: https://www.nve.no/reguleringsmyndigheten/nettjenester/nettleie/tariffer-for-produksjon/innmatingstariffer/.

[65] L. Boscán and R. Poudineh, "Chapter 19 - Business Models for Power System Flexibility: New Actors, New Roles, New Rules," in *Future of Utilities Utilities of the Future*, F. P. Sioshansi, Ed., Boston: Academic Press, Mar. 2016, pp. 363–382, ISBN: 978-0-12-804249-6.

[66] Python Software Foundation, *About Python*, [Last accessed: 09 Jun 2021], Jun. 2021. [Online]. Available: https://www.python.org/about/.

[67] W. E. Hart, J.-P. Watson, and D. L. Woodruff, "Pyomo: Modelling and solving mathematical programs in python," *Mathematical Programming Computation*, vol. 3, no. 3, pp. 219–260, Aug. 2011. DOI: https://doi.org/10.1007/s12532-011-0026-8.

[68] Nordkraft, *Om nordkraft*, [Last accessed: 09 Jun 2021], Jun. 2021. [Online]. Available: https://www.nordkraft.no/om-nordkraft/category813.html.

[69] A. E. Feijoo and J. Cidras, "Modeling of wind farms in the load flow analysis," *IEEE Transactions on Power Systems*, vol. 15, no. 1, Feb. 2000. DOI: 10.1109/59.852108.

[70] Y. Wu, J. Zeng, G. Lu, S. Chau, and Y. Chiang, "Development of an equivalent wind farm model for frequency regulation," *IEEE Transactions on Industry Applications*, vol. 56, no. 3, pp. 2360–2374, Nov. 2020. DOI: https://doi.org/10.1109/ias.2019.8912030.

[71] Norsk Klimaservicesenter, *Observasjoner og værstatistikk*, [Last accessed: 09 Jun 2021], May 2021. [Online]. Available: https://seklima.met.no/.

[72] ——, *Om Norsk klimaservicesenter*, [Last accessed: 09 Jun 2021], 2021. [Online]. Available: https://klimaservicesenter.no/kss/om-oss/om-kss.

[73] Nord Pool, *Day-ahead prices*, [Last accessed: 09 Jun 2021], Jun. 2021. [Online]. Available: https://www.nordpoolgroup.com/Market-data1/Dayahead/Area-Prices/NO/Daily1/?view=table.

[74] Energy Exemplar, *PLEXOS Market Simulation Software*, [Last accessed: 09 Jun 2021], Dec. 2020. [Online]. Available: https://energyexemplar.com/solutions/plexos/.

[75] J. Nocedal and S. J. Wright, *Numerical Optimization*, second. New York, NY, USA: Springer, Jul. 2006, ISBN: 0387303030. DOI: https://doi.org/10.1007/978-0-387-40065-5.

[76] Gurobi Optimization, *Gurobi optimizer*, [Last accessed: 09 Jun 2021], Dec. 2020. [Online]. Available: https://www.gurobi.com/products/gurobi-optimizer/.

[77] ——, *Concurrent Optimizer*, [Last accessed: 09 Jun 2021], Dec. 2020. [Online]. Available: https://www.gurobi.com/documentation/9.1/refman/concurrent_optimizer.html#sec:Concurrent.

[78] Siemens Gamesa, *Legacy Siemens - Onshore wind turbines*, [Last accessed: 09 Jun 2021], Jun. 2020. [Online]. Available: https://www.siemensgamesa.com/products-and-services/onshore/siemens-legacy-products.

[79] Norwegian Meteorological Institute, *Nord-Norge siden 1900*, [Last accessed: 9 Jun 2021], Jan. 2021. [Online]. Available: https://www.met.no/vaer-og-klima/klima-siste-150-ar/regionale-kurver/nord-norge-siden-1900.

[80] M. L. Fossdal and B. Bergesen, "Energibruksrapporten 2012," NVE, Tech. Rep., Oct. 2012, [Last accessed: 09 Jun 2021]. [Online]. Available: http://publikasjoner.nve.no/rapport/2012/rapport2012_30.pdf.

[81] M. Sidelnikova, D. E. Weir, L. H. Groth, K. Nybakke, K. E. Stensby, B. Langseth, J. E. Fonneløp, O. Isachsen, I. Haukeli, S.-L. Paulen, I. Magnussen, L. I. Husabø, T. Ericson, and T. H. Qureishy, "Kostnader i energisektoren," NVE, Tech. Rep., Oct. 2015, [Last accessed: 09 Jun 2021]. [Online]. Available: https://publikasjoner.nve.no/rapport/2015/rapport2015_02a.pdf.

Appendix

A Close-Up Plots of Power Production Scheduling

In this Appendix, plots focusing on specific parts of the presented power production scheduling in Section 5 are presented. The purpose is here to increase the understanding and accuracy of the resulting power production plots from the simulation and optimisation models.

A.1 Simulation Plots

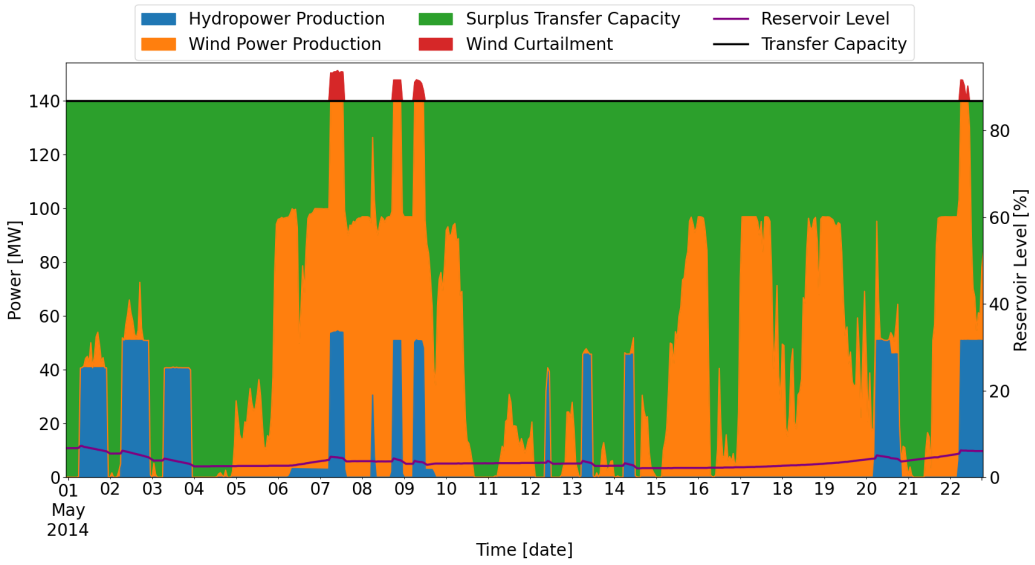

Figure 20: Close-up of the resulting production scheduling in May 2014 from the simulation of the reference case with SLR. Here, it is confirmed that there is hydropower production in the start of May, which substantiates the reservoir level trajectory shown in Figure 10

A.2 Optimisation Plots

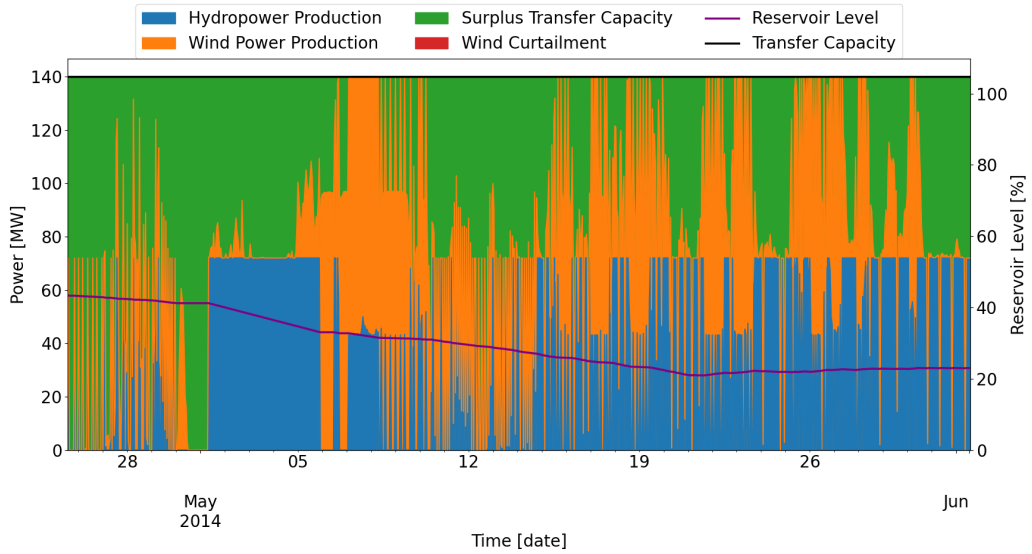

Figure 21: Close-up of the resulting production scheduling in May 2014 from the simulation of the reference case. Here, it is confirmed that there is hydropower production in the start of May, which substantiates the reservoir level trajectory shown in Figure 12

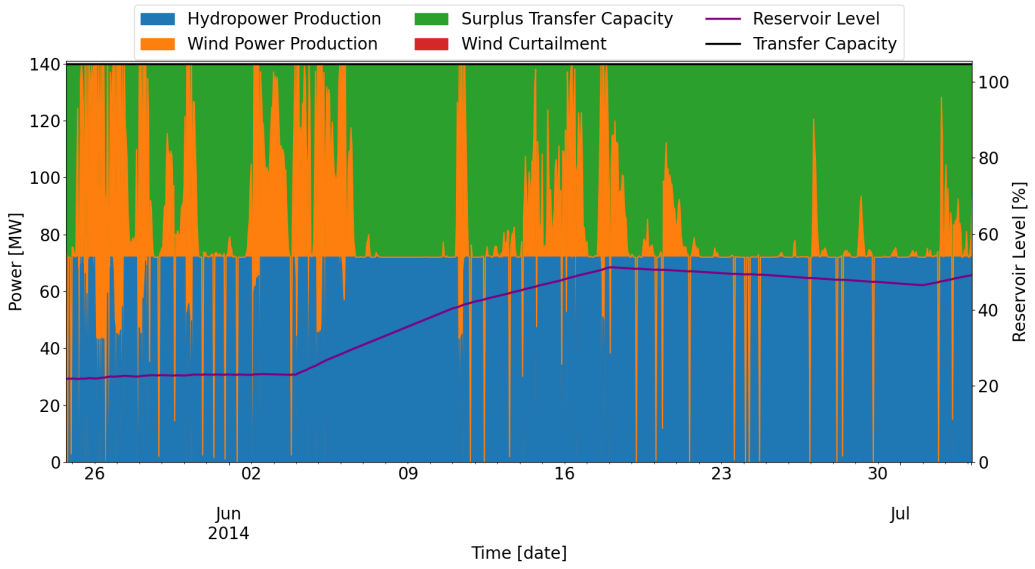

Figure 22: Close-up of the resulting production scheduling in June 2014 from the optimisation of the reference case. Here, it is confirmed that there is hydropower production in the end of June, which substantiates the reservoir level trajectory shown in Figure 12

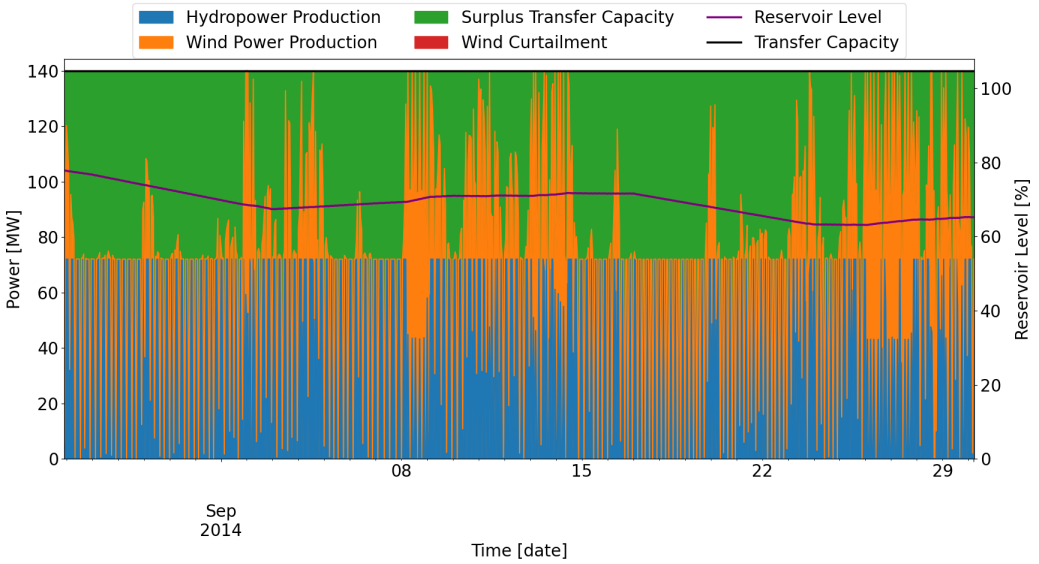

Figure 23: Close-up of the resulting production scheduling in September 2014 from the optimisation of the reference case with SLR. Here, it is confirmed that there is hydropower production in the end of September, which substantiates the reservoir level trajectory shown in Figure 12

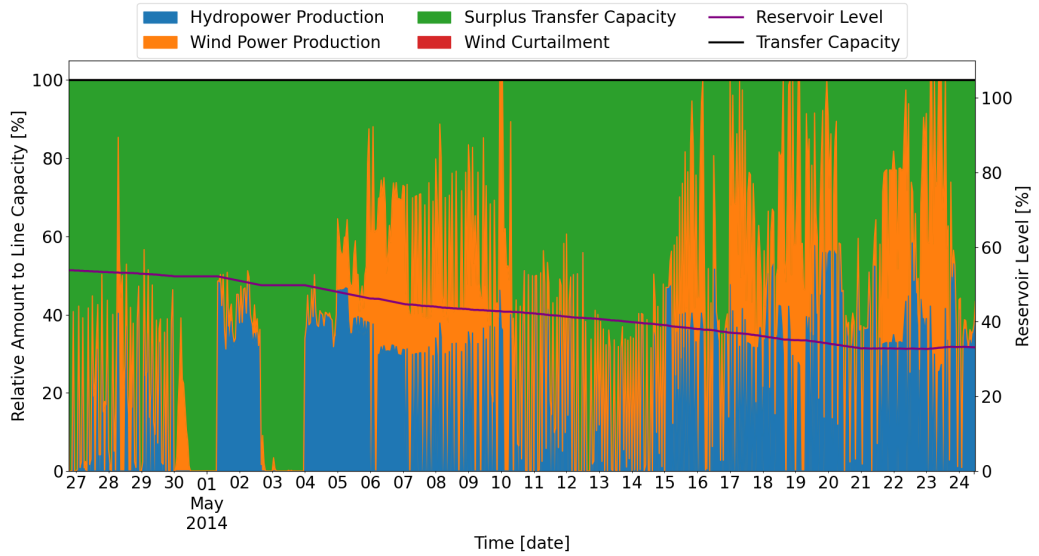

Figure 24: Close-up of the resulting production scheduling in May 2014 from the optimisation of the reference case with DLR. Here, it is confirmed that there is hydropower production in the end of May, which substantiates the reservoir level trajectory shown in Figure 15

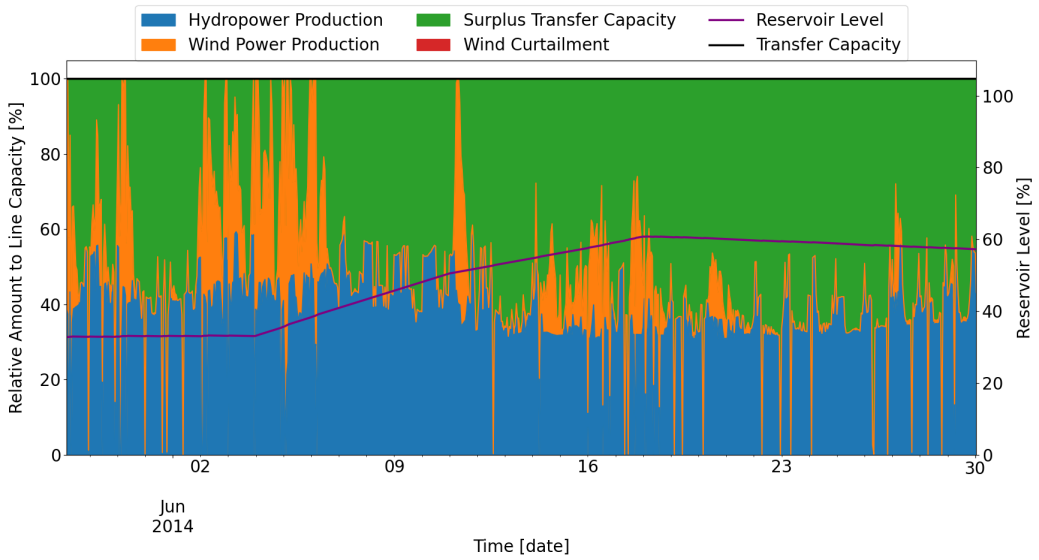

Figure 25: Close-up of the resulting production scheduling in June 2014 from the optimisation of the reference case with DLR. Here, it is confirmed that there is hydropower production in the end of June, which substantiates the reservoir level trajectory shown in Figure 15

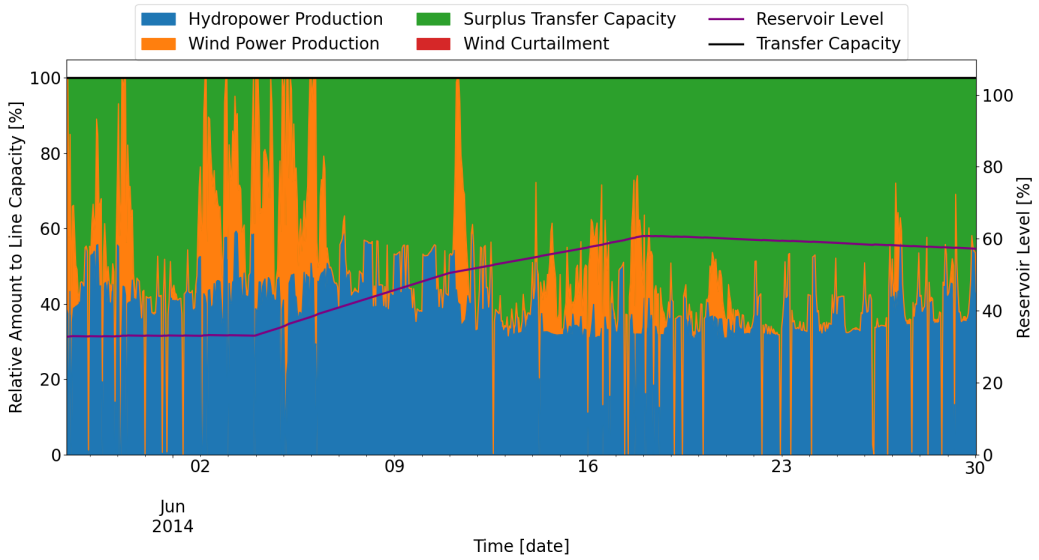

Figure 26: Close-up of the resulting production scheduling in June 2014 from the optimisation of the reference case with DLR. Here, it is confirmed that there is hydropower production in the end of September, which substantiates the reservoir level trajectory shown in Figure 15

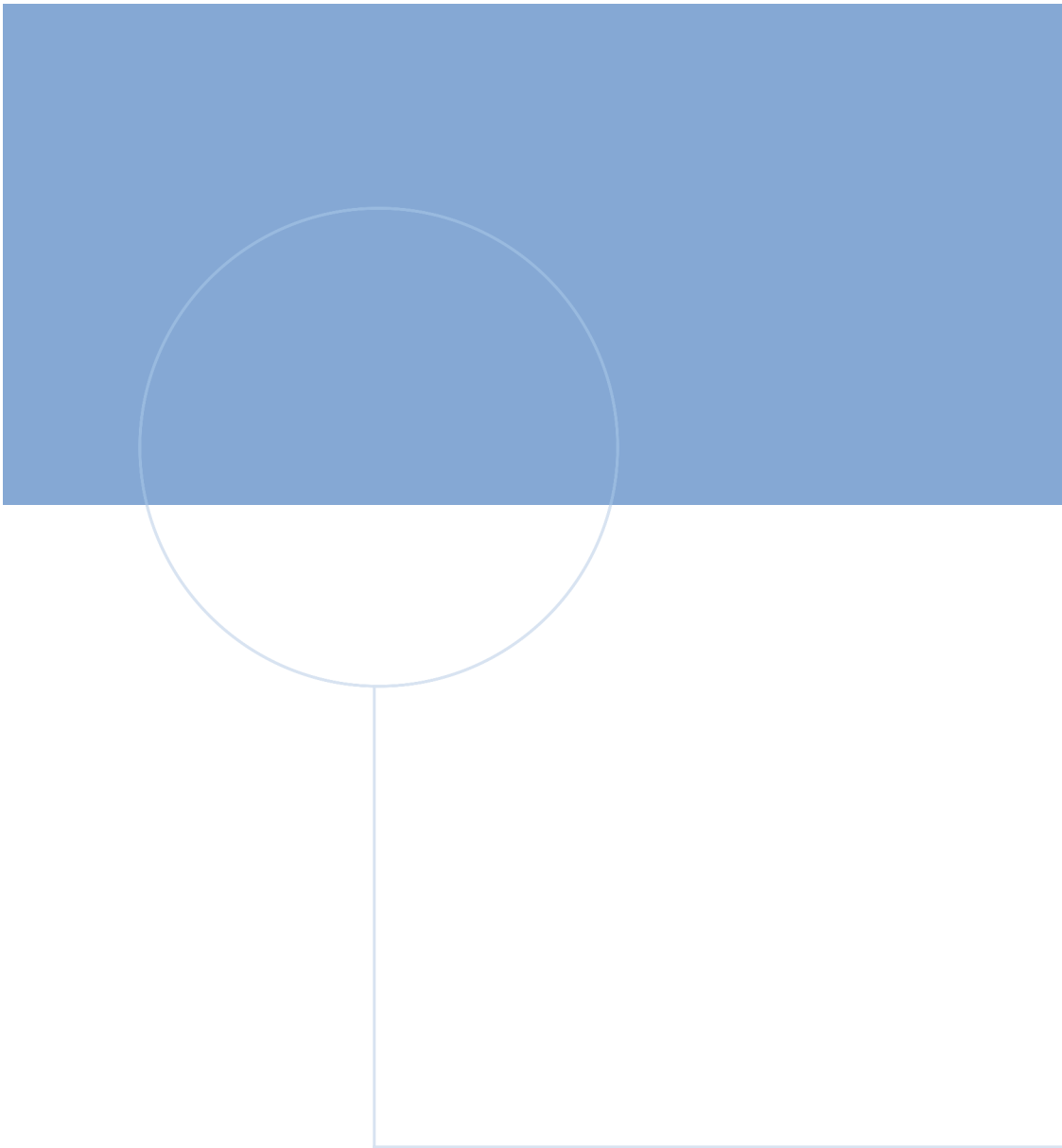

NTNU

Norwegian University of
Science and Technology